TRANSPORTATION RESEARCH RECORD 653

Track Systems and Other Related Railroad Topics

TRANSPORTATION RESEARCH BOARD

COMMISSION ON SOCIOTECHNICAL SYSTEMS
NATIONAL RESEARCH COUNCIL

NATIONAL ACADEMY OF SCIENCES
WASHINGTON, D.C. 1977

Transportation Research Record 653
Price $4.80
Edited for TRB by Frances R. Zwanzig

subject areas
03 rail transport
33 construction

Transportation Research Board publications are available by ordering directly from the board. They may also be obtained on a regular basis through organizational or individual supporting membership in the board; members or library subscribers are eligible for substantial discounts. For further information, write to the Transportation Research Board, National Academy of Sciences, 2101 Constitution Avenue, N.W., Washington, D.C. 20418.

Library of Congress Cataloging in Publication Data
National Research Council. Transportation Research Board.
Track systems and other related railroad topics.

(Transportation research record; 653)
1. Railroads—Track—Congresses. I. Title. II. Series.
TE7.H5 no. 653 [TF240] 380.5'08s [625.1'4] 78-11249
ISBN 0-309-02682-2

Sponsorship of the Papers in This Transportation Research Record

Group 2—DESIGN AND CONSTRUCTION OF TRANSPORTATION FACILITIES
Eldon J. Yoder, Purdue University, chairman

Railway Systems Section
Thomas B. Hutcheson, Seaboard Coast Line Railroad Company, chairman

Committee on Track Structure System Design
M. E. Harr, Purdue University, chairman
Gilbert L. Butler, John S. Collins, Harold D. Decker, John H. Eick, Jr., C. Page Fisher, Lewis D. Freeman, Amir N. Hanna, John B. Heagler, Jr., William P. Hofmann, James D. Jardine, C. R. Kaelin, Arnold D. Kerr, W. S. Lovelace, R. Michael McCafferty, John T. O'Neill, A. C. Parker, Jr., Gerald P. Raymond, Robert N. Schmidt, Paul S. Settle, Donald A. Shoff, Marshall R. Thompson, G. H. Way, Jr.

Edward J. Ward, Transportation Research Board staff

The organizational units and officers and members are as of December 31, 1976.

Contents

Part 1
Track Systems

Effect of Design Parameters on Track Support Systems

Shiraz D. Tayabji,* Department of Civil Engineering, Drexel University
Marshall R. Thompson, Department of Civil Engineering, University of Illinois at Urbana-Champaign

A finite-element structural-analysis model for conventional railway-track support systems previously developed was used as the basis of a study of design parameters to establish the effects of the various parameters on the instantaneous-elastic response of a support system. The parameters studied were type and depth of ballast, type and depth of subballast, subgrade-support conditions, rail size, tie spacing, wheel loading, and number of missing ties. The study indicated that type of ballast and rail size do not significantly affect the instantaneous-elastic response of a support system, but the stabilized subballast, the subgrade-support condition, and the wheel loading are major parameters that do.

Over the years, sporadic efforts have been made to develop analytical methods for the evaluation of the structural response of railway-track support systems. The early attempts to model these systems were hampered by the lack of satisfactory theories for representing the behavior of their various components. In the last quarter century, however, extensive developments in track and pavement-system modeling have coincided with developments in electronic computer technology.

One of the major limitations of the track-system behavior models that have been developed is the inadequate representation of the structural behavior of the ballast and subgrade soil materials. In most models of track support systems, the ballast and subgrade system has been represented by an elastic half space or by a spring constant. The various types of models are listed below:

1. Beam on elastic foundation (1, 2),
2. Finite beam on elastic foundation (3, 4, 5, 6, 7),
3. Analytical solution for track structure subjected to moving and oscillating loads (8),
4. General Boussinesq (9),
5. Semiempirical [e.g. Japanese National Railway Equation (10)], and
6. Finite-element (11, 12, 13).

Numerous theories, techniques, and procedures have been developed for calculating stress and strain and deflection or deformation conditions in track support systems. Even the most recent developments in the methodology of track-structure analysis have concentrated on realistic representations of the rail, fastener, and tie components, while representing the ballast and subgrade either as springs or as linear-elastic-homogeneous materials. Most of the attention has been directed to the behavior of the rail, rather than to that of the ballast and subgrade soil.

Recent developments in highway and airfield-pavement technology have demonstrated that the repeated-load response of granular materials and subgrade soils is very much dependent on the stress conditions existing in the materials (14, 15, 16). Thus, a realistic representation of these materials in a model for track-system analysis requires that their stress-dependent nature be adequately considered. With the limitations of the existing methods and the requirements of a realistic analytical model in mind, a finite-element model—ILLI-TRACK—was developed that incorporates the basic components of the conventional railway-track support system (CRTSS) and can accommodate the stress-dependent structural response characteristics of the ballast, the subballast, and the subgrade. A detailed discussion of the development of the model has been given by Tayabji (17), and a brief description of it is presented below.

ILLI-TRACK MODEL

Figure 1 shows a typical longitudinal section and a typical transverse section of a CRTSS. Because of the three-dimensional geometry and the nonuniform loading conditions, an analysis of the conventional railway track structure should use a three-dimensional finite-element model to represent the system. However, the amount of discretization and the computer costs required for solution of the problem would be high and probably impractical.

However, when the symmetrical nature of the loading in the transverse direction is examined, it is apparent that a two-stage analysis might provide a reasonable engineering approach. In this analysis, the longitudinal analysis is followed by the transverse analysis.

The longitudinal analysis considers the point loads (corresponding to wheel loads), acting on a single rail sitting on a tie-ballast-subgrade system. Figure 2 shows a typical finite-element mesh, such as is used for this analysis. The rail and tie subsystem is represented as a continuous beam supported on tie springs. Rectangular planar elements are used to represent the ballast, the subballast, and the subgrade materials. The thickness of the elements is varied with depth by using a pseudoplane strain technique to account for the spread of loading in the direction perpendicular to the plane. This allows a two-dimensional model to simulate the three-dimensional load spread that is known to exist in practice. The displacement components are assumed to vary linearly over each element.

The transverse analysis uses an output from the longitudinal analysis as its input. Either the maximum reaction or the maximum deflection at a tie obtained from the longitudinal analysis is used as the input at a tie that rests on the ballast and subgrade subsystem. Again the pseudoplane strain technique is used. The tie can be represented either as a two-dimensional body or as a beam resting on the ballast. A rectangular element representation is used for the ballast, the subballast, and the subgrade materials, and the displacement components are assumed to vary linearly over each element. Figure 3 shows the finite-element mesh used for the transverse analysis. Triangular elements can be used to incorporate sloping ballast shoulders.

This finite-element model has been validated by using measured responses at section 9 of the Kansas Test Track (17). Good agreement was obtained between the measured responses and those calculated by using the model. As more appropriate field response data become available, it is expected that the model will be further validated. In its present state, the ILLI-TRACK model is not a design model, but rather an analysis tool.

The characteristics of stress-dependent materials can be determined in terms of the resilient modulus. For ballast materials and sandy soils, the stress-dependent

resilient response can be incorporated by using Equation 1.

$$E_R = K\theta^n \quad (1)$$

where

E_R = resilient modulus = repeated deviator stress/elastic or recoverable strain,
θ = sum of principal stresses = $\sigma_1 + \sigma_2 + \sigma_3$, and
K and n = constants determined from laboratory tests.

For fine-grained soils, the resilient modulus generally decreases as the deviator stress ($\sigma_d = \sigma_1 - \sigma_3$) increases. At higher values of the deviator stress, the resilient modulus is almost constant.

Stress-dependent characteristics have been incorporated in the ILLI-TRACK model. However, failure criteria and constitutive response models for granular materials subjected to stress states in which the confining stress is close to zero (tending to go into tension) or in which the principal stress ratio (σ_1/σ_3) exceeds a limiting value are not well defined. At present, when granular material element in the structural model satisfies the failure criteria [in terms of the minimum allowable minor principal stress (σ_3) or of the maximum principal stress ratio (σ_1/σ_3)], it can be assigned a low modulus value of 27.59 MPa (4000 lbf/in^2) to be used in the next step loading analysis. Analyses can also be carried out in which no failure criteria for granular materials are used; it is then assumed that the granular material would be stable under any state of stress and that the resilient modulus of a granular material element determined by using Equation 1 is valid, even when the failure criteria are satisfied. The omission of failure criteria considerations make the analysis less conservative, and thus the calculated responses are less severe.

With these considerations in mind, a study of the

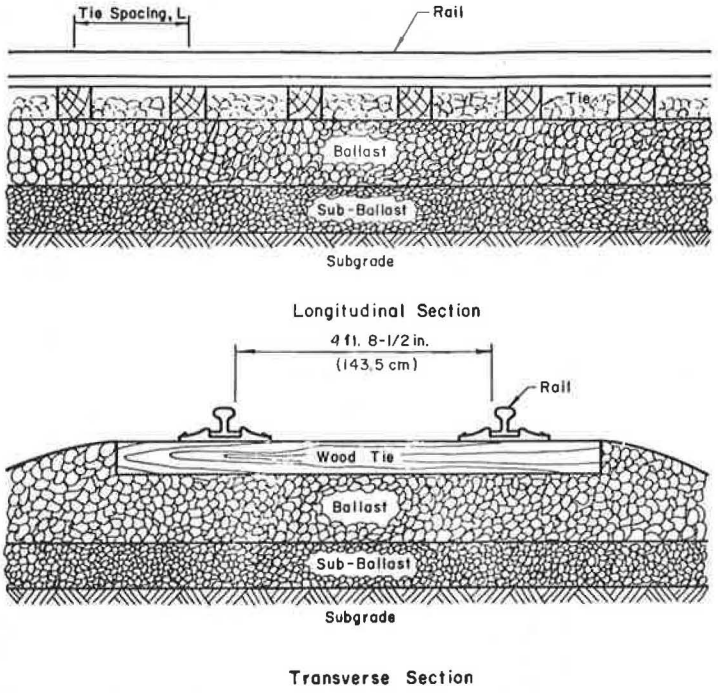

Figure 1. Typical longitudinal and transverse sections of conventional railway track.

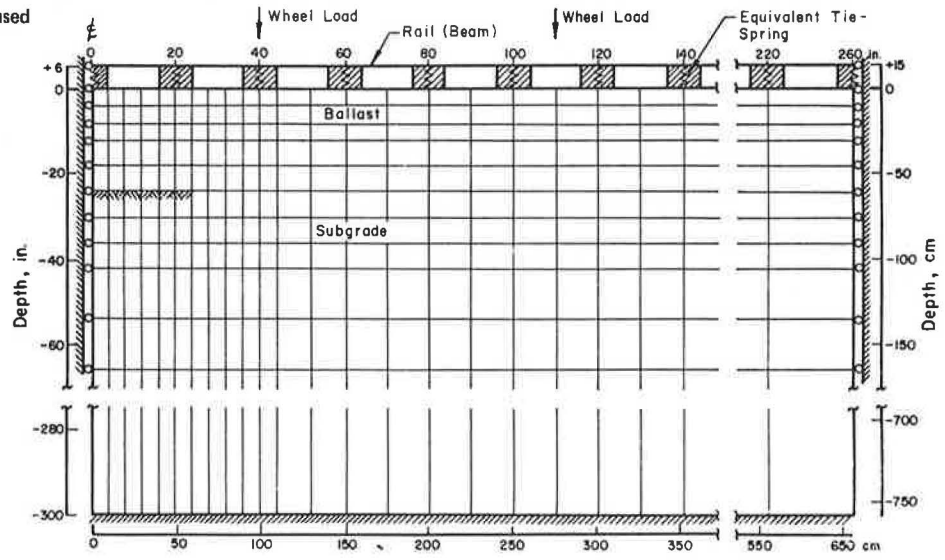

Figure 2. Typical finite-element mesh used for longitudinal analysis.

design parameters was conducted to evaluate the relative differences among the responses of different track systems. The failure criteria selected for the ballast were a σ_1/σ_3 value of 10 and a σ_3 value of 0. Loading was applied in three increments. Because the selection of the failure criteria was arbitrary, the study also included analyses of track sections for which no failure criteria were used.

STUDY OF DESIGN PARAMETERS

An important feature of the design of a track support system is the judicious selection of the optimum design based on factors such as available resources, anticipated performance, and level-of-service requirements. One method used in the selection of an optimum design is to conduct a parameter study or a sensitivity analysis and evaluate the effects of the critical design parameters on the response of the system. The structural model used to evaluate the response of a track support system should therefore be capable of incorporating the critical design parameters. The ILLI-TRACK model possesses this capability and was used to study the effects of various design parameters on the response of the track support system.

Reference Track

A reference track was designed to allow the comparison of the structural responses of track support systems with different design parameters. The characteristics of the track are given below (1 kg/m = 2.0 lb/yd, 1 cm^4 = 0.023 in^4, 1 GPa = 145 037 lbf/in^2, and 1 m = 3.3 ft):

Characteristic	Value
Rail	
Linear mass, kg/m	68
Moment of inertia, cm^4	3954
E, GPa	20.7
Timber ties	
Size, m	0.23 by 0.18 by 2.59
Spacing, m	0.51
Compressive modulus, MPa	8618
Crushed stone ballast	
Resilent response model, E_R	$5082\theta^{0.58}$
Poisson's ratio	0.35
Subballast	—
Subgrade (embankment)	
Poisson's ratio	0.47

The resilient-response curve data for the average subgrade are given below (1 kPa = 0.145 lbf/in^2):

σ_D (kPa)	E_R (kPa)
0.7	102 180.0
42.8	55 160.0
249.6	19 990.0

The reference loading was taken to be two trucks of two adjacent freight cars, each car having a gross mass of 108.8 Mg (240 000 lb), thus giving an approximate wheel load of 133 kN (30 000 lbf). The truck spacing was 3.81 m (150 in), and the axle spacing was 1.78 m (70 in).

The structural responses of particular interest were

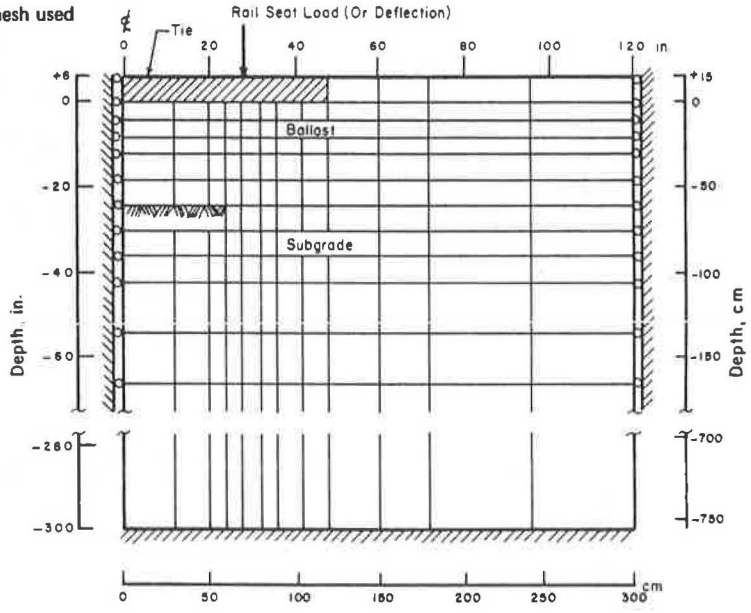

Figure 3. Typical finite-element mesh used for transverse analysis.

Table 1. Responses of sections with type of ballast as variable.

Response	Failure Criteria Used			No Failure Criteria Used		
	Crushed Stone	Blast-Furnace Slag	Well-Graded Crushed Stone	Crushed Stone	Blast-Furnace Slag	Well-Graded Crushed Stone
Maximum rail deflection, mm	2.5	2.0	2.3	1.8	1.8	1.8
Maximum rail moment, kN·m	33.6	29.3	31.5	27.1	27.6	27.7
Maximum ballast vertical stress, kPa	788.1	533.7	564.0	369.5	367.5	396.5
Maximum subgrade vertical stress, kPa	162.0	140.0	143.4	135.1	136.5	137.2
Maximum subgrade vertical strain	0.001 15	0.000 71	0.000 83	0.000 75	0.000 79	0.000 80

Note: 1 mm = 0.039 in, 1 kN·m = 8820 lbf·in, and 1 kPa = 0.145 lbf/in^2.

the rail deflections and moments, the ballast and subgrade vertical stresses, and the subgrade vertical strain. When considering the effect of a particular design parameter, only its input value was changed; all other design parameters were kept constant.

Variable: Type of Ballast

The following types of ballast were evaluated (1 cm = 0.39 in):

Section	Description
1 (reference)	No. 4 gradation crushed stone, $E_R = 5092\theta^{0.58}$
2	No. 4 gradation blast-furnace slag, $E_R = 1957\theta^{0.77}$
3	Well-graded crushed stone (max size 2.5 cm, 20 percent smaller than no. 40, E_R $3582\theta^{0.59}$)

The comparison of the responses of the three sections shown in Table 1 indicates that the influence of type of ballast on the transient response of the track support system is not large. However, different ballast materials have characteristically different permanent deformations (rutting or loss of alignment) behavior and particle breakdown (degradation) when subjected to repeated application of a particular state of stress. While the transient responses when different ballasts are used may be similar, the ballasts may have different durability properties. Therefore, when ballast types are compared, the factors affecting their long-term behavior must be considered in addition to their transient structural responses.

Variable: Depth of Ballast

The following depths of crushed stone ballast were evaluated for 68 and 57 kg/m (136 and 115 lb/yd) rails (1 cm = 0.39 in):

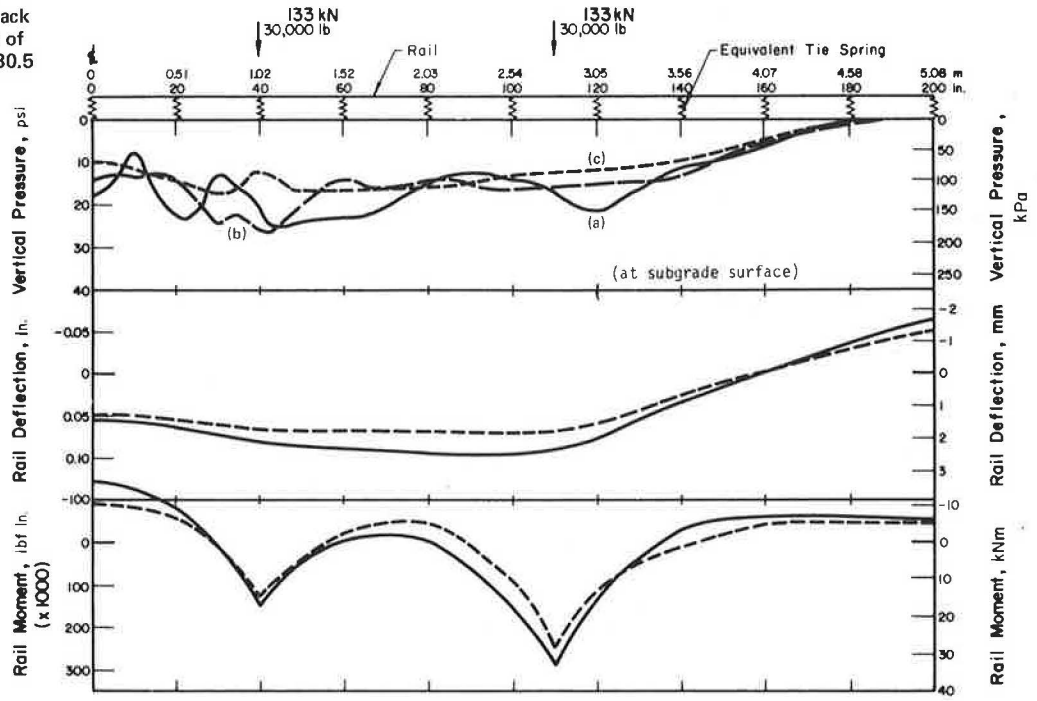

Figure 4. Responses of track system for varying depths of ballast: (a) 20.3 cm, (b) 30.5 cm, and (c) 61 cm.

Table 2. Responses of sections with depth of ballast as variable (68 kg/m rail).

	Depth of Ballast (cm)					
	Failure Criteria Used			No Failure Criteria Used		
Response	20.3	30.5	61.0	20.3	30.5	61.0
Maximum rail deflection, mm	2.5	2.5	1.8	1.8	1.8	1.5
Maximum rail moment, kN·m	33.1	33.6	29.3	27.6	27.1	25.6
Maximum ballast vertical stress, kPa	606.8	788.1	633.0	347.5	369.5	416.5
Maximum subgrade vertical stress, kPa	166.9	182.0	121.4	147.5	135.1	109.6
Maximum subgrade vertical strain	0.001 09	0.001 15	0.000 65	0.000 86	0.000 75	0.000 54

Note: 1 mm = 0.039 in, 1 kN·m = 8820 lbf·in, and 1 kPa = 0.145 lbf/in².

Table 3. Responses of sections with depth of ballast as variable (57 kg/m rail).

	Depth of Ballast (cm)					
	Failure Criteria Used			No Failure Criteria Used		
Response	20.3	30.5	61.0	20.3	30.5	61.0
Maximum rail deflection, mm	2.8	2.3	2.0	1.8	1.8	1.5
Maximum rail moment, kN·m	30.1	25.6	26.6	25.5	25.3	23.5
Maximum ballast vertical stress, kPa	750.9	649.5	757.1	364.7	392.3	449.5
Maximum subgrade vertical stress, kPa	193.1	182.0	130.3	152.4	140.0	111.7
Maximum subgrade vertical strain	0.001 52	0.000 94	0.000 78	0.000 94	0.000 83	0.000 60

Note: 1 mm = 0.039 in, 1 kN·m = 8820 lbf·in, and 1 kPa = 0.145 lbf/in².

Section	Depth (cm)
1	20.3
2 (reference)	30.5
3	61.0

The response of the track system is shown for the 68-kg/m rail in Figure 4. There was little difference in the responses for the 20.3 and 30.5-cm ballast depths, but there was a significant reduction in rail deflection and subgrade stress and strain when the 61.0-cm ballast depth was used. The pertinent results are summarized in Table 2.

The effect of the depth of ballast when 57-kg/m rail was used is summarized in Table 3. The trends in the responses are similar to those for the 68-kg/m rail. The rail moment remains relatively constant for the 20.3 and 30.5-cm depths of ballast. The 61.0-cm thick ballast layer tends to transmit the vertical stress on the subgrade more uniformly than do the thinner ballast layers for both of the types of rail considered.

To evaluate the effect of using a stabilized-soil layer, similar analyses were conducted for the 68-kg/m rail and the three depths of ballast, but with a 15.2-cm (6 in) layer of stabilized-soil subballast having a constant modulus value of 345 MPa (50 000 lbf/in^2) incorporated into the sections. The results are summarized in Table 4. The use of the stabilized-soil layer tends to minimize the differences in the structural responses caused by changes in the ballast depth.

Table 4. Responses of sections incorporating stabilized subballast with depth of ballast as variable (68 kg/m rail).

Response	Depth of Ballast (cm)		
	20.3	30.5	61.0
Maximum rail deflection, mm	1.8	1.8	1.8
Maximum rail moment, kN·m	28.2	27.1	27.5
Maximum ballast vertical stress, kPa	566.8	595.7	635.0
Maximum subgrade vertical stress, kPa	138.6	129.6	102.0
Maximum subgrade vertical strain	0.000 79	0.000 71	0.000 48

Note: 1 mm = 0.039 in, 1 kN·m = 8820 lbf·in, and 1 kPa = 0.145 lbf/in^2.

Table 5. Responses of sections with type of subballast as variable.

Response	Failure Criteria Used				No Failure Criteria Used		
	None	Stabilized Soil (E = 345 MPa)	Stabilized Soil (E = 6900 MPa)	Sandy	None	Stabilized Soil (E = 345 MPa)	Stabilized Soil (E = 6900 MPa)
Maximum rail deflection, mm	2.5	1.8	1.5	2.0	1.8	1.5	1.5
Maximum rail moment, kN·m	33.6	27.1	23.6	28.4	27.1	26.0	23.5
Maximum ballast vertical stress, kPa	788.1	595.7	537.8	738.5	369.5	406.8	477.8
Maximum subgrade vertical stress, kPa	182.0	129.6	122.7	138.6	135.1	121.3	122.0
Maximum subgrade vertical strain	0.001 15	0.000 71	0.000 42	0.000 77	0.000 75	0.000 63	0.000 40

Note: 1 mm = 0.039 in, 1 kN·m = 8820 lbf·in, and 1 kPa = 0.145 lbf/in^2.

Table 6. Responses of sections with depth of stabilized subballast as variable.

Response	Depth of Subballast (cm)					
	Failure Criteria Used			No Failure Criteria Used		
	0	15.2	30.5	0	15.2	30.5
Maximum rail deflection, mm	2.5	1.8	1.8	1.8	1.5	1.5
Maximum rail moment, kN·m	33.6	27.1	27.7	27.1	26.0	25.0
Maximum ballast vertical stress, kPa	788.1	595.7	608.1	369.5	406.8	430.2
Maximum subgrade vertical stress, kPa	182.0	129.6	113.8	135.1	121.3	110.3
Maximum subgrade vertical strain	0.001 15	0.000 71	0.000 57	0.000 75	0.000 63	0.000 50

Note: 1 mm = 0.039 in, 1 kN·m = 8820 lbf·in, and 1 kPa = 0.145 lbf/in^2.

Figure 5. Bounds for resilient-response curves for fine-grained soils used in study.

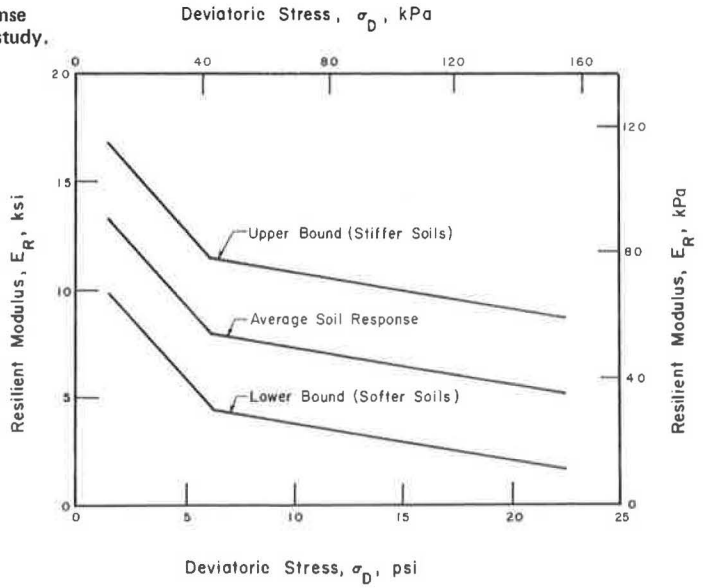

Variable: Type of Subballast

The materials normally used as subballasts are lower quality granular materials (usually used as a filter layer) or stabilized soils. The thicknesses of subballast commonly used range from about 15 to 31 cm. The following types were evaluated (1 MPa = 145 lbf/in^2):

Section	Description
1 (reference)	No subballast
2	15.2-cm deep stabilized soil layer, constant E = 345 MPa
3	15.2-cm deep stabilized soil layer, constant E = 6900 MPa
4	15.2-cm deep sandy subballast, E_R $6700\theta^{0.36}$

The effect of type of subballast is shown in Table 5. The inclusion of a stabilized soil layer has a significant effect on the structural response of the track support system. The rail deflections and moments are reduced, and the vertical stress is uniformly transmitted to the subgrade. The section with no subballast has localized zones of high vertical stresses at the subgrade surface under the tie below the wheel load. The slab-type behavioral mechanism of the stiffer stabilized layer tends to minimize the development of tensile stresses and the dilation tendency within the ballast layer, which allows the ballast material to achieve higher moduli values. There is also a significant reduction in the vertical strain at the surface of the subgrade in the stabilized layer sections. The responses with and without the use of ballast failure criteria are similar for sections with stabilized-soil layers.

Variable: Depth of Subballast

The following depths of stabilized subballast having a constant E-value of 345 MPa were evaluated (1 cm = 0.39 in):

Section	Depth (cm)
1 (reference)	No subballast
2	15.2
3	30.5

The effect of the depth of the stabilized subballast is shown in Table 6. The use of a 15.2-cm stabilized-soil layer greatly improves the structural response of the track support system. However, except for a reduction in the subgrade strain, there was no appreciable difference in the responses of sections with 15.2 and 30.5-cm stabilized soil layers.

Variable: Subgrade

The subgrade is one of the most variable of the components of a track support system. The resilient response of fine-grained subgrade soils primarily depends on the type of soil and its degree of saturation, volumetric water content, compaction, and stress state.

Typical average, upper bound, and lower bound resilient-response curves for fine-grained soils are shown in Figure 5 (15). The upper bound response corresponds to stiffer (stronger) soils, and the lower bound response corresponds to softer (weaker) soils. The following stiffnesses of soils were evaluated:

Section	Stiffness
1	Softer
2 (reference)	Average
3	Stiffer

The effect of subgrade stiffness is shown in Table 7. Comparison of the rail deflections for the three subgrade soils indicates that the resilient response of the subgrade has a substantial effect. Although the vertical subgrade stresses tend to be similar in all three cases, the softer subgrade will also have a lower shear strength and a lower resistance to the accumulation of permanent deformation with repeated-load applications. The analysis without the use of failure criteria indicates that as the support system becomes stiffer, the maximum ballast vertical stress increases. When the subgrade becomes stiffer, the maximum subgrade vertical stress also increases. This can be attributed to the fact that as the track support system becomes stiffer, there is less rail deformation, and the wheel loads are distributed to fewer ties.

Variable: Rail

There are many types of rails currently in use in the United States. Rail weights usually range from 57 kg/m (115 lb/yd) for lines with light traffic density to 70 kg/m (140 lb/yd) for lines with heavy traffic density. For this study, the following types of rail were evaluated (1 kg/m = 2.0 lb/yd and 1 cm^4 = 0.023 in^4):

Section	Linear Mass (kg/m)	Moment of Inertia (cm^4)
1	57	2730
2	66	3671
3	68	3950

The effect of type of rail is shown in Table 8. The responses of the track support system are similar for the 66 and 68 kg/m rails. The maximum rail deflection and the maximum rail moment of the 57 kg/m rail are slightly lower than those of the 66 and 69 kg/m rails. This probably indicates that for a well-maintained track, the type of rail has minimal influence on the transient response of the track support system. Although the rail moments of stiffer rails are larger, the maximum tensile rail stress is almost constant when ballast failure criteria are used and decreases from 70 MPa^2 (10 200 lbf/in^2) for the 57 kg/m rail to 58 MPa^2 (8500 lbf/in^2) for the 69 kg/m rail when ballast failure criteria are not used.

Variable: Tie Spacing

Normal tie spacings for CRTSSs in the United States range from 50.8 cm to 61.0 cm. In this study, the following tie spacings were evaluated (1 cm = 0.39 in):

Section	Tie Spacing (cm)
1	50.8
2	61.0
3	76.2

The responses of the three tracks to the loading of 133-kN (30 000 lbf) wheel loads are summarized in Table 9. The effect of tie spacing is twofold. Closer spacing leads to an increase in the overlapping effects of adjacent ties in the ballast and the subgrade, but smaller tie reactions at each tie. An increase in the tie spacing leads to a decrease in the overlapping effects in the ballast and the subgrade, but larger tie reactions. Thus, when the tie spacing is small, the overlapping effects of adjacent ties dominate, while when the tie spacing is larger, the effects of individual tie reactions dominate the response under the ties. Nevertheless, the overall effect of an increase in tie spacing is to produce more severe responses in the track support system. An in-

Table 7. Responses of sections with stiffness of subgrade as variable.

Response	Failure Criteria Used			No Failure Criteria Used		
	Softer	Average	Stiffer	Softer	Average	Stiffer
Maximum rail deflection, mm	3.0	2.5	2.0	2.3	1.8	1.5
Maximum rail moment, kN·m	34.9	33.6	32.4	29.0	27.1	25.9
Maximum ballast vertical stress, lbf/in^2	637.1	788.1	725.4	348.2	369.5	389.6
Maximum subgrade vertical stress, lbf/in^2	168.2	182.0	171.0	128.2	135.1	144.1
Maximum subgrade vertical strain	0.001 30	0.001 15	0.000 80	0.001 00	0.000 75	0.000 61

Note: 1 mm = 0.039 in, 1 kN·m = 8820 lbf·in, and 1 kPa = 0.145 lbf/in^2.

Table 8. Responses of sections with type of rail as variable.

Response	Type of Rail (kg/m)					
	Failure Criteria Used			No Failure Criteria Used		
	57	66	68	57	66	68
Maximum rail deflection, mm	2.3	2.5	2.5	1.8	1.8	1.8
Maximum rail moment, kN·m	25.6	31.7	33.6	25.3	26.7	27.1
Maximum ballast vertical stress, kPa	649.5	791.5	788.1	392.3	375.1	369.5
Maximum subgrade vertical stress, kPa	182.0	183.4	182.0	140.0	136.5	135.1
Maximum subgrade vertical strain	0.000 94	0.001 16	0.001 15	0.000 83	0.000 77	0.000 75

Note: 1 mm = 0.039 in, 1 kN·m = 8820 lbf·in, and 1 kPa = 0.145 lbf/in^2.

Table 9. Responses of sections with tie spacing as variable.

Response	Tie Spacing (cm)					
	Failure Criteria Used			No Failure Criteria Used		
	50.8	61.0	76.2	50.8	61.0	76.2
Maximum rail deflection, mm	2.5	2.8	3.3	1.8	2.0	2.3
Maximum rail moment, kN·m	33.6	30.4	34.6	27.1	27.8	29.9
Maximum ballast vertical stress, kPa	788.1	599.9	842.6	369.5	398.5	466.1
Maximum subgrade vertical stress, kPa	182.0	151.0	193.7	135.1	142.0	146.1
Maximum subgrade vertical strain	0.001 15	0.001 08	0.001 40	0.000 75	0.000 85	0.000 95

Note: 1 mm = 0.039 in, 1 kN·m = 8820 lbf·in, 1 kPa = 0.145 lbf/in^2.

Table 10. Responses of sections with wheel loads as variable.

Response	Wheel Load (kN)						
	Failure Criteria Used				No Failure Criteria Used		
	89	133	267	356	89	133	267
Maximum rail deflection, mm	1.5	2.5	6.4	8.9	1.0	1.8	4.1
Maximum rail moment, kN·m	20.2	33.6	67.3	91.3	17.7	27.1	55.1
Maximum ballast vertical stress, kPa	357.9	788.1	899.8	1210.1	251.7	369.5	732.2
Maximum subgrade vertical stress, kPa	106.8	182.0	304.8	385.4	93.1	135.1	265.4
Maximum subgrade vertical strain	0.000 48	0.001 15	0.002 00	0.002 79	0.000 47	0.000 75	0.001 60

Note: 1 mm = 0.039 in, 1 kN·m = 8820 lbf·in, and 1 kPa = 0.145 lbf/in^2.

crease in tie spacing leads to an increase in rail deflection and moment, an increase in ballast vertical stress, and an increase in subgrade vertical stress and strain.

Variable: Loading

The four wheel loads shown below were evaluated (1 kN = 224 lbf):

Section	Wheel Load (kN)
1	89
2	133
3	267
4	356

The effect of loading is shown in Table 10. Increases in the wheel load lead to increasingly detrimental responses of the track support system. For example, an increase from 89 kN (20 000 lbf) to 267 kN (60 000 lbf) increases the maximum rail deflection and the maximum subgrade vertical strain by a factor of more than four and the maximum rail moment and the maximum subgrade vertical stress by factors of about three. The increase in rail moment with increased loading is significant because it can lead to earlier rail failures due to fatigue.

Variable: Number of Missing Ties

The effects of missing or hanging ties on the response of the following systems were evaluated:

Section	Ties Missing
1 (reference)	0
2	1
3	2 in a row
4	3 in a row

These sections are illustrated in Figure 6. Figure 7 shows the deflection profile of the ballast surface relative to that of the rail, demonstrating the detrimental effect of missing ties. In a normal track section without missing ties, this relative displacement of ballast particles is small, but when there are missing ties, it is greatly accentuated. The significance of this can be realized if the permanent deformation characteristics of the open-graded ballast-aggregate matrix are considered. The overall strain of an aggregate mass is a result of the deformation of individual particles and of

the relative sliding between the particles. In an open-graded aggregate matrix, the portion of the strain due to the sliding tends to dominate, especially at higher values of σ_1/σ_3. The relative sliding between aggregate particles is largely irreversible, and thus the deflection profile of the ballast surface (Figure 7) that develops due to missing ties can lead to a loss of alignment in the ballast surface at a faster rate and result in poorly performing track.

These results also show that an increase in the number of adjacent missing ties results in an increase in the maximum rail deflection, the maximum subgrade vertical strain, and the maximum tie reaction.

DISCUSSION OF RESULTS

In this design parameter study, it was assumed that all sections considered were properly maintained sections, i.e., there were no gaps between rail and tie or between tie and ballast. Firm seating was assumed of the rail on the tie and of the tie on the ballast; this factor must be considered when interpreting the results of the study.

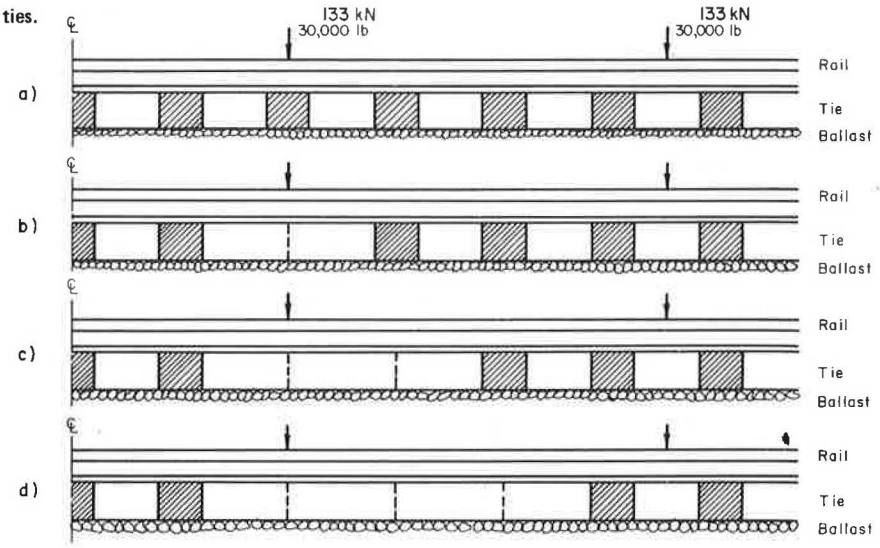

Figure 6. Sections with missing ties.

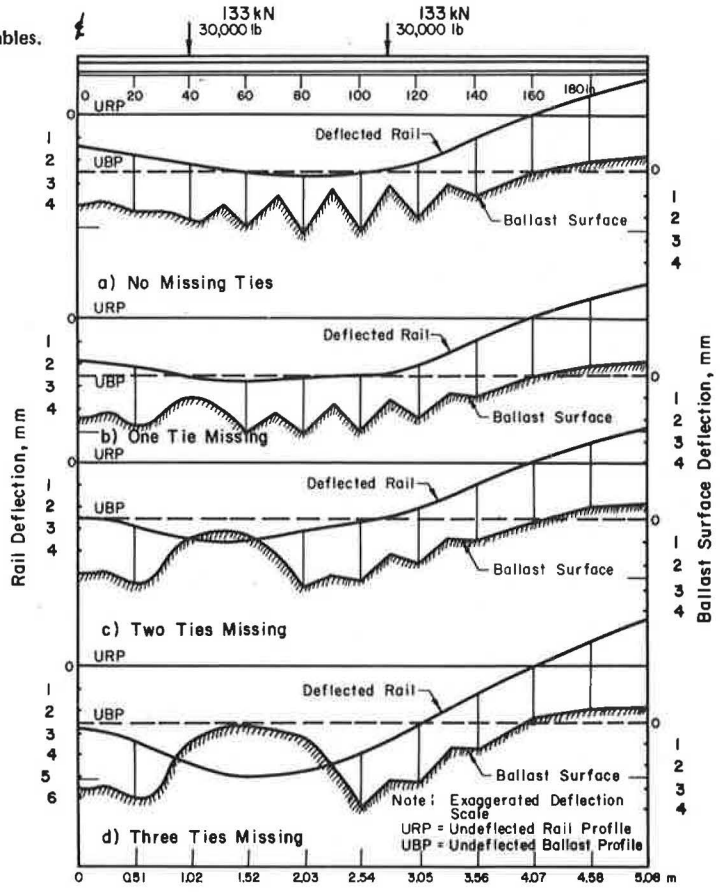

Figure 7. Deflection profiles of sections with missing ties as variables.

Use of the failure criteria for ballast leads to generally more detrimental responses, and the magnitude as well as the distribution of pressure in the ballast layer is affected. When the ballast failure criteria are not used, the responses of the track support system are less detrimental, and the trend of them is as expected.

Basically, the stiffness of a CRTSS is derived from two sources—the rail subsystem and the foundation subsystem, which includes the ballast, the subballast, and the subgrade. The variability in the stiffness of the foundation subsystem has less effect on the response of the CRTSS when the stiffness of the rail subsystem is high (i.e., the 68 kg/m rail). Thus, the use of a stiffer rail might be advantageous for a poorly maintained track with substantial foundation subsystem variability and poorly maintained ties.

The primary response of a CRTSS is not very dependent on the type of ballast used: The E_R versus θ resilient-response curves for most ballasts lie in a very narrow band (18). Thus, standardized E_R versus θ resilient-response curves for the various types of ballast could be used in analyzing the primary response of a CRTSS.

However, the long-term behavior of ballast under repeated (traffic) loading and changing environmental conditions is significantly dependent on the type of ballast, and this should be considered when evaluating different ballast types.

The effect of a variable foundation subsystem can be reduced by using a stabilized subballast. This type of subballast aids in distributing the load more uniformly on the subgrade and maintains the ballast-aggregate matrix in a more confined state, which allows the ballast to develop higher stiffness.

The development of stiffness at the bottom of the ballast layer is very much dependent on the stiffness of the underlying layer (19). When the ratio of the moduli values of the ballast layer and the layer under it is less than a certain value, a horizontal compressive stress will develop at the bottom of the ballast layer. When that ratio is above a certain value, a horizontal tensile stress will develop at the bottom of the ballast layer. With the use of a stabilized layer, a very low modular ratio can be maintained, which results in the development of a horizontal compressive stress at the bottom of the ballast layer. Thus, the ballast layer can develop higher stiffness; the response of a CRTSS with a stabilized layer is more favorable under traffic loading than is that of a CRTSS without a stabilized layer.

One of the more variable components in a CRTSS is the subgrade. Variation in the subgrade support can result from such conditions as type of soil, moisture content, frost action, and compaction. The variation in the strength of the subgrade soils is one of the most important parameters affecting the response of a CRTSS. Thus, on a given track section with a nonuniform (in terms of stiffness) subgrade, the response due to traffic loading can be very erratic. The desirability of uniform and stable subgrades is apparent.

The results of the study indicate that the type of rail has little effect on the system response of a CRTSS subjected to vertical loading. However, the use of stiffer rail might be advantageous for lateral stability considerations and for a track with substantial variability of the support system.

Increased tie spacing leads to detrimental responses in terms of the maximum rail deflection and the pattern of subgrade vertical stress. Increased tie spacing leads to localized concentration of stress on the subgrade (below the ties).

Over the years, many tracks in the United States have been deteriorating because of increased traffic frequency, heavier wheel loads, and inadequate maintenance. Increased wheel loading leads to an increasingly detrimental response of the CRTSS and results in an early failure of the CRTSS. When increased wheel loading is anticipated on a given line, it is necessary to evaluate the CRTSS to ensure that the response patterns in all of the components (rail, tie, ballast, subballast, and subgrade) are acceptable.

SUMMARY AND CONCLUSIONS

Summary

An acceptable structural analysis of a CRTSS cannot consider it as composed of only rails and ties. A large portion of the structural strength is derived from the ballast, the subballast, and the subgrade—i.e., the ballast, the subballast, and the subgrade also act as load-carrying media. Like other structural materials, the ballast, the subballast, and the subgrade have limiting (or allowable) response patterns. Therefore any analysis of a CRTSS should include the evaluation of the response patterns within all the components.

The mechanistic characterization of the ballast and the subgrade has been achieved by using the results of repeated-load triaxial tests. However, the open-graded nature of the ballast-aggregate matrix, when considered as a part of a CRTSS, does not lend itself to proper simulation in the structural model because the ballast in crib and shoulder areas is in a free state—i.e., it is subject to unrestricted displacement in at least one direction when subjected to loading. In a confined state, ballast has a potential for developing very high stiffness, but in a free state, it can generate very little resistance to loading.

The finite-element model should be considered as an input to a larger model or system for predicting the performance of a CRTSS. Because performance is evaluated with respect to the ability of the CRTSS to fulfill its functional requirements, it is essential to establish performance criteria for the whole system as well as for each subsystem.

Conclusions

The following conclusions were derived from this study:

1. When the developmental state of procedures for material characterization and the lack of availability of pertinent field response data are considered, the ILLITRACK model adequately characterizes the primary response of a CRTSS when subjected to vertical loading.
2. There are a large number of conditions that exist in an actual CRTSS, and it would be impracticable to attempt to satisfy all of them in a theoretical model. In certain cases, the effects of some conditions can be evaluated by using the results of the finite-element model and incorporating them carefully.
3. One of the most critical design factors appears to be that of the interface of the ballast and the subgrade. Ballast laid directly on a low-strength subgrade can be detrimental to the satisfactory performance of a CRTSS. The desirability of a stiff layer (e.g., a stabilized subballast) between the ballast and the subgrade has been demonstrated in this study.
4. The material testing, analysis, and design of a CRTSS should direct special attention to the ballast, the subballast, and the subgrade materials.

ACKNOWLEDGMENT

This paper is based on the results of a ballast and foun-

dation materials research program conducted by the Transportation Research Laboratory of the Department of Civil Engineering, University of Illinois at Urbana-Champaign. The research was sponsored as a subcontract between the Research and Test Department, Association of American Railroads, and the University of Illinois. This subcontract is part of a larger contract that is a cooperative effort between the Federal Railroad Administration and the Association of American Railroads on improved track structures. This paper represents our views and positions and does not necessarily reflect those of the Federal Railroad Administration or the Association of American Railroads.

REFERENCES

1. A. N. Talbot. Stress in Railroad Track. Proc., AREA, Vol. 19, 1918, pp. 873-1062, and Vol. 21, 1920, pp. 645-814.
2. H. C. Meacham and others. Studies for Rail Vehicle Track Structures. Office of High-Speed Ground Transportation, Federal Railroad Administration, Rept. FRA-RT-71-45, April 30, 1970.
3. M. Hetenyi. Beams on Elastic Foundations. Univ. of Michigan Press, 1946.
4. R. H. Prause and others. Assessment of Design Tools and Criteria for Urban Rail Track Structures: Vol. 1, At-Grade Tie-Ballast Track. Office of Research and Development, Urban Mass Transportation Administration, Rept. UMTA-MA-06-0025-74-3, April 1974.
5. L. Barden. Distribution of Contact Pressure Under Foundations. Geotechnique, Vol. 13, No. 3, Sept. 1962.
6. H. B. Harrison. General Computer Analysis of Beams on Elastic Foundations. Proc., Institute of Civil Engineers, London, Vol. 55, Pt. 2, Sept. 1973.
7. Y. K. Cheung and D. K. Nag. Plates and Beams on Elastic Foundations: Linear and Nonlinear Behavior. Geotechnique, Vol. 18, No. 2, 1968.
8. F. S. Rostler and others. Study of Methods of Stabilizing Conventional Ballast Using Polymers. Materials Research and Development, Oakland, CA, Dec. 1966.
9. H. O. Ireland. Railroad Subgrade Stresses. Proc., AREA, Vol. 75, Bull. 641, Jan.-Feb. 1973.
10. Construction and Maintenance Operations. Proc., AREA, Vol. 75, Bull. 645, Nov.-Dec. 1973.
11. J. R. Lundgren and others. A Simulation Model of Ballast Support and the Modulus of Track Elasticity. Civil Engineering Studies, Transportation Engineering Series 4, Univ. of Illinois, Urbana-Champaign, Sept. 1970.
12. O. J. Svec and others. Analytical and Experimental Investigation of a Rail Track Structure. Paper presented at the Second Symposium on Applications of Solid Mechanics, McMaster Univ., Hamilton, Ontario, June 17-18, 1974.
13. S. W. Fateen. A Finite-Element Analysis of Full-Depth Asphalt Railway Track. Univ. of Maryland, College Park, MS thesis, 1972.
14. H. B. Seed and others. Prediction of Flexible Pavement Deflections from Laboratory Repeated-Load Tests. NCHRP, Rept. 35, 1964.
15. M. R. Thompson and Q. L. Robnett. Resilient Properties of Subgrade Soils. Civil Engineering Studies, Transportation Engineering Series 14 and Illinois Cooperative Highway and Transportation Series 160, Univ. of Illinois, Urbana-Champaign, June 1976.
16. J. M. Duncan, C. L. Monismith, and E. L. Wilson. Finite-Element Analysis of Pavements. HRB, Highway Research Record 228, 1968.
17. S. D. Tayabji. Considerations in the Analysis of Conventional Railway Track Support Systems. Univ. of Illinois, Urbana-Champaign, PhD thesis, 1976.
18. R. Knutson. Factors Influencing the Repeated-Load Behavior of Railway Ballast. Univ. of Illinois, Urbana-Champaign, PhD thesis, 1976.
19. W. Heukelom and T. J. G. Klomp. Road Design and Dynamic Loading. Proc., AAPT, Vol. 33, Feb. 1964, pp. 92-125.

**Dr. Tayabji was at the University of Illinois when this work was performed.*

Improvement in Rail Support

Gerald Patrick Raymond, Department of Civil Engineering, Queen's University, Canada

An on-going investigation on rail support material is briefly summarized. Static and repeated-load triaxial compression and extension tests on a dolomite ballast are reported, and their significance to track design is discussed. Model tests using static and repeated loading on a small scale with Ottawa sand as a foundation material and on a large scale with rail track, ballast, subballast, and sandy subgrade were made, and the significance to tie and track design of their results is discussed.

The replacement and upkeep of fills and tracks cost Canadian railways an estimated $100 000 000 annually, of which about 40 percent is spent for the procurement, distribution, and rehabilitation of ballast. The potential savings that would accrue from research and the better use of track-support materials is therefore very large. A complete assessment of the economic importance of ballast in policies and practice, however, should include the costs of derailments and of the restricted speed and other delays caused by deteriorating track support.

The Canadian railways are at present mainly freight carriers, but as high-speed passenger trains are developed and put into service, the length of track traveled per vehicle will increase, and the technical and financial requirements of the track will tend to dominate these costs. Despite this, in comparison with the research effort devoted to such items as control systems, switching, and guidance systems, there has been little research devoted to track design. It is not surprising then that the Canadian Institute of Guided Ground Trans-

port requested a feasibility study on the types of research that are needed in the track-support area in 1969.

The first efforts of this study were concentrated in the area of ballast selection and have been reported elsewhere (1, 2, 3, 4). This paper will discuss certain aspects of the work in relation to track design.

TRIAXIAL ONE-CYCLE TESTS OF RAILROAD BALLAST

Two properties have been found to have a dominant effect on the performance of a ballast under load. The first is the hardness of the ballast, which is sometimes difficult to assess because ballast is composed of different minerals of different hardnesses, and the second is the toughness of the ballast, which is best measured by the crushing-value test. Another property of importance is the ability of the ballast to resist chemical weathering. Four materials were selected for study, (a) a dolomite with a Mohr's hardness of 3.5 to 4, which is relatively soft, but has a crushing value of 16.4, which indicates a relatively tough material; (b) Sudbury slag, which is hard and tough; (c) Kenora granite, which is hard, but weak and brittle; and (d) marble, which is soft and also weak and brittle. Thus far, extensive testing has been restricted to the dolomite.

Immediately after the maintenance cycle, when the ballast material is in its loosest condition, the major concerns for its performance are its strength against bearing failure and its ability to withstand lateral forces. The ability to resist bearing failure can best be assessed in the laboratory by standard triaxial compression tests. The ability to withstand lateral forces, on the other hand, is best assessed by extension tests. Each of these types of tests has been performed on the dolomite ballast for a variety of different densities. Of the most interest to the track engineer is the performance of the ballast in its densest condition because the effect of the in-track compaction is to place the ballast in as dense a packing as possible. For the compression and extension tests, specimens 0.2 m (9 in) in diameter by 0.45 m (18 in) high were prepared at dry densities varying from 1.4 to 1.7 g/cm^3 (87 lb/ft^3 to 106 lb/ft^3). To ensure uniform density throughout the sample, a precalculated weight of ballast [e.g., 25 kg (55 lb) for a density of 1.4 g/cm^3] was prepared, divided into four equal parts and placed in the specimen preparation mold, which was marked in four equal 0.11-m (4.5-in) increments of height for a total of 0.45 m (18 in). The sample with a dry density of 1.7 g/cm^3 was prepared by a vibratory compaction process, again in four equal increments of height. In every test, the dimensions of the specimen were measured to verify the actual densities. The samples were saturated before removal of the molding forms.

The tests performed on the ballast were constant strain rate, saturated, drained tests. The volume changes were continually monitored by using a large burette connected to the bottom of the specimen. The strain rate was slow enough to prevent any buildup of pore pressure. A cell with a rotating bushing was used. Figure 1 compares the results obtained from compression and extension triaxial tests that used the maximum placement density that could be achieved in the laboratory. This figure shows that the material is considerably stiffer in the extension tests than in the compression tests and that the failure is higher in the compression tests. This is to be expected because in the extension tests, the cell pressure is the major principal stress, but in the compression tests, it is the minor principal stress. Thus, a direct comparison of the strength is rather misleading. Far more realistic is a comparison on a Mohr circle (Figure 2). The failure envelope from the compression tests in Figure 2a is imposed on Figure 2b. Somewhat surprisingly, the failure envelope from the extension tests is considerably less than that from the compression tests. Somewhat surprisingly, because Green (5) had found that for rounded dense sand, the angle of internal friction (ϕ) was greater in extension than in compression, but that for loose sand, there was very little difference between the two values of ϕ. In these results, ϕ is greater in compression than in extension. Green attributed the observed difference in his values of ϕ to anisotropy introduced during the setting-up period. However, the difference is more likely caused by ballast particle packing and shape that, of course, may be related to anisotropy, but is more likely due to random nonhomogeneity.

An alternative method of interpreting the Mohr circle diagrams is to consider each sample a different material and, because ballasts are granular in performance, assume them to be noncohesive. Under such circumstances, the Mohr circle would be represented by a friction angle only. Figure 3 shows a comparison of the compression and extension values of ϕ obtained by such an interpretation and an average line developed by Leps from compression tests on rock fill for earth dams (6). Most of the samples tested by Leps consisted of large-size specimens with particle sizes up to 15.2 cm (6 in). Leps tests were performed at high pressures similar to those occurring in earth dams, but ours were performed at low pressures because the height of ballast in track is small and therefore the confining pressures are small. In particular, the resistance mobilized to prevent the phenomenon known as sun kinks will occur at low confining pressures. From Figure 3, it can be seen that at low pressures, a zero cohesion intercept results in friction angles at failure that are greater than 45°. However, a value of ϕ greater than 45° is meaningless, which means that a considerable portion of the strength at low confining pressures is obtained from interlock forces. Also, crushing and the crushed faces of a ballast will be important; it is not surprising that specifications dealing with railroad ballast specify particles having a high percentage of crushed faces.

The importance of good compaction at low confining stress can be seen from Figure 4, which shows the differences in the triaxial stress at failure obtained for the dolomite ballast. At low cell pressures, the density of placement has an immense effect on the ballast failure resistance. This difference is less significant at higher confining pressures, as when the ballast is subject to the weight of a loaded train. Intermediate confining pressures would result from a lightly loaded or an unloaded train. Proper compaction and the achievement of high densities during maintenance cycles would therefore be valuable in resisting sun kinks and in maintaining the stability on curves of unloaded trains traveling at high speeds. Under heavily loaded trains the high frictional resistance will cause considerable ballast resistance, and the ballast density or good compaction will be of less immediate importance. However, this ignores the possibility of large deformations occurring in the ballast due to a large number of repetitive loads. To assess this, it becomes important to look at the performance of a ballast under repeated loading.

TRIAXIAL REPEATED-LOAD TESTS OF DOLOMITE BALLAST

Triaxial repeated-load strain tests on the dolomite ballast were carried out with different fractions of the difference in the axial stresses at static failure. In both

Figure 1. Results of stress versus strain tests.

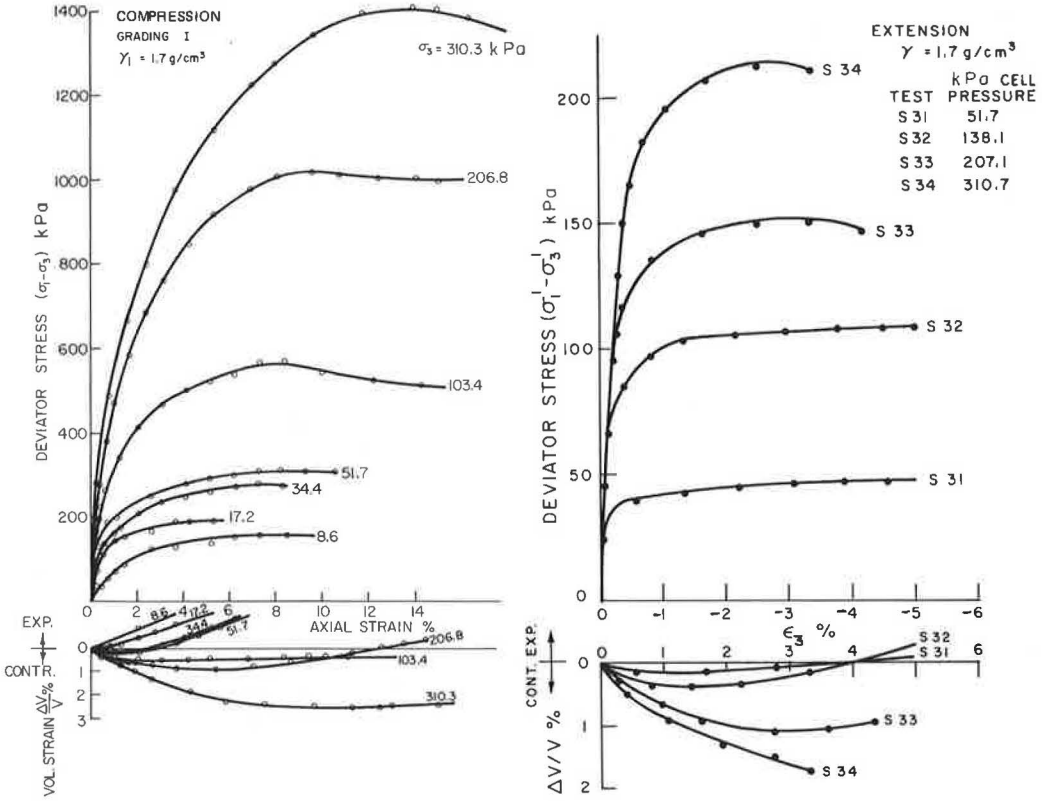

Figure 2. Mohr circles for dense samples.

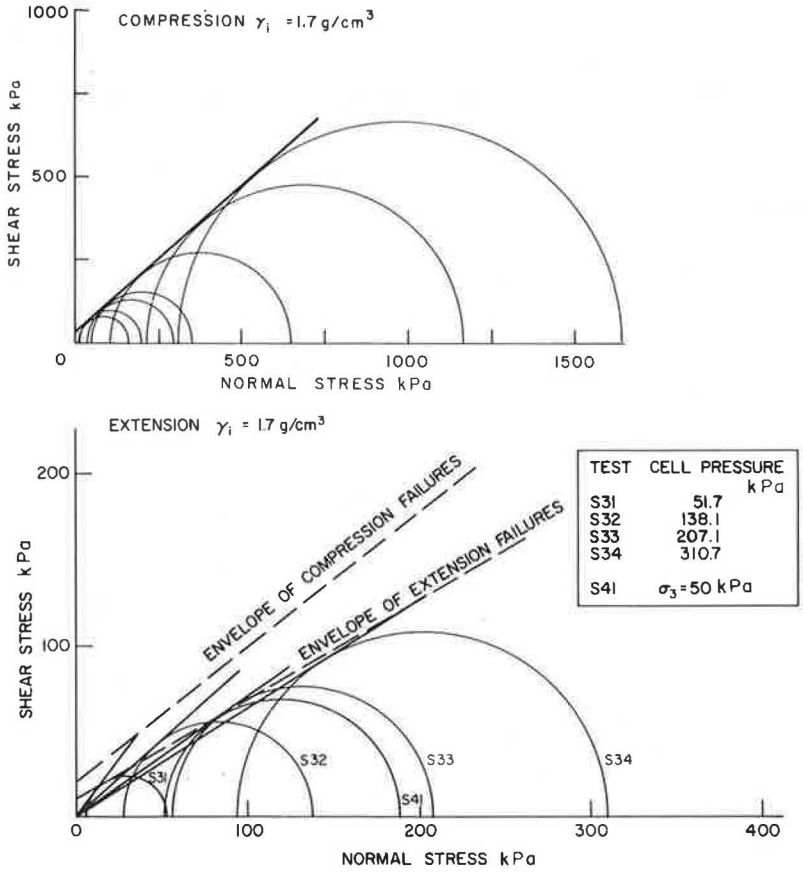

Figure 3. Interpretation of test results representing Mohr circle as friction angle.

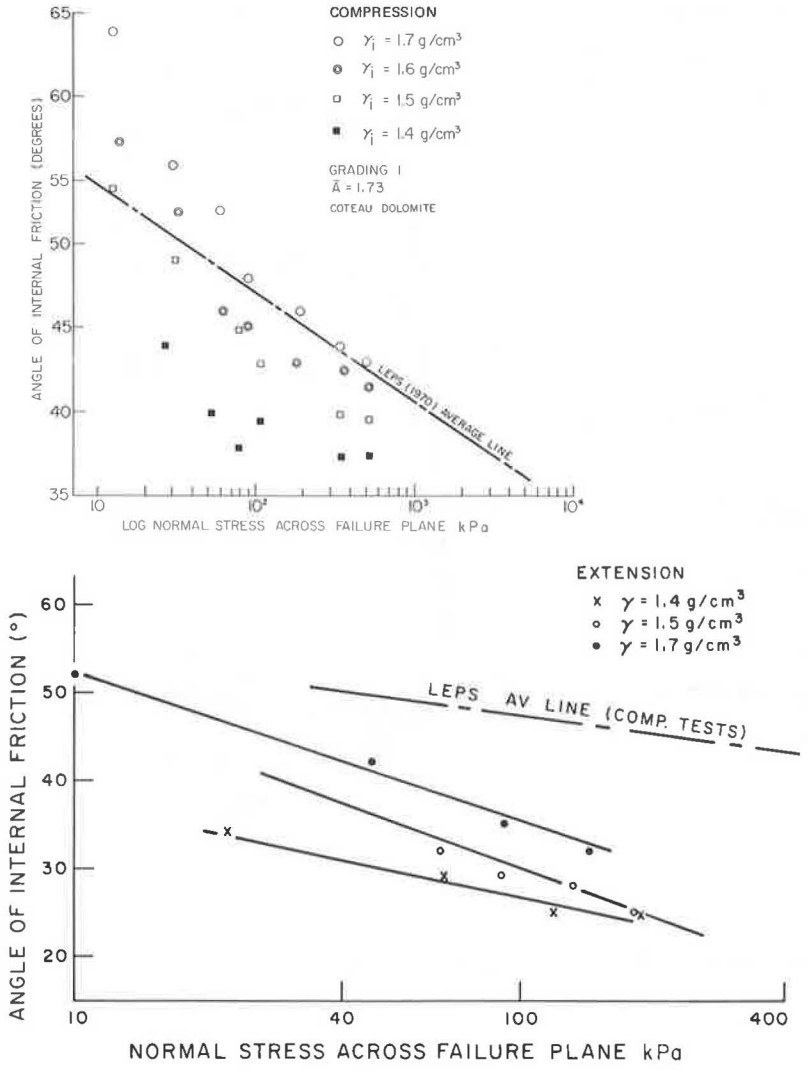

Figure 4. Failure stresses.

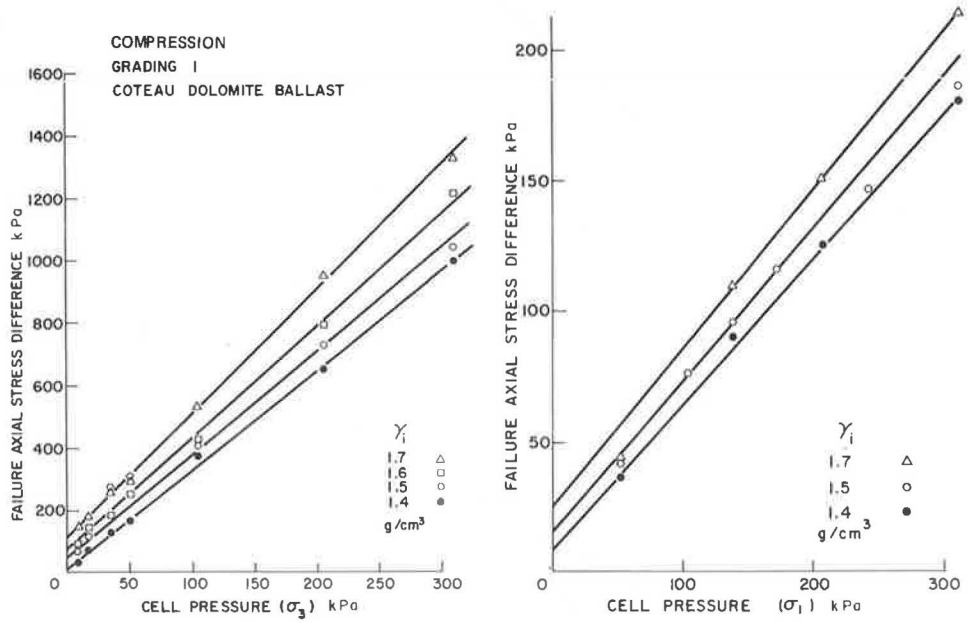

the compression and the extension repeated-load tests, the minor principal stress was maintained constant. Figure 5a shows the results of the plastic axial and volume strains plotted against the logarithm of the number of repeated loads in the compression tests, and Figure 5b shows the same type of plots for the extension tests. As in the static tests, the first cycle of strain is considerably less for the extension test than for the compression test. The slope of the line shown in Figure 5 is an indication of the change in strain per logarithm of the number of the repeated loads. These slopes are shown in Figures 6a and 6b for the compression and extension tests respectively. There is considerable difference in performance between the compression and the extension repeated-load tests. In the compression test, the axial strain is approximately proportional to the fraction of the

Figure 5. Plastic axial strains.

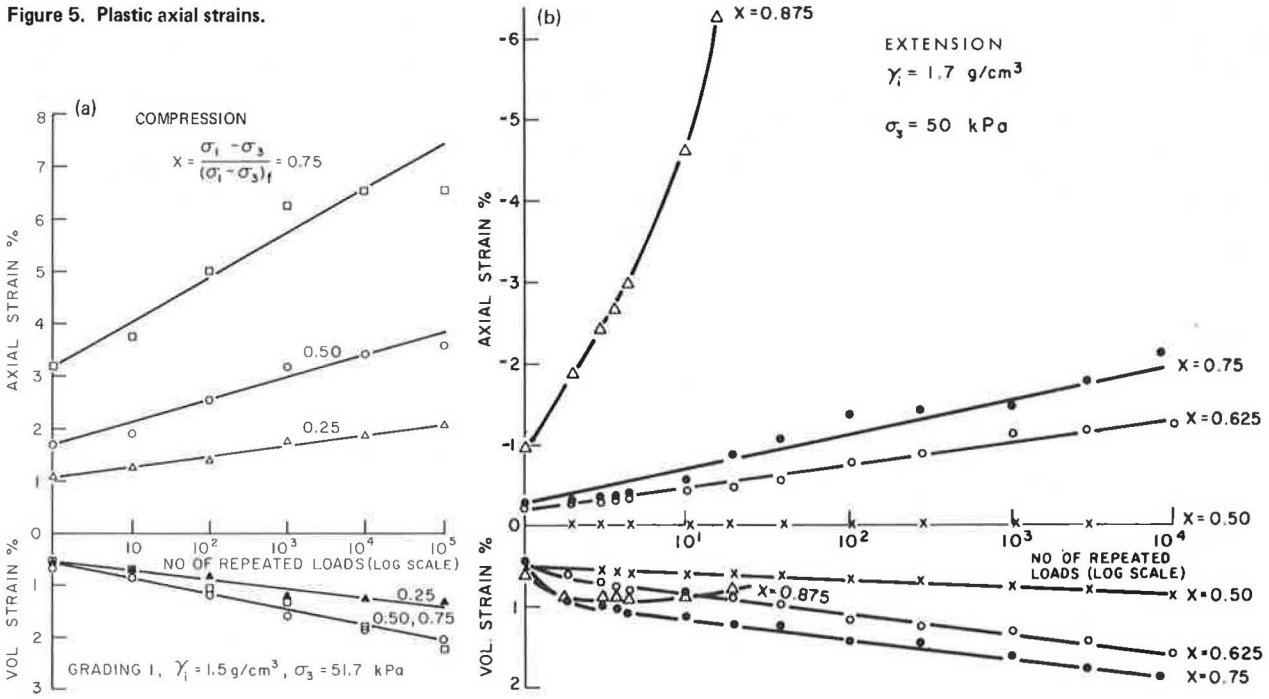

Figure 6. Rates of plastic strain.

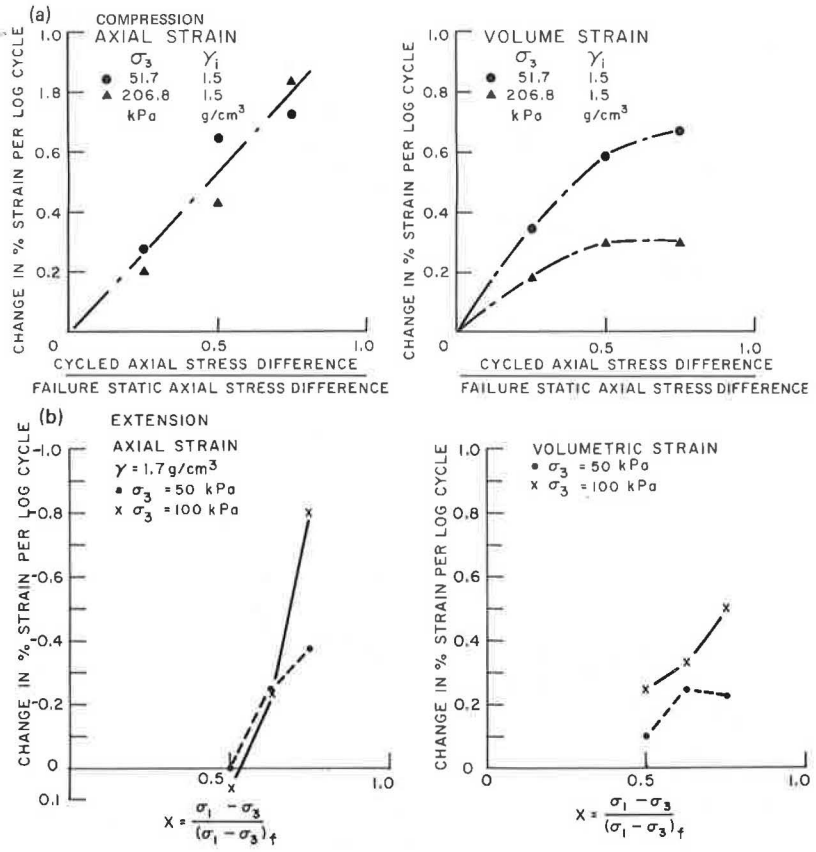

axial-stress difference used, whereas in the extension tests, there is little strain up to a value of about ½, but it then increases rapidly as the stress fraction increases. The axial strain at low stress fractions decreases. If the stress fraction used is constant, the change in axial strain per logarithm of the cycle of repeated load is similar; however, the compression and expansion tests will show different behavior with regard to the volumetric strains. At high values of the minor principal stress, the curve of the volumetric strain versus the logarithm of the number of repeated loads in the compression test is less than that at lower values. The behavior in the extension test is directly opposite. Because the axial strain in the extension test is the minor principal strain, the deduced major principal strain must be calculated from the volumetric and axial strains. It becomes obvious that the rate of change of the major principal strain per logarithm of the number of repeated loads in the extension test, is greater for larger values of the minor principal stress and similar deviator-stress fractions.

Repeating the stress difference causes the ballast to become stiffer. The increase in stiffness of the ballast with repeated loading is shown in Figure 7. The static tests showed that the axial secant modulus in the extension test was larger than that in the compression test, however; Figure 7 shows that, after a large number of repeated loads, the axial secant modulus in the compression test becomes larger than that in the extension test. Furthermore, after a large number of repeated loads, the sample failed in the extension test, but there were no failures in the compression test.

Figure 8 shows the number of repeated loads required to cause failure in the extension test as higher values of the stress fraction were used. As the logarithm of the number of loads increases, the fraction of the repeated-load deviator stress required to cause failure decreases approximately linearly, down to a value of about 0.5. At fractions less than 0.5, failure was not observed after 100 000 cycles of load. Whether failure would have occurred with further loading is unknown—more testing is

Figure 7. Secant moduli.

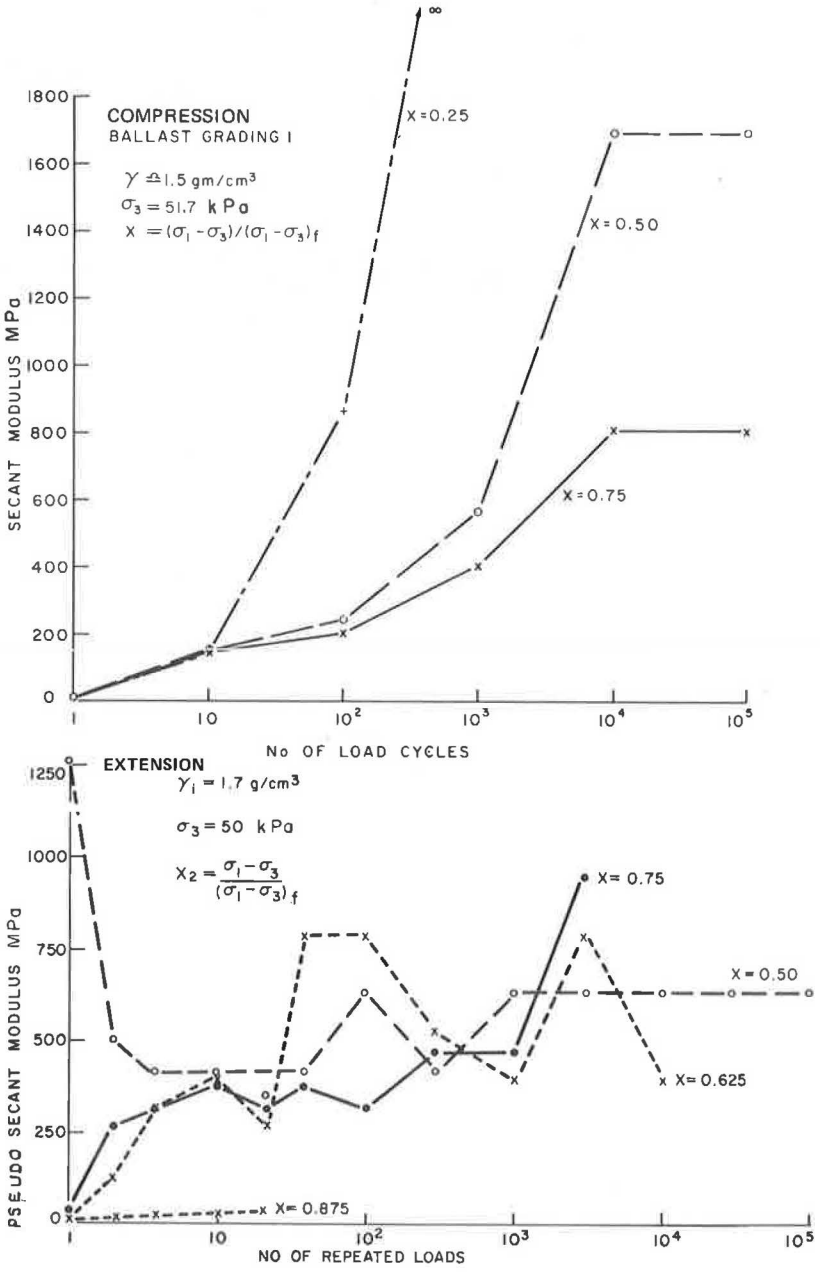

Figure 8. Repeated loads to failure.

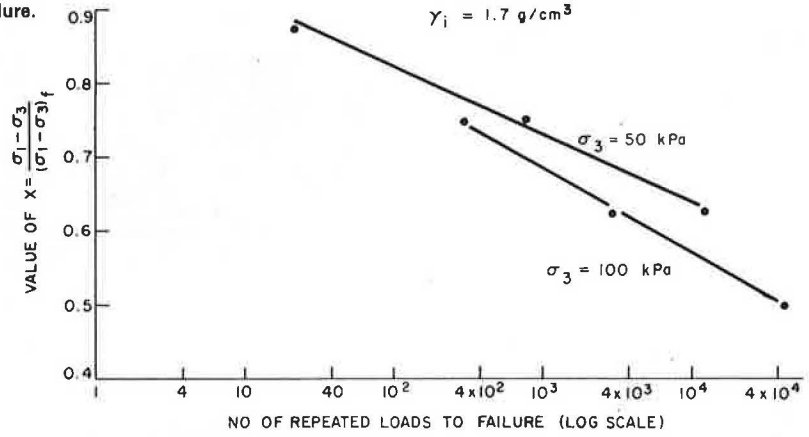

required to clarify this point. Because the change in strain per logarithm of the number of repeated loads for the extension test (shown in Figure 6) is negative at low values of deviator-stress fraction, it is speculated that failure would not occur. If so, then there is a fatigue limit of 0.5 for extension repeated loads for the dolomite ballast.

During the compressive static and repeated loading, the ballast breakdown after testing was measured. The breakdown, recorded as the percentage of the material passing a 4.75-mm (no. 4) sieve, is plotted against the cell pressure for the static test (Figure 9) and against the fraction of the deviator stress used for the repeated loading test (Figure 10). Figure 10 shows that the breakdown increases as the deviator-stress fraction used increases. The results for the static test would be expected to fit onto the relation shown in Figure 10 had the deviator stress been used. In the compression repeated-load test, the minor principal stress appears to have little effect on the relation. From this, it is clear that the higher the shear strength (and thus the density) of the ballast, the better it will perform in service, again showing the importance of good initial compaction.

A number of practical factors can be derived from the triaxial repeated-load tests. First, the practice of using train loads to compact ballast in situ after maintenance seems to be a realistic one because the ballast stiffens as the number of loads increases. Second, if the breakdown is independent of the minor principal stress, then any practical application that causes higher confining pressures will result in better performance because, for the same deviator stress, the factor of safety will decrease. This means that broader ties and smaller ratios of tie spacing to tie breadth would decrease the rates of breakdown and of plastic deformation. If the tie breadth is increased, however, the rate of decrease of stress with depth would decrease so that the depth of ballast might have to be increased. While it is possible to calculate these effects theoretically, caution should be exercised until more knowledge is obtained about the validity of the theories in use. For this reason, model studies have been undertaken to attempt to rationalize the theoretical or semiempirical performance of foundations subject to repeated loads on granular material.

MODEL STUDIES

Model studies have been undertaken on a small scale as shown in Figure 11 and on a large scale as shown in Figure 12. These studies confirmed the evidence that the strength and deformation characteristics of a foundation soil are greatly affected by the repeated application of stresses caused by live loads. These characteristics cannot be predicted satisfactorily by conventional static tests. Our studies used a repeated load that returned to zero at the end of each cycle; this is characteristic of a train wheel load passing over a railroad tie. Of equal importance is the case of a repeated load imposed on a dead load; it is hoped to extend our studies to this in future years. Space limitations do not permit a complete presentation of our work.

Four series of tests were conducted by using the small-scale test apparatus. Series A consisted of static load tests incrementally applied to failure. The results of these tests provided a basis for comparison with subsequent repeated-load tests. Series B consisted of applying repeated loads that varied between zero and an upper limit of 90 percent of the static failure load. The upper limit was constant for any given test but was varied among tests. Series C consisted of repeated-load tests that were a continuation of the series B tests. The foundation soil was not renewed between the series B and the series C tests, and the compaction resulting from the series B tests was left untouched. Only the berms caused by the sinking of the footing during the series B tests were removed before the start of the series C tests. Series D was essentially a repetition of series A on the now-compacted foundation soil; however, the berms thrown up during the series C tests were removed before the series D tests were performed.

Typical plastic vertical deformations observed during repeated loading are plotted against the number of loads on a logarithmic scale in Figure 13. This figure shows that the permanent vertical deformation increased as the number of loads and as the percentage of the static failure load increased. At the end of 100 000 loadings, the vertical settlement was 1.8 mm under 13.5 percent of the static failure load, and 18 mm under 50 percent of the static failure load. This difference of 16.2 mm is primarily due to the repeated loading. The difference after the first loading for the same two tests was only 1.5 mm.

The relation of the plastic deformations and the number of loadings is nonlinear and can be fitted to a hyperbolic equation as is commonly done for modeling stress versus strain triaxial-test results. However, Figure 13 is based on the following modified equation:

$$\text{Log } N = S/(a + bS) \quad (1)$$

where

S = deformation after first loading,
N = number of loadings, and
a and b = experimentally determined constants.

The values of a and b were determined for tests conducted on 75- and 228-mm broad footings. Regression analysis was used to fit these values to the percentage of the static failure load used and to the footing breadth. The equations resulting from these fits are

$$a = -0.151 + 0.000\,069\,B^{1.18}(F + 6.09) \quad (2)$$

and

$$b = 0.154 + 0.000\,036\,B^{0.82}(F - 23.1) \quad (3)$$

where F = percentage of failure load used and B = footing width (mm). Equation 3 indicates that the strength in terms of excessive deformation does not vary in proportion to the footing breadth squared, which is the well-known result for static loading of a footing on granular soil. The strength increases, however, at a greater rate than does the breadth of the footing. Thus, under

Figure 9. Breakdown in one-cycle compression tests.

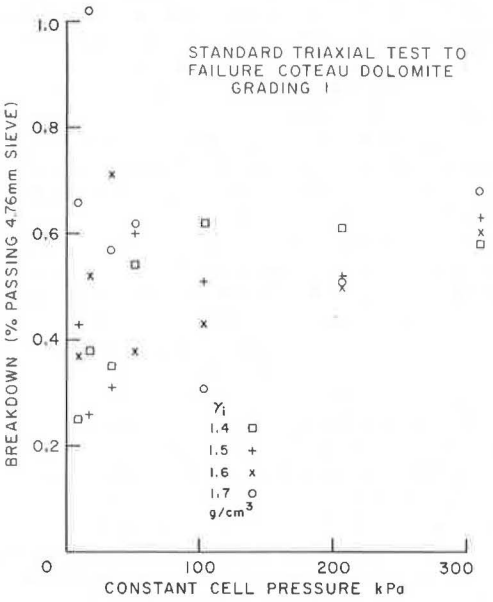

Figure 10. Breakdown in repeated-load compression tests.

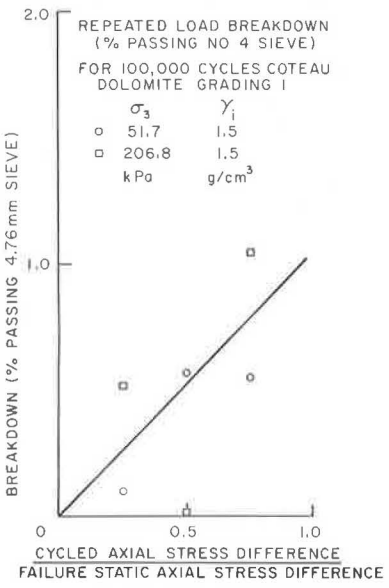

Figure 11. Small-scale planar strain model equipment.

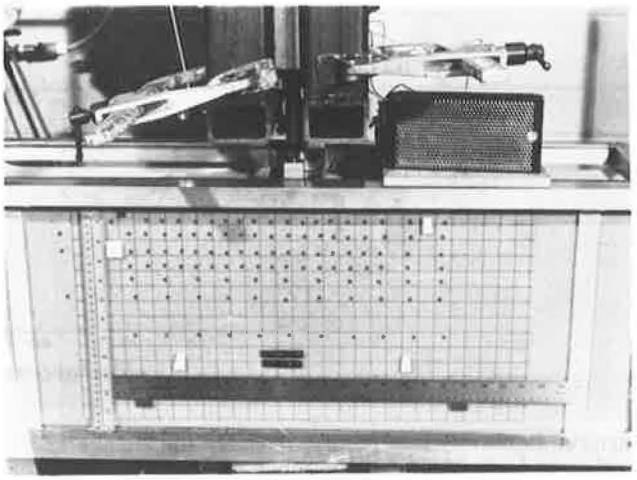

Figure 12. Full-scale model equipment.

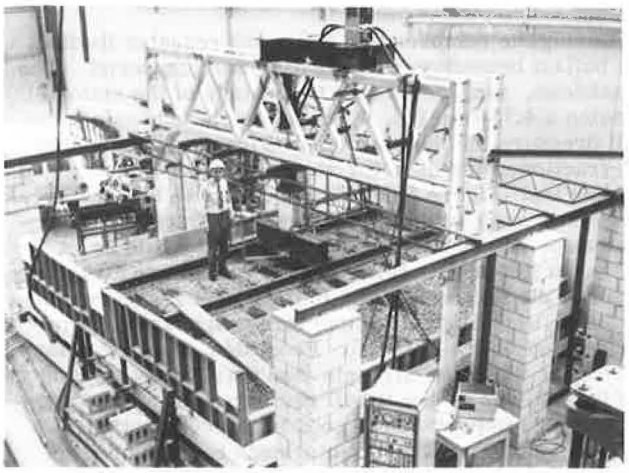

Figure 13. Deformations in small-scale planar strain tests.

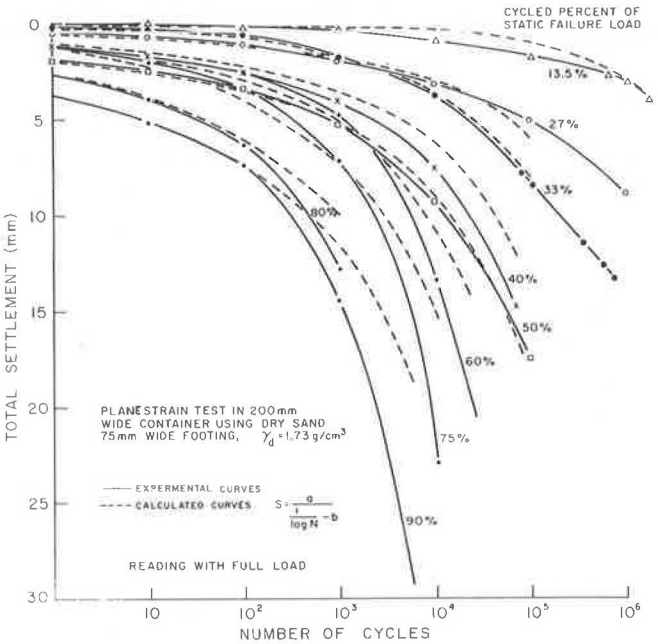

Figure 14. Rebound deformations in small-scale planar strain tests.

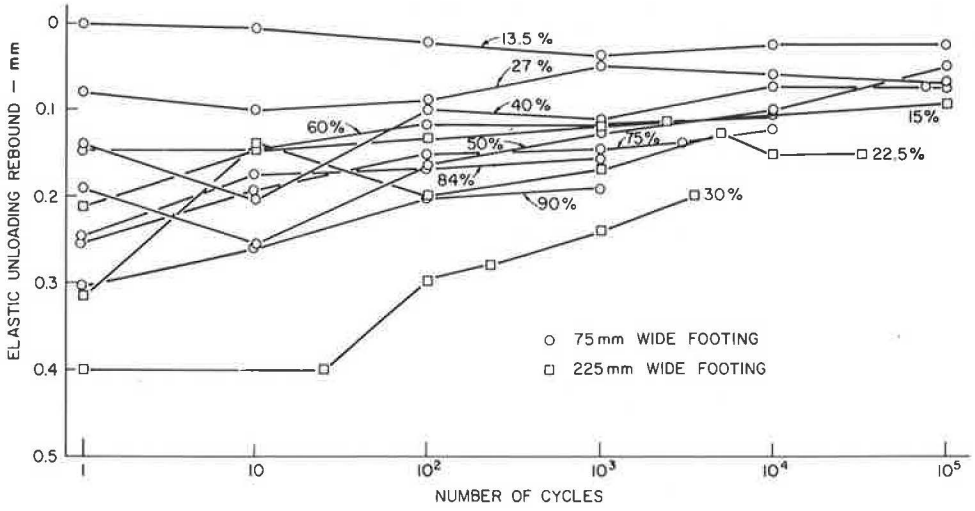

Figure 15. Average contact pressure: rebound results for small-scale planar strain tests.

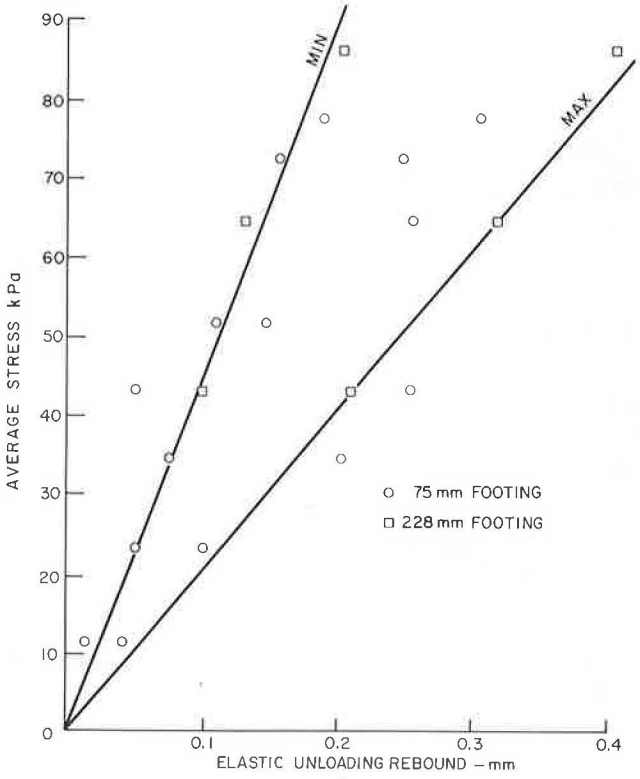

repeated loading, a broad footing loaded with an equal pressure will deform less than a narrow footing.

Figure 14 shows typical rebound readings recorded under 75 and 228-mm broad footings at different percentages of their failure loads. The failure load of the larger footing would be approximately nine times greater than that of the smaller footing. As the number of loadings increases, the rebound deformation decreases, as is to be expected, because repeated loading causes an increase in the soil density. The rebound from the first loading was neglected, because of the possibility of a rough initial sand surface, and the minimum and maximum deformations were selected. Typical values are plotted against the average footing contact pressure in Figure 15. While the maximum values for the smaller footing show some scatter, the minimum values approximate a straight line. The scatter of the maximum values would seem to occur with the nonuniformity of placement. Only after complete bedding down under many loadings does the sand tend to act in conformity with the Winkler foundation concept of a constant deformation modulus. Even so, Figure 14 indicates that the rebound under the larger footing is decreasing, while that for the smaller footing is almost constant. This means that if the loadings were continued, the foundation rebound for the larger footing would decrease, which would make the foundation rigidity for the larger footing greater than that for the smaller footing. Another advantage of the larger footing is that it has a three times larger average contact stress for the same percentage of failure load.

Confirmation of these conclusions and observations is being sought from the full-scale tests. It is also possible to measure the pressure distribution within the track bed. A set of pressure distributions for a single tie is shown in Figure 16. After relatively few applications of the load, the vertical pressures registered beneath the centerline of the loaded tie began to increase, but the vertical pressures measured beneath the rails decreased. This phenomenon was also observed for an 11-tie test and is associated with center binding.

If the load had been evenly distributed over the contact surface of the interface between the tie and the ballast, the average contact pressure would have been 371 kPa. At 100 loadings, the maximum pressure under the rail was about 60 percent greater than the average value. After 1 000 000 loadings, the pressure under the centerline, however, was about 20 percent greater than the average.

Figure 17 shows, for three of the dial gauges on the tie, the deformations for the single tie and its foundation after various numbers of loadings. In each case, the plastic deformations from previous loadings have been deducted. Thus, each loading curve starts from zero. After the first loading, the deformation curves at the rail and the free end do not fit smoothly through the origin. If a linear relation was fitted to the higher load readings, a considerable gap would exist at zero load. This is consistent with the pressure readings and with the phenomenon of center binding already mentioned.

Figure 16. Pressures below single tie (full-scale test).

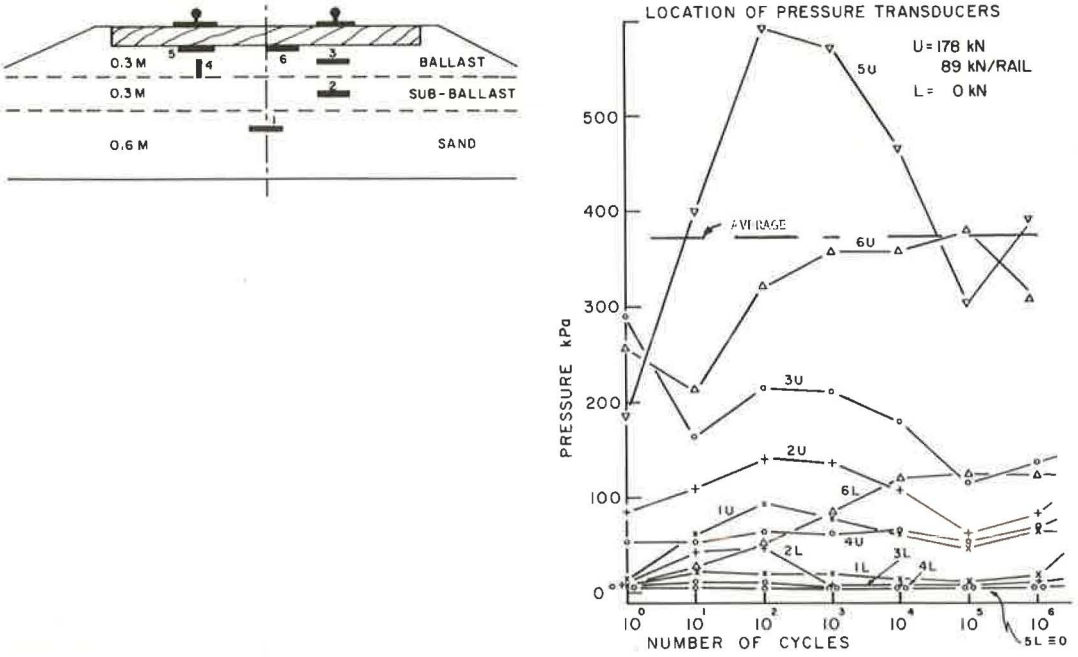

Figure 17. Deformations of top of tie (single-tie test).

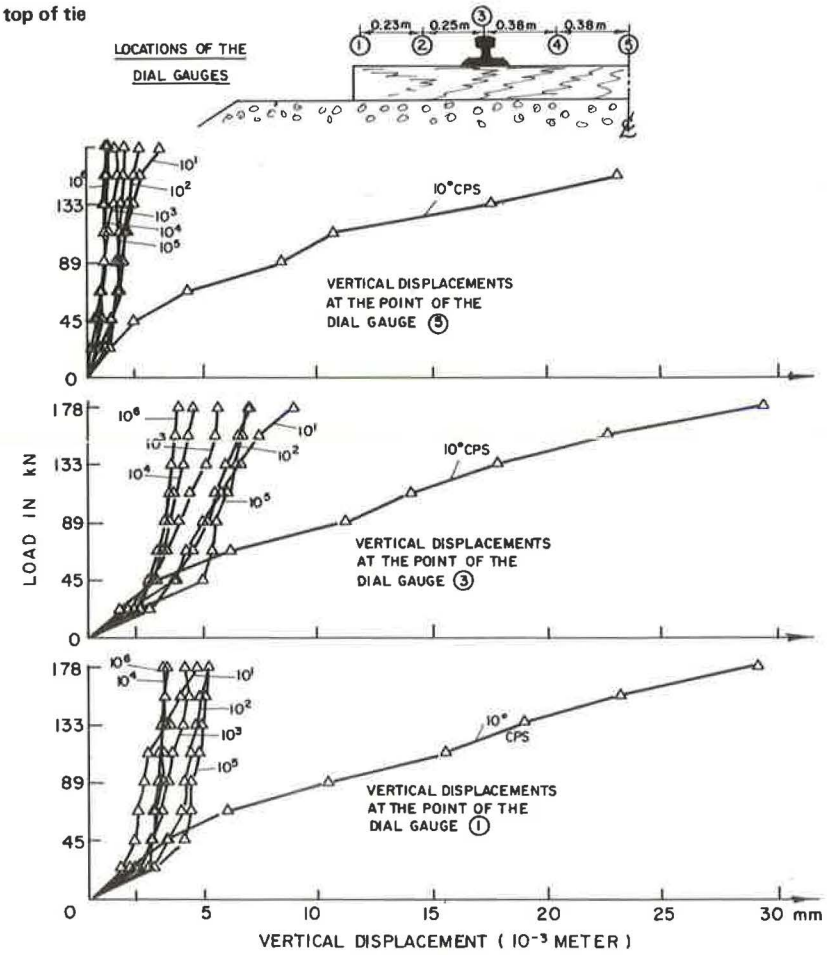

CONCLUSIONS

1. In static triaxial compression tests, ballast breakdown is only slightly affected by cell pressure and is closely related to the factor of safety.
2. In repeated-load triaxial compression tests, the breakdown of ballast is related to the fraction of the failure stress used, rather than to the confining stress. Higher shear strength means less breakdown.
3. Factors one and two may be associated with broader ties and a smaller ratio of tie spacing to tie breadth.
4. Cycling the stress causes ballast to become stiffer, which confirms the practice of using train loads to further compact ballast in track.
5. The extension tests tended to confirm the results of the compression tests; however, failure was observed in the repeated-load extension tests. The number of loadings required to cause failure in the extension tests decreased as the fraction of the deviator stress used increased. The repeated-load failure in the extension tests is important with regard to track stability. There appeared to be a fatigue limit of about one-half the static failure for the dolomite tested.
6. The results of the small-scale model tests reinforce the conclusion that broader ties should perform better than narrow ones in minimizing plastic deformations.
7. The footing rebounds measured suggest that, because of repeated loading, a broader footing should produce a marginally higher foundation stiffness.
8. The plastic deformation of a footing on Ottawa sand subjected to repeated loading has been quantified by using a hyperbolic equation.
9. After parameters for the quantification of plastic deformation of different ballast materials have been obtained, then a design methodology for track maintenance (in terms of plastic deformation) can be formulated.
10. The full-scale model tests indicated that equilibrium in terms of zero plastic strain at the interface of the tie and the ballast is never reached. The displacement is not uniform across the tie. The settlements under the rails are greater than those at the tie centerline. This leads to a center binding phenomenon, the ultimate result of which is fatigue failure of the tie at or near its midpoint. To counteract this phenomenon, tie geometry and dimensions could be changed to encourage a more uniform displacement. The advent of synthetic ties that more readily lend themselves to nonuniform shapes may make such changes practical. Further full-scale testing of ties of various geometries would be a potentially fruitful course of action.

ACKNOWLEDGMENTS

The work presented here forms part of a general study on the geotechnical problems of railroad structures and fills that is being financed by the Canadian National Railways and the Canadian Pacific Rail and Transportation Development Agency of the Ministry of Transport under a project of the Canadian Institute of Guided Ground Transport at Queen's University. I also acknowledge the advice and help obtained from personnel from Canadian National Railways and Canadian Pacific Railways, particularly N. Caldwell, C. J. Dalton, J. D. Jardine, F. L. Peckover, and L. D. Tufts.

REFERENCES

1. P. N. Gaskin and G. P. Raymond. Contribution to Selection of Railroad Ballast. Transportation Engineering Journal, Proc., ASCE, Vol. 102, No. TE2, 1976, pp. 377-394.
2. G. P. Raymond, C. J. Boon, R. W. Lake, and V. Y. Diyaljee. Characteristics of Acceptable Railway Ballast. Paper presented at the 55th Annual Meeting, TRB, 1976.
3. G. P. Raymond, P. N. Gaskin, J. R. Davies, K. Van Dalen, and O. J. Svec. Laboratory Performance of Railroad Ballast. Proc., 2nd Australia-New Zealand Geomechanics Conference, Brisbane, Vol. 1, 1975, pp. 238-242.
4. G. P. Raymond, P. N. Gaskin, and O. J. Svec. Selection and Performance of Railroad Ballast. Proc., Symposium on Railroad Track Mechanics, Princeton Univ., 1975, in press.
5. G. E. Green. Small Scale Laboratory Measurements of Stress-Strain Parameters. Proc., Roscoe Memorial Symposium, Henley-on-Thames, England, 1971, pp. 285-323.
6. T. M. Leps. Review of Shearing Strength of Rockfill. Journal of the Soil Mechanics and Foundations Division, Proc., ASCE, Vol. 96, No. SM4, 1970, pp. 1159-1170.

Track Structure Systems

George H. Way, Jr., Research and Test Department, Association of American Railroads

The railway track-system concept is a way of looking at things that takes into account secondary and tertiary effects in the totality of cause and effect. A track system is not simply a collection of curves, tangents, switches, frogs, turnouts, crossings, and crossovers, but includes the interrelations among the various components—the rails, ties, ballast, fasteners, and subgrade. One of the earliest railway engineers to employ system thinking was Robert L. Stevens of New Jersey, who in 1830 conceived the flat-bottomed-tee rail and the first cut spikes and joint bars. Later, he evolved the idea of wooden crossties. He single-handedly developed the basic system of mutually complimentary components used in railroad trackage today. The next system thinker to have a profound influence on track technology in North America was Arthur N. Talbot of the University of Illinois, who developed the concept of the modulus of elastic track support, first reported in 1918. This was a quantifiable response to load of ties, ballast, fasteners, and subgrade material that can be used to predict track deformation under vertical load. The Stevens' legacy was a system design of railway track, and Talbot's contribution was a system analysis of track structure. Talbot also left a challenge because, while track performance can be predicted when the modulus is known, how to design to a modulus has not yet been learned. The rate of return on incremental investment in individual track components can be determined only by full-scale experiments. The new full-scale laboratory the Association of American Railroads is building in Chicago should bring about validation of mathematical models of track that are being developed.

This new laboratory will permit applications of calibrated loads to full-scale test sections of track, and the resulting deformations and stresses can be measured. The really important system is not the track system nor the equipment system, but the train-and-track system. An example of train-and-track system thinking occurred in 1934 when the Pennsylvania Railroad chose the GG-1 locomotive over its competitor because of lower wheel and axle loadings. Technical decisions must be influenced by economic and political factors, and track systems are no exception. An example today is the question of proper superelevation on curves, and the answer depends in part on the kind and amount of intercity rail passenger service that will be provided, which is a political question. Even more significant is the question of right-of-way ownership. Would a private company choose a lower axle-load locomotive if it were to be operated over track the company did not own?

The phrase railway track system has a rather nice ring to it and will probably be in use long enough for us to spend a little time discussing it in an attempt to at least avoid semantic confusion.

The simple word system has been part of our language for a long time, but it seems to have come into concentrated use (if not confused overuse and misuse) with the advent of computer technology. It was in the middle 1960s that it became the prefix to all passwords to technical acceptance, and system approach was surely the most popular of these passwords. To gain acceptance, nearly every proposal then, and to some degree today, had to call attention to the system approach used by its proponents.

This apparently new technique represents a very sound and realistic approach to technological problems; however, it is not at all unlike the approach formerly described as the engineering approach. The point I am trying to make here is that, regardless of what we choose to call it, the system approach is simply a concept, a way of looking at things that we hope takes aspects of a situation into account that at first may not be readily apparent, but that are none the less important. Thus, secondary and tertiary effects are to be considered in the totality of causes and effects. The concept is important. The words we use to describe it are much less so. Words are words, concepts are concepts, and the relation between them is not necessarily one-to-one. New words and terms do not, of and by themselves, represent new concepts.

I frequently find myself amused or even annoyed at those who redress good but older ideas in new clothes and present them as progress. But, so be it. If changing the dress code of semantics helps in the understanding and acceptance of useful ideas, then the process is for a good cause, even if it contributes to some confusion.

Thus, we come to the concept of railway track as a system. If you had asked me in 1955 to describe a track system, I would have responded with little hesitation that it was a collection of curves, tangents, switches, frogs, turnouts, crossings, and crossovers making up a network suitable for the conduct of rail transport. Today, while not incorrect, such an answer would be incomplete. That description of a track system is analogous to a plan view; in the language of a draftsman, the side and front elevations are missing. The interrelations among the various components—the rails, ties, ballast, fasteners, and subgrade—are of equal interest.

One of the earliest railway engineers to employ systems thinking in the area of railway track was Robert L. Stevens of New Jersey, the son of Colonel John Stevens. Robert Stevens was the president and builder of the Camden and Amboy Railroad and Transportation Company, which became an important link in the northeast corridor in the 1830s and 1840s. At that time, travel between Washington, New York City, and Boston was largely intermodal (yet another new term for a rather old concept).

The overland portion across New Jersey was slow and burdensome in comparison with travel on the natural waterways of the Chesapeake and Raritan bays, the Delaware River, and Long Island Sound. Many canals were proposed, and many were built to connect natural waterways. But the successes of the Stockton and Darlington Railway of England attracted considerable attention and led to proposals for railroads as alternatives to canals. In particular, the Camden and Amboy was chartered at the same time as the Delaware and Raritan Canal, which had been first proposed in 1804. In 1830, Robert Stevens traveled to England to purchase iron rail and a steam locomotive for use on the Camden and Amboy. During his crossing of the Atlantic, Stevens considered the question of rail and fastenings. While carving out of wood, a section of Birkinshaw rail, such as was popular in England, and which had only a head and a base, he conceived the classic flat-bottomed-tee rail now in general use throughout the world. Had he stopped here, his accomplishment would have been significant, but he did not. Stevens went on to design the first cut or hook spikes and the fishplates or joint bars, as we now know them, to join the rails together. In England, Stevens induced a reluctant supplier to roll his oddly shaped rails and negotiated the purchase of the John Bull locomotive from Robert Stephenson. This locomotive is now in Washington at the Smithsonian Institution. Construction of the Camden and Amboy proceeded; the portion between South Amboy and Bordentown receiving the highest priority because it connected steamer lines operating to and from Philadelphia and New York City. The track construction involved spiking the iron rails to wooden plugs that were driven into holes drilled in large stone blocks. This type of track work was also used on portions of the Baltimore and Ohio Railroad and the level portions of the state of Pennsylvania Public Works rail crossing of the Allegheny Mountains. The stone blocks for use in the Camden and Amboy line were shipped from their source at Sing Sing Prison on the east shore of the Hudson River above New York. It had been hoped to complete the line to Bordentown before work stopped for the winter in 1832, but the slow delivery of the stone blocks was an obstacle to this goal. Stevens then came to the idea of placing logs crosswise to the track and spiking the rails directly onto them. The result was not only efficient and economical of materials, but also a vastly improved track structure. The crossties or sleepers distributed the rail load as did the stone blocks and also maintained the gauge and held the rails in a common plane as the blocks did not. Thus, Stevens single-handedly developed the basic system of mutually complimentary components that with many refinements of materials and detail design makes up the largest part of worldwide railway trackage even today.

The next systems thinker to have a profound influence on track technology in North America did not come along for nearly 100 years. Advances were made in individual components—steel replaced iron for rails, tie plates were introduced, and wood preserving extended crosstie life—and such progress continues today. But it was not until Arthur N. Talbot of the University of Illinois addressed the subject of railway track performance in his report on stresses in track published in 1918 that an understanding of the track response as a system was evolved. Talbot, working with and for the American Society of Civil Engineers and the American Railway Engineering Association, developed the concept of the modulus of elastic track support. This was a single quantifiable term that grouped the response to load of ties, ballast, fastenings, and subgrade material. To-

gether with the geometric and material properties of the rail, it could be used to predict the manner in which a track would deform under vertical loading and what stresses would be developed in resisting the load.

If Stevens' legacy was a systems design of railway track, then Talbot's contribution was to teach us how to perform a system analysis of a track structure. But Talbot left us a challange as well. While we can predict the performance of a track rather well after we have determined its modulus, we have not yet learned how to design to a modulus or to make the economic trade-offs between components that Talbot's analysis makes possible. We know, for example, that larger ties or more ties per length of rail increase track modulus. We also know that increased depth of ballast increases track modulus. By using Talbot's equations, we can compare the effectiveness of any of these increases in track modulus with changes in the moment of inertia of the rail section in reducing track deflection under load, flexure stress in the rail, or rolling resistance to trains. But we cannot yet determine the rate of return on incremental investment in individual track components in a reliable, convenient way, except by full-scale experiments. Nor do we even know what degree of track stiffness is optimal for specified levels of traffic and wheel loadings.

The new full-scale track laboratory the AAR is building in Chicago should enable us to validate the several track models that are being developed. This new facility will permit applications of carefully calibrated loads to full-scale test sections of track and detailed measurements of the resulting deformations and stresses. It is particularly important that the track configuration, rail section, tie spacing, and ballast depth and material can be altered, and the entire structure can be compacted under simulated traffic. The data produced can be used, among other things, to calibrate and validate the new track models, which in turn can suggest detailed track configurations for evaluation amd comparison. At last, we may be able to determine the most economical fashion to achieve a given track modulus.

I would like to turn at this point to some comparatively more recent railway engineering history that would seem, but is not, unrelated to the subject of track systems. That is the development of one of the most successful locomotive designs of all time—the class GG-1 electric of the former Pennsylvania Railroad. This locomotive was developed between 1933 and 1935, and 139 units were built between 1934 and 1943. Of these, about 100 are still in service, long after locomotives 20 years newer have been retired. The single-locomotive unit was measured to have developed 6.95 MW rail power (9300 hp), equivalent to 8.21 MW diesel-electric power (11 000 hp). It accelerated from 0 to 160 km/h (0 to 100 mph) in 64.5 s. In 1942, the GG-1 fleet regularly hauled 416 passenger trains/d. Typically these trains were 18 cars long and covered the distance from New York to Washington [326 km (226 miles)] in 215 min including five station stops.

What does this have to do with track systems? It has to do with the only system that is really important—not the equipment system, not the track system—but the train-and-track system. Historically, track has been the concern of civil engineers, and equipment has been the prerogative of mechanical and electrical engineers. Railroad managements did little to correct the separation begun in universities by grouping the civil engineering track people in engineering departments and the mechanical engineering equipment people in mechanical departments. Fortunately, both groups were responsible to one operating vice president and sometimes the system worked to the common good.

It worked exceedingly well in 1933 on the Pennsylvania Railroad. The GG-1 prototype, locomotive 4900, was one of several designs being considered for the expansion of the electric locomotive fleet. Among its competitors was locomotive 4800, representing class R-1, which was even more powerful. In 1934, both prototypes were taken to Claymont, Delaware, where comparative tests were to be run on a test track that included 300 instrumented steel crossties. The GG-1 design was selected despite its somewhat lower power and anticipated greater maintenance cost (it had 12 motors to the 8 of the R-1 and included an articulated frame). The GG-1 was chosen because it produced lower track stress, especially lateral loads.

In 1934, the Pennsylvania Railroad had the strongest and best track in the world, especially in the territory to be served by the new electric locomotives. The standard track consisted of 45.7 cm (18 in) of crushed granite trap-rock ballast on top of 30.5 cm (12 in) of cinder subballast, 17.8 mm by 2.59 m (7 in by 8.5 ft) crossties laid at 49.5 cm (19.5 in) spacing, and 76-kg/m (152-lb/yd) rail laid in 39.3-cm (15.5-in) tie plates. Thus, it was not the kind of track that might collapse under the loading of the R-1 (the R-1 prototype was renumbered to 4999 and used until 1958 in regular service). The GG-1 was selected over the R-1 because its lower axle loadings and lower dynamic lateral loads would contribute to a lower total cost of the track-and-train system. It was not chosen, as have been some more recent designs, because of high axle and lateral loads that were below some arbitrary standard. It is more than significant that a locomotive chosen for use on the best possible trackage weighed over 220 Mg (200 tons) but had a maximum wheel load of only about 11 300 kg (25 000 lb) and this on 1.42-m (56-in) diameter driving wheels. This is a very favorable ratio of less than 8900-kg/m (500-lb/in) wheel diameter.

Finally, let us spend a few moments to consider how the concept of system engineering as applied to track-structure systems or to track-and-train systems leads us into other areas, particularly those of economic and political concern. Specifically, let us explore the way systems thinking about track and trains should influence our economic and political perspectives on the railroad industry.

Some will say that, as technologists and engineers, we should not be concerned about such things, that we have more than enough to do to keep freight and passenger trains on the rails and on time. I disagree and strongly so. There are important interactions between political, technical, and economic issues. The way technologists react to the political and macroeconomic issues the industry faces will be relevant to whether or not we are able to deal effectively with what may appear to be purely technical problems.

It is the political and economic climate that provides the basis for reference in which technology must guide itself. Technical decisions must frequently be made because of political pressures but, if they are made on a basis of improper or poor appreciation of the political or economic issues at hand, they will be just as wrong as if they were made on a basis of poor technical data.

One small example among the difficult technical track problems we face today relates to the proper superelevation on curves. The answer, however, depends in part on the kind and amount of intercity passenger service the industry is going to provide, and that is a political question. I, for one, do not think that intercity passenger trains will be eliminated, regardless of their economics. But, the answer to this question is one on which track-system people base important technical decisions every day.

Even more significant is the question of right-of-way

ownership. Some transportation planners have advocated, as a solution to the problem of nonequal treatment of transportation modes by government, a system in which railroad rights-of-way would be publicly owned, as are highways, but the private sector would own and operate the trains in a manner analogous to the trucking or barge companies. Considered only as a political question, this proposal has some significant appeal. But, when the subject is considered from the systems perspective and the secondary technological effects are evaluated, some rather serious questions arise. For example, Would a private company choose a GG-1 locomotive in preference to an R-1 to operate over trackage it did not own and need not maintain? The private railroads have made errors with respect to track-and-train system compatibility, but these errors have probably not been as numerous or as serious as they would have been without the incentives that common ownership and responsibility provide.

Combinations of public and private ownership and enterprise have considerable appeal today. Their advocates tell us that they combine the private enterprise incentive with public responsibility—but in this case, I am afraid that the limitation to system thinking imposed by the separation of track responsibility from equipment responsibility is too high a price.

Railroads are excellent examples of industrial systems. They include a variety of mutually dependent organizational and technical subgroups that make up a unified whole. In fact, many railroads historically included the word system in their corporate title. Track, the fundamental subgroup of a railroad system, is a system itself. But, systems thinking can lead us into trouble in such a complex environment as railroading by setting the limits of the system under consideration either too narrow to include all the essentials or so broad as to be incomprehensible, and either can lead to disastrous consequences. The really successful system engineer is the one who knows, guesses, intuitively understands, and sets the appropriate limits to the system analysis required by the specific problem. In this respect, track systems are no different from any other kind—they still require qualitative, personal judgment.

Problems and Needs in Tie and Fastener Research

Thomas B. Hutcheson, Seaboard Coast Line Railroad Company

The advantages of the timber crosstie—relatively low cost; traditional ready availability; toughness, resilience, and strength; allowance for a flexible system of support; relatively long useful life; and availability of a relatively inexpensive fastening system—are compared with its disadvantages—increasing cost; decreasing availability; economic relation to competing demands for timber; suitability for increased train lengths, equipment configurations, and wheel loads; and availability of satisfactory substitutes. Similarly, the advantages of the crosstie fastening system used in North America—relatively low cost, ease of application, satisfactory service for many years, and flexibility of tie loading—are compared with its disadvantages—selective loading of individual ties and mechanical wear in the tie plate and spike holes. Areas for research suggested by the disadvantages are enumerated.

Since the early nineteenth century, after brief experiments with longitudinal support in various forms involving the use of timber, stones, and other materials, American railroads have used the timber crosstie to transmit wheel loads through the rails to the subgrade. At first this was done directly, but then as loads and speeds increased, selected materials were applied as ballast and subballast to assist in maintaining the line and the surface of the track and to facilitate drainage.

During this period, extending for more than 140 years, the solid timber crosstie has served North American railroads well. It represents a considerable improvement over the longitudinal support system used on the earliest roads. The discrete support of the rail and loading of the ballast and subsoil provides a flexible means of load distribution that is highly desirable.

An interesting discussion of the development of stress analysis in rails and ties using this loading system is given by Kerr (1).

As loads have increased, the physical aspects of the crosstie and its use have undergone changes, generally of minor and apparent natures. The length has varied, first with the gauge of the track, and then with the load. Current North American practice uses tie lengths of 2.59 to 2.74 m (8.5 to 9 ft). The size of the tie has been standardized for many years at 17.8 by 22.9 cm (7 by 9 in) for the largest recommended size. Tie spacing, center to center, has varied from about 1.83 m (6 ft) in the earliest practice to the 48.3 to 50.8 cm (19 to 20 in) commonly used in current heavy-duty main tracks.

During this period of time, at least on the North American continent, the timber crosstie has withstood competition from other materials and methods of support. Among its advantages are that

1. It is relatively inexpensive;
2. It was for many years generally in adequate supply, and the raw materials were widely distributed over the continent;
3. It offers excellent physical characteristics of toughness, resilience, and strength in the most favored species;
4. It provides a desirable discretely flexible system of support that allows inexpensive correction of deviations in line and surface;
5. When properly treated with readily available preservatives, it has a relatively long useful life, and
6. The current North American fastening system, involving the cut spike, a steel tie plate, and base anchors is relatively inexpensive and easily applied.

On the other hand, there are new factors that make it desirable to reexamine the function and role of the timber crosstie in terms of changed conditions of service and

load, some accumulated over time and some of rather recent vintage. Some of these factors are that

1. The cost of timber crossties has increased at a sharper rate than both forest products generally and other railroad materials and supplies during the 5-year period from 1971 to 1975,
2. Timber of the size and species required for solid timber crossties has a long growing cycle and is increasingly scarce,
3. Competition for suitable crosstie timber fluctuates widely with housing starts and economic factors related to other timber uses, such as pallets and dunnage, whose economies are related to operations rather than to material cost,
4. Current train lengths, equipment configurations, and wheel loads have increased the dynamic forces and actions of trains and produced much higher vertical, lateral, and longitudinal forces, which brings into question not only tie and fastening strength, but also size, length, and shape, and
5. New technologies have produced methods and materials that may provide a satisfactory substitute for a solid timber tie.

The continued availability of an adequate supply of timber for solid timber crossties is an important problem. Increasingly, over the past 10 years, the availability of timber has been questioned, even though tie installations have been at considerably less than the estimated requirements. In the 10-year period from 1966 to 1975, average tie insertions in the United States have been at an annual level of 37/km (60/mile) of maintained track; whereas a conservative estimate of annual requirements is approximately 62/km (100/mile) of maintained track. In addition, during this period, railroads have of necessity purchased less desirable species, including mixed hardwoods that are difficult to satisfactorily dry and treat, and some softwoods that will not satisfactorily withstand current axle loads. Tie insertions on class 1 railroads over the past 10 years have averaged 17 800 000 ties annually, but the requirements, estimated on a basis of an annual replacement of 67 ties/km of maintained track are 28 870 000; i.e., there is a shortfall of 11 070 000 ties on the basis of the 1975 kilometers of track using crossties.

These supply problems suggest the following areas for research:

1. Study of forest growth rates to determine the expected future availability of timber of suitable species and dimensions to produce satisfactory crossties for current service conditions;
2. Study of methods for producing ties of adequate dimensions and shapes by using available timber and lamination, doweling, chipping, fabrication, and other means;
3. Study of refabrication of released ties by chipping and recasting, using resins or other binders;
4. Study of methods for extending the life of ties by improvement in treating methods, materials, coatings, and otherwise inhibiting fungus attack;
5. Study of methods of reducing mechanical wear on conventional ties by improved fastening methods;
6. Study of the cost and demand factors that affect the movement of timber of suitable size and acceptable species to the crosstie market; and
7. Study of the economic factors that create the large swings of demand in the crosstie market, to assess the cost to the tie industry and railroads of an unstable market.

The increase in the cost of ties and the need to purchase undesirable species to secure adequate replacements indicate a need to locate a satisfactory substitute for the timber tie. Also, the current train lengths, axle loads, and dynamic forces transferred to the track structure suggest that increased track moduli may be desirable for current and prospective service, and these facts suggest the need for increased research into the development of a suitable substitute for the timber tie.

Work in this area thus far has produced mixed results under North American conditions. Although the concrete crosstie has gained general acceptance in the United Kingdom and is widely used throughout Europe, its use in North America has generally been restricted to test installations. There are a number of reasons why this is so. Some of these are that

1. The 10-year replacement rate of 37 ties/km of maintained track (an average of about 17 800 000 ties/year), which is determined by economic rather than need considerations, has been met by available timber-tie production in recent years;
2. Timber demand in the construction and furniture industries and other normally higher priced markets has been lower in recent years;
3. Track maintenance practices in Europe call for complete track replacement, but cyclic tie replacement is the current practice in North America;
4. Accounting practices dictated by the Interstate Commerce Commission favor cyclic maintenance as opposed to complete replacement maintenance;
5. The lighter European axle loads and shorter train consists do not load the track as severely as is done in North America;
6. European methods of tie and rail fastenings have traditionally used more expensive and responsive fastenings than have American methods; and
7. Early American tests of concrete ties experienced severe fastening and load problems due, in large part, to attempts to compete with the wooden tie by using inadequate fastening systems and wider spacing, which resulted in failure in the fastening, the tie itself, and the ballast and subgrade section.

Thus, the concrete tie has had only limited use in North America, and at the same time, for largely economic reasons, timber-tie replacements have lagged significantly behind the actual requirement. Also, for reasons dictated by current economic conditions, there has been only limited research and service testing of concrete ties, and research and testing of reconstituted ties and laminated or other composite ties are in their early stages.

Other matters requiring evaluation and research under North American conditions are

1. The size and length of ties required to meet current conditions of vertical and lateral loads;
2. The economic and load relation between tie spacing and ballast-section depth and width;
3. The effect of tie shape on the lateral stability of track;
4. The determination of an optimum replacement philosophy and maintenance practice, including the impact of current accounting procedures on life-cycle cost factors;
5. The development of life-cycle cost-accounting procedures, including disposal costs;
6. Methods of extending the life of timber ties by reducing mechanical wear and improving resistance to fungus attack; and
7. Acceptable substitutes for conventional timber ties.

Work is under way in many of these areas, but continued effort will be required to bring about acceptable changes and improvements.

The crosstie fastening system used in North America has remained basically unchanged over many years. The conventional cut spike, steel tie plate, and base-applied rail-anchor system is relatively inexpensive, easy to apply in the field and, until recent years when dynamic loads, speeds, and axle loads increased significantly, has given satisfactory service. To keep pace with change, tie plates have become longer, heavier, and wider. The spiking practice has been changed by increasing the size of the spikes and the number used, and recently, plate hold-down spikes having a more positive locking feature have been introduced. The number of base rail anchors applied has increased with train lengths, and the generally accepted current practice is for every other tie to be box anchored. Disadvantages of this system are that (a) the base-anchoring system loads individual ties selectively (as opposed to uniform longitudinal loading of all ties) and (b) the spike-held tie plates allow serious mechanical wear in the tie plate seat and spike holes. Its major advantage is that it provides a more flexible system of individual tie loading, which limits pumping action.

The European system of track fastening is much more positive than is the North American system. Heavier plates are used, and these are more or less rigidly anchored to the tie with bolts or lag screws. The rail is anchored through the plate system with a heavy clamping or spring force, which controls longitudinal movement of the rail and inhibits rail overturn. Rail cant is provided through the tie plate in both fastening systems.

Early limited use of the European system under the North American loads of the time resulted in loss of surface and line, principally because of pumping. Thus, the more flexible fastening system has continued to be used. However, recent problems related to mechanical wear in ties, rail cant, rail overturning, loss of gauge, track movement or buckling, and other problems of lateral, vertical, and longitudinal stability suggest that the system of tie plate, base rail anchor, and cut spike is operating at the upper limits of its ability to withstand current train load forces.

This suggests the following areas for research:

1. The effect of alternative fastening systems on the lateral, vertical, and longitudinal stability of the track system;
2. The engineering and economic aspects of rigid versus flexible fastening systems, including the effect on the ballast section under North American loading conditions;
3. The determination of the optimum rail cant to reduce both rail damage and timber-tie mechanical wear; and
4. The determination of the level of restraint required or desirable to prevent rail overturn and the means to provide such restraint.

While the timber tie and its unique fastening system developed for North American use has served well, changed conditions now indicate that a critical review, involving economic and engineering research, is desirable to determine a direction for the future. This review should include investigation of the economic philosophy of track maintenance to determine whether the North American practice of individual component renewal and adjustment results in a lower life-cycle cost than does the European system of complete rebuilding of the entire track system near the end of its economical service life. It should also include a critical examination of the fastening system to determine whether current and future force levels can be satisfactorily met with the flexible spike, tie plate, and base anchor fastening system or whether the life-cycle costs will be lower if a more positive restraint system, such as is commonly found in British and European practice, is used.

REFERENCE

1. A. D. Kerr. On the Stress Analysis of Rails and Ties. Proc., AREA, Bull. 659, Vol. 78, Oct. 1976.

Track-Structure Analysis: Methodology and Verification

Amir N. Hanna, Transportation Development Section, Portland Cement Association

Track behavior under traffic and environmental conditions can be predicted by using appropriate methods of analysis. Well-developed concepts and procedures in the structural engineering field are used to illustrate methods of track analysis. These procedures are based on assumptions that often require verification by laboratory or field tests. In this paper, some of the approaches to the analysis of track structure and the methods for laboratory and field tests are discussed.

The purpose of a track structure is to support and guide railway vehicles. In performing this function, the track is subjected to repeated loads, which it must withstand to provide a safe and acceptable ride to the passengers and a nondamaging environment for the movement of goods.

To evaluate the performance and safety of a track and to plan for its maintenance, it is necessary to understand its behavior under traffic and environmental conditions. This can be accomplished by using a systematic procedure such as that illustrated in Figure 1, which consists primarily of a method of analysis that uses two sets of input data. These data are

1. Factors external to the track that contribute to its performance and behavior, i.e., (a) rolling stock characteristics, such as axle loads, arrangement of axles, and diameter of wheels; (b) operating conditions, such as volume and type of traffic and operating speed; (c) environmental conditions, such as frost action and tem-

perature changes; and (d) subgrade characteristics, such as soil strength and stability and susceptibility to frost and moisture and

2. Structural details that influence its behavior, i.e., (a) geometry, such as degree of curvature and gradient; (b) components, such as rail profile, type and dimension of crossties, spacing of ties, type of fastenings, and ballast depth and properties; and (c) type, such as continuously welded or jointed rail.

Methods of analysis generally determine the response of a track in terms of structural values such as deflections, strains, stresses, accelerations, and deformations. These values can be compared with appropriate evaluation criteria to predict track performance. Performance is related to the distress of the track or its components that results from overstressing or from long-term changes in track geometry caused by variations in gauge alignment and surface.

METHODS OF ANALYSIS

Well-developed concepts and procedures in the structural engineering field have been used for track analysis (1). Some of the approaches to the analysis of track structure and the methods for determining stresses in track structure components are outlined below.

In normal operations, railroad tracks are subjected to loads from numerous external and internal forces. The external forces are induced by the rolling stock. They include vertical and lateral forces, as well as the longitudinal forces caused by traction and braking and cause longitudinal bending stresses in the track and high contact stresses in the vicinity of the contact area between the wheel and the rail. The internal forces result principally from temperature changes and residual stresses and produce bending and axial stresses in the track.

Rail Stresses

Flexural Stresses

Generally, the wheels of rolling stock exert vertical and lateral forces on the rail. The vertical load is usually eccentric with an eccentrictiy towards the gauge side. The lateral force acts below the top of the rail head. For the analysis of the track structure, these forces can be replaced by a vertical load applied at the center of the rail head, plus a lateral force and a torque, both acting at the center of twist of the rail cross section, as shown in Figure 2.

The deflection and bending moments due to vertical loads can be determined by any of many methods. One of these methods considers the rail as a long beam supported continuously on an elastic foundation, as shown in Figure 3. The rigidity of this system is defined by the track modulus and determined from the vertical deflection of the rail. To simplify the mathematical analysis, assumptions are made regarding the relations among rail deflection, foundation reaction, and track modulus (2). Work by the ASCE-AREA Special Committee on Stresses in Railroad Track (3) has demonstrated the validity of this method for predicting rail deflections and rail bending stresses due to vertical wheel loads.

Another method considers a continuous rail supported on individual elastic supports, as shown in Figure 4. The rigidity of this system is defined by the spring constant of the individual elastic supports. To simplify the mathematical analysis, assumptions are made regarding the relations among rail deflection, foundation reaction, and spring constant (4). By varying the spring constant of the individual supports, the case of a nonuniform track under normal operating and maintenance conditions can be evaluated.

Both the track modulus with respect to the vertical deflection and the spring constant of the individual supports vary with the service life and operation of the track. They depend on the resilience of the track components, including the rail, pad, tie, ballast, and subgrade. A combined track modulus or spring constant can be determined by considering these components as springs arranged in a series, as shown in Figure 5.

In addition to the bending stresses that result from the beam action of the rail, there are secondary bending stresses in the rail head that are due to the bending of the rail head on the web. These stresses can be determined approximately by assuming that the rail head behaves as a beam on an elastic foundation. The modulus of support reaction of this foundation can be estimated from the compression of the rail web (5).

The stresses that are due to vertical bending of the rail consist of the bending stresses that are due to the beam action of the rail and the secondary stresses that are due to the additional bending of the rail head, as shown in Figure 6. The rail head is subjected to compressive stresses, and the rail base is subjected to tensile stresses.

The lateral force and the torque at the center of twist of the rail cross section result in a lateral deflection and a twisting of the rail cross section. The method of solving for these stresses is based on the assumption that the rail is supported on a continuous elastic system that resists both lateral deflection and twisting of the rail. The rigidity of this system is defined by the moduli of the track with respect to twist and lateral deflection. To simplify the mathematical analysis, assumptions can be made regarding the relations among the angle of twist, the lateral deflection, the reactive moments, the shearing forces, and the moduli of the track. The general solution for the lateral deflection and twist of the rail is defined by two simultaneous differential equations that can be solved by using computer techniques (6).

Another method of analysis for the lateral bending of the track assumes that the rail acts as a short beam fixed rigidly at the fastenings (4), although this assumption does not represent actual track conditions. This analysis shows that the lateral force will produce tensile stresses on the field side of both the rail head and the rail base and compressive stresses on the gauge side, as shown in Figure 7.

The moment of twist will produce tensile stresses on the field side of the rail head and the gauge side of the rail base and compressive stresses on the gauge side of the rail head and the field side of the rail base, as shown in Figure 8. By using this analysis, rail deflections and bending stresses, as well as loads transmitted to the ties, can be determined.

Contact Stresses

The rail head is subjected to localized high stresses in the area of load application. These stresses depend on the magnitude of the load and the curvature of the wheel and the rail at the point of contact. Because of service, progressive wear of both rail and wheel occur during their lifetime, which results in a shift in the position of contact between the wheel and the rail and variations in their curvatures.

The solution for contact stresses in the rail head is based on the approach developed by Hertz for the contact of elastic bodies under normal loading (7). According to Hertz, the pressure between two elastic bodies is distributed over an elliptical area of contact in the shape of a

semiellipsoid, as shown in Figure 9a. However, theoretical and experimental studies (8) have shown that under heavy axle loads, plastic deformation occurs in the upper layer of the rail head, so that the assumption of elastic bodies in contact is not entirely valid. The pressure distribution over the contact area varies from the Hertzian distribution and tends to be uniform, as shown in Figure 9b. As a first approximation, a uniformly distributed pressure acting on the elliptical area of contact, as shown in Figure 9c, can be assumed for the calculation of stresses in the interior of the rail head.

By following this procedure, the distribution of stresses in the interior of the rail head can be calculated by integrating the principal Boussinesq equations

Figure 1. Approach to track analysis.

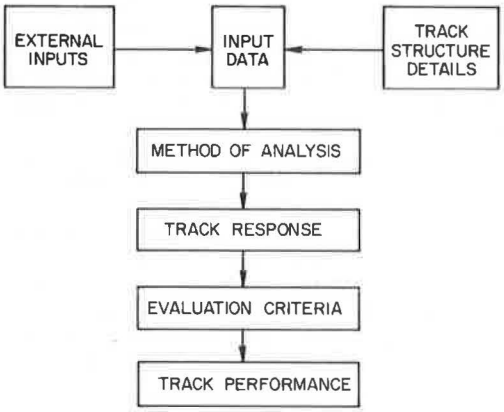

Figure 2. Resolution of forces acting on rail.

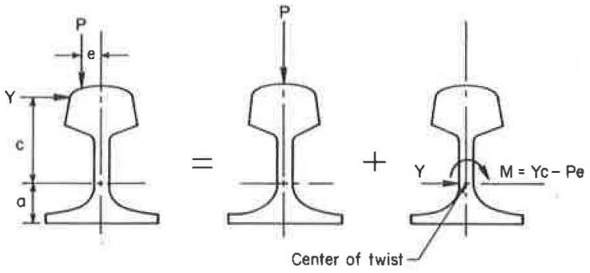

Figure 3. Rail as beam on continuous elastic foundation.

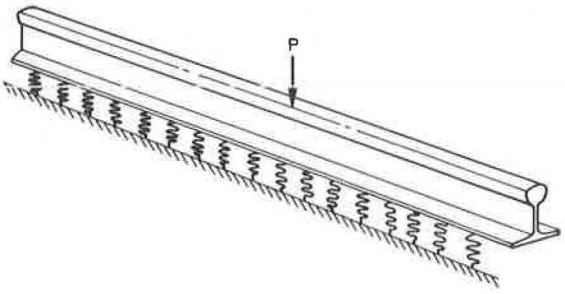

Figure 4. Rail as beam on individual elastic supports.

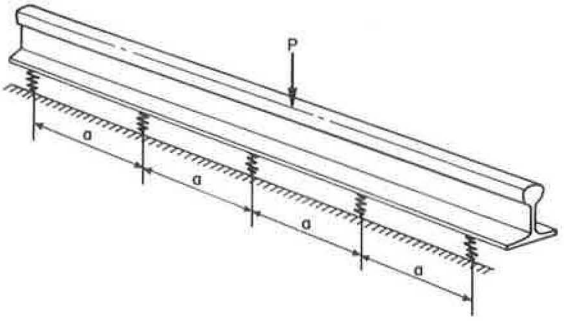

Figure 5. Track as series of springs.

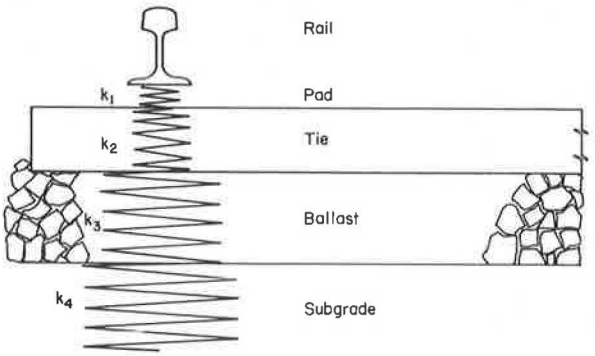

Figure 6. Stress distribution due to vertical bending.

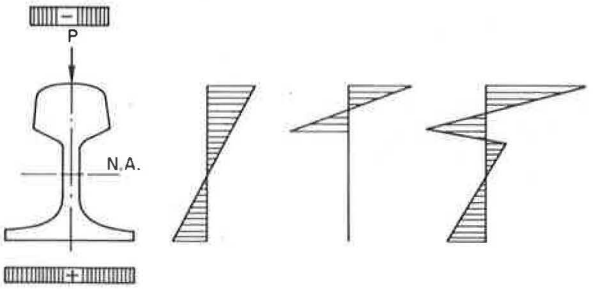

Figure 7. Stress distribution due to lateral bending.

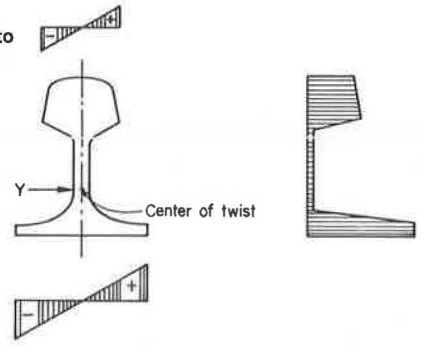

Figure 8. Stress distribution due to twist.

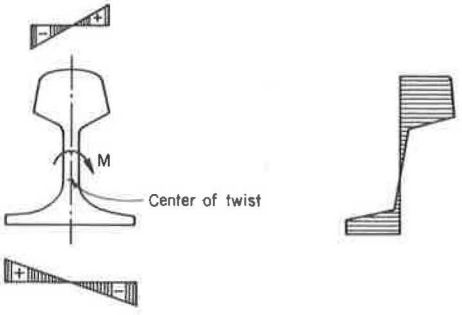

for a single load (9). Experimental studies using model-analogy techniques and photoelastic investigations have verified the validity of this solution (8).

The distribution of stresses in the rail head can also be obtained by using the finite-element method. A three-dimensional finite-element model for the rail head has been used to determine the stresses for a Hertzian pressure distribution (10). This model can also be used to determine the contact stresses due to tangential forces.

By using this analysis, the three-dimensional stress state in the rail head can be determined. To evaluate the effect of this stress state on the material strength, the stresses should be expressed in terms of a single stress designated the significant stress. The significant stress can be determined by using distortion-energy theory (11).

Thermal Stresses

Temperature changes also cause stresses in the rail. For a jointed rail, these stresses depend on the change in temperature from that at which the rail was laid, the length of the rail between two joints, the width of the joint between two rail ends, and the resistance of the joints and of the rail to longitudinal movement. Longitudinal restraint depends on the type of tie plate, the rail fastening, the longitudinal resistance (friction) of the rail on the tie, and the resistance of the tie on the ballast.

As temperature decreases, the rail tends to contract. This movement, however, is restrained by the resistance of the joint bar and the longitudinal rail restraint. The length of rail required to provide full restraint to movement as illustrated in Figure 10 is ℓ. If the rail length between joints is larger than ℓ, the intermediate portion will encounter no movement and will be subjected to the maximum force.

The behavior of a jointed rail laid at a temperature of t_o is shown in Figure 11.

1. As the temperature decreases below t_o, the rail will tend to contract. In the case of free movement, as the rail contracts, the joint width will increase, and no axial forces will be developed. However, if there are joint and longitudinal restraints, the joint width will remain unchanged, and tensile forces in the rail will develop. After the restraint is overcome, the joint opening will gradually increase, and no additional forces will develop until the temperature reaches its minimum (t_{min}), at which time the joint width will reach its maximum.
2. At the temperature increases above t_{min}, the tensile force in the rail will change to a compressive force to overcome the restraint. At a certain temperature, the joint will close, and any additional increase in temperature will result in an additional compressive force.

For a continuously welded rail or a jointed rail of length longer than ℓ, the potential change in the rail length due to temperature change is restrained by the track resistance. In this case, thermal stress is largest.

Residual Stresses

Residual stresses in the rail originate during the manufacturing process from cooling and straightening and can be determined experimentally. The magnitudes and signs of these stresses depend on the manufacturing process. In general, the distribution of residual stress over the rail cross section is irregular and does not follow a definite pattern.

Residual stresses also originate in the welding process. The amount and distribution of these stresses depend on the welding method.

Basically, there are two methods for measuring the residual stresses in rail. One is to release them by cutting and then measure the strains caused by their release. The other is a photoelastic method that combines the shear difference procedure with the stress-freezing process (12).

Tie Stresses

It is possible to determine the load transfer between track components, particularly rail and tie, by using an established method of analysis. These loads can then be used for the analysis of the tie stresses.

The design and analysis of crossties can be performed by considering the tie as a finite-length beam supported on an elastic foundation. To simplify the mathematical analysis of the problem, assumptions are made regarding the relations among tie deflection, tie and ballast pressure, and modulus of support reaction.

Other methods of tie analysis are based on assumed distribution of tie and ballast pressure that vary with service life and operation of track. Pressure variation can include the support conditions encountered shortly after tamping (Figure 12a), as traffic continues (Figure 12b), and at a full center-bound condition (Figure 12c).

After the support conditions are established, it is possible to determine the maximum bending moments and stresses in the tie. For prestressed concrete ties, the stresses depend not only on tie dimensions, but also on the prestressing force and the location of the prestressing tendons. In the analysis, consideration must be given to the prestress losses that occur during the tie life.

Ballast and Subgrade Stresses

By using an appropriate method of analysis, the pressure on the ballast can be determined. Then, the stress distribution in the ballast and the subgrade can be calculated by using Boussinesq equations for a semi-infinite solid or by using a layered-system analysis (13) similar to that used in pavement analysis. The analysis considers the effects of the subgrade, subballast, and ballast properties; the shape and spacing of the ties; and the depth of ballast and subballast on the stresses in the subgrade.

Dynamic Stresses

The dynamic deflections and stresses of a track under the action of the moving wheels of rolling stock may be much larger than those calculated on the basis of static formulas. There are many factors that contribute to increases in deflection and stress, including

1. Differences in irregularities in the shape of the wheel or rail, such as flat spots on the rim of the wheel, low spots in the rail, and discontinuities at the rail joints;
2. Vibration in the forces acting on the rail caused by variable spring forces on the wheels; and
3. Vibration of the track under moving loads.

Dynamic stresses produced in track by the effect of a low spot in the rail (a corrugated rail profile) or a flattened wheel can be determined analytically (14). For this purpose, the shape of the geometric irregularity can be represented in a mathematical equation. Similarly, the dynamic loads developed near rail joints can be determined analytically. For this purpose, the math-

ematical model should consider the change in track stiffness at the rail joint.

Dynamic stresses can be accounted for by using an impact factor. Extensive measurements by European railways (15) have shown that the dynamic stresses in railroad track depend on the condition of track and rolling stock and the speed of operation. An appropriate dynamic impact model has been developed to account for the effect of these three factors.

For the analysis of ties, European railroads have used impact factors that reflect the most severe track conditions. A similar approach was followed by the AREA Special Committee on Concrete Ties (16).

Figure 9. Pressure distribution between wheel and rail.

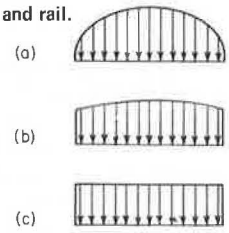

Figure 10. Joint and longitudinal track-restraint forces.

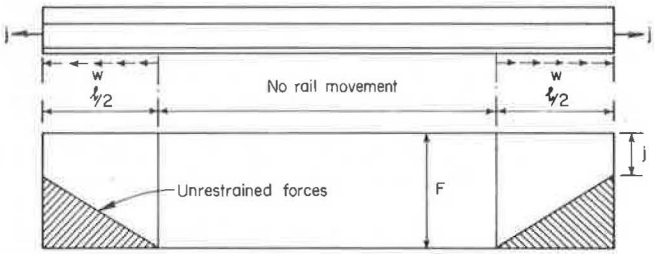

Figure 11. Variation in joint opening and axial force with temperature change.

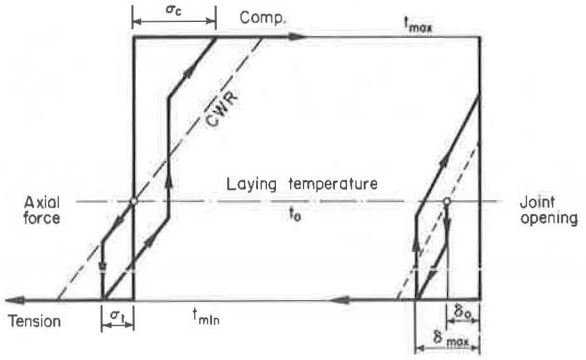

Figure 12. Typical tie-support conditions.

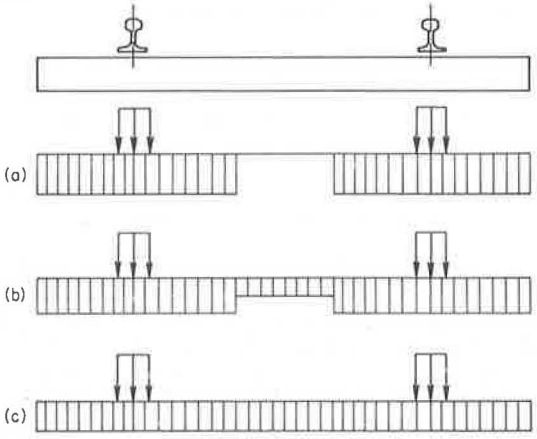

EVALUATION

By using the results of these analyses, track deflections and stresses at the critical locations can be determined. The locations of critical stresses are illustrated in Figure 13. Critical stresses include

1. Bending stresses that can result in plastic deformations of the rail head (location a) and the rail base (location b),
2. Bending stresses that can result in fatigue failure of the rail (location c),

Figure 13. Locations of maximum stresses.

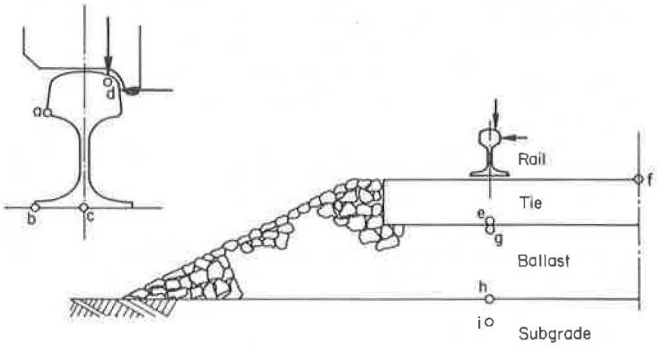

Figure 14. Loading cycle simulating axle and truck spacing.

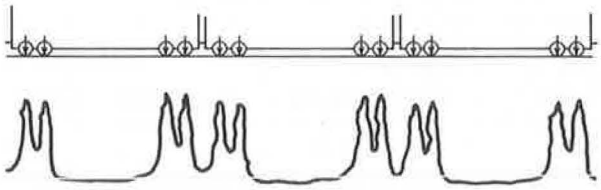

Figure 15. Laboratory tests on tie supported on ballast and subgrade.

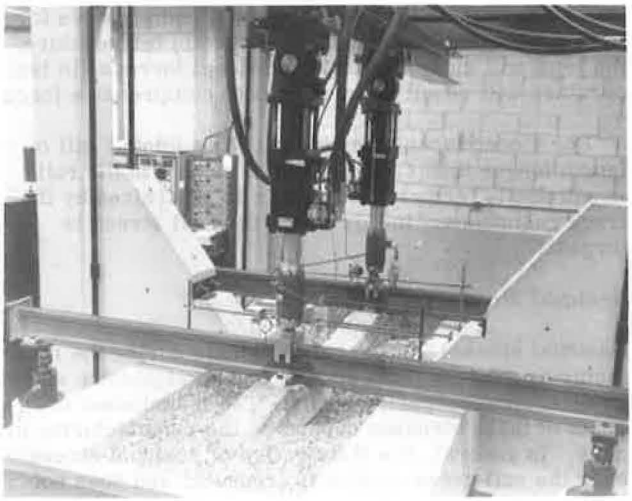

Figure 16. Track instrumentation: general layout.

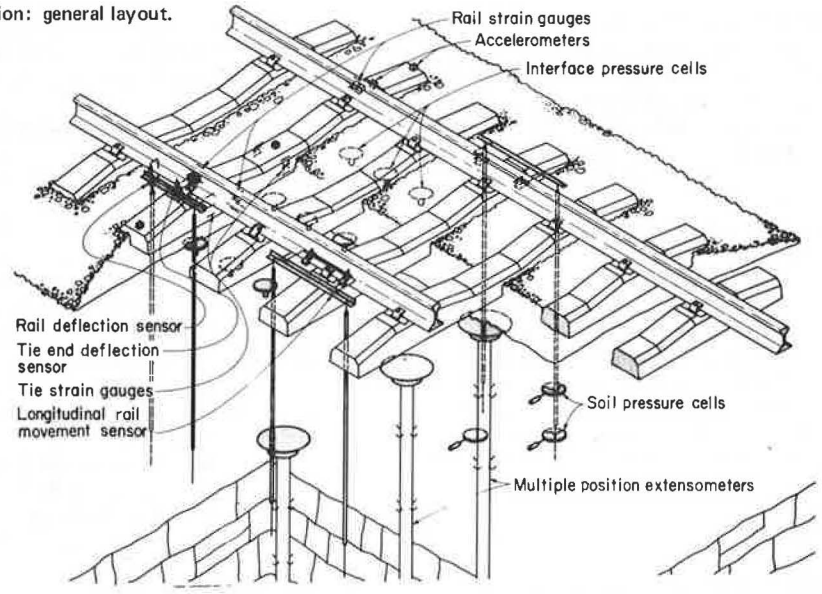

3. Contact stresses that can result in shelling or fatigue failure of the rail head (location d),
4. Bending stresses that can result in flexural cracking of the crossties under the rail seat (location e) and at the tie center (location f),
5. Pressures that can cause degradation and deformation of the ballast (location g), and
6. Pressures and shear stresses that can result in permanent deformation and shear failure of the subgrade (locations h and i).

Stresses at the critical locations can be used in conjunction with limiting values and theories of failure to forecast the service life and the safety of track components. Thus, remedial actions may be taken at appropriate times.

VERIFICATION

As outlined above, methods of track analysis are complex and based on many assumptions. Therefore, the applicability of the methods and the validity of the assumptions should be verified. This can be accomplished in three different ways:

1. By laboratory testing of track sections or track components,
2. By field investigations of track sections, or
3. By accelerated testing.

Laboratory Tests

In conducting laboratory tests on track systems and components, efforts should be made to simulate the field support condition and the loading environment. This requires a proper selection of track support, loading magnitude and frequency, and pattern of loading cycle. Laboratory tests, when properly designed and conducted, can provide adequate data on the response of a track to traffic loads.

Attempts to provide good simulation should include programming the loading cycles to simulate the effects of axle and truck spacings, as shown in Figure 14, and of speed of operation. Methods of simulating the support of ties and track sections on representative ballast and subgrade have been developed, as shown in Figure 15.

In laboratory tests, appropriate instrumentation can provide quantitative measures of track response. However, laboratory tests can also be designed to provide qualitative information on the performance and properties of track components. In these cases, no instrumentation is provided, and the test elements are examined visually.

Field Tests

In designing a field-test installation, consideration should be given to the site selection. This includes principally the selection of the desired characteristics of speed, traffic volume, track alignment, and environment. Further consideration should be given to the selection of the track structure. A most important consideration in a field-test installation is the design and installation of appropriate instrumentation to measure the required information.

Relatively complete instrumentation of a field-test section, as shown in Figure 16, includes the following:

1. Strain gauges for the measurement of rail and tie strains;
2. Transducers for the measurement of rail and tie displacements, including longitudinal, lateral, and vertical movements of the rail and the tie;
3. Accelerometers for the measurement of rail, tie, and ballast vertical accelerations;
4. Transducers for the measurement of load transfer from the rail to the fastener and to the tie seat;
5. Pressure cells for the measurement of pressure beneath the tie—i.e., at the tie-ballast interface, the ballast-subgrade interface, and various depths; and
6. Vertical and lateral extensometers for the measurement of the soil strains produced by load applications.

A similar array of instruments can also be used for the evaluation of track structure in laboratory tests.

Accelerated Tests

Accelerated tests can be conduced in the laboratory or on a railroad track under accelerated service conditions. An example of a field-test track is the Facility for Accelerated Service Testing at the U.S. Department of Transportation Test Center in Pueblo, Colorado. The

test loop has 7.7 km (4.8 miles) of track and consists of 22 test sections. The purpose of the facility is to subject various track components and types of construction to accelerated testing. The track components and types to be tested cover a wide range of variables; these include rail metallurgy, steel, reconstituted, laminated, concrete, and wooden ties, ballast, rubber pads, tie plates, and many others.

In accelerated tests, appropriate instrumentation should be provided to measure the track response. This instrumentation can be similar to that used in ordinary field tests.

The information generated from verification studies, whether conducted in the laboratory, in the field, or in an accelerated service loop, is useful only to the extent that the test corresponds to actual conditions. Therefore, verification studies should be designed and conducted carefully and, of more importance, the data must be interpreted properly.

CONCLUDING REMARKS

A systematic procedure for the analysis of a track structure is described. The procedure uses methods of analysis that are well developed in the structural engineering field. Methods for verifying the analysis by means of laboratory, field, and accelerated tests are presented.

The present standards of track have been evolved from previous practices through a process involving trial, judgment, and experience. This practice has not yet provided a track structure that fulfills its intended purpose. Therefore, railroad track should be developed in a manner similar to that followed in the development of other engineering structures. Analysis and experimentation can contribute significantly to the orderly development and upgrading of our railroad system.

REFERENCES

1. A. N. Hanna. Railway Track Research: Theoretical and Experimental. Portland Cement Association, Research and Development Bull. RD030.01R, 1975.
2. H. Zimmermann. The Calculation of Railroad Permanent Way. W. Ernst and Sohn Verlag, Berlin, 3rd Ed., 1941.
3. Fifth Progress Report. ASCE-AREA Special Committee on Stresses in Railroad Track, AREA, Bull., Vol. 31, 1929.
4. H. Luber. Analysis of Elastic-Supported Railway Tracks Under Vertical Loads. Institute for Railway and Highway Construction, Technical Univ. of Munich, Bull. 1, 1962.
5. J. Eisenmann. Theoretical Views on the Stresses in the Rail Head Near the Point of Load Application. Eisenbahn-Technische Rundschau, Vol. 14, No. 12, Dec. 1965, pp. 25-34.
6. A. N. Hanna. Solution of the Stresses in the Rail Due to Lateral Forces. Strasse-Brücke-Tunnel, Vol. 22, No. 3, March 1970, pp. 70-73.
7. H. Hertz. On the Contact of Solid Elastic Bodies. Journal für die Reine und Angewandte Mathematik, 92, 1882, pp. 156-171.
8. A. N. Hanna. Theoretical and Experimental Examination of the Stresses in the Interior of the Rail Head. Institute for Railway and Highway Construction, Technical Univ. of Munich, Bull. 10, 1967.
9. J. Heymann. Semi-Infinite Space Under Uniform Loading with an Elliptical Boundary. Zeitschrift für Angewandte Mechanik, Vol. 42, No. 12, Feb. 1963, pp. 568-572.
10. G. C. Martin and W. W. Hay. The Influence of Wheel-Rail Contact Forces on the Formation of Rail Shells. Paper presented at the Winter Annual Meeting, New York, ASME, Nov. 26-30, Paper 72-WA/RT-8, 1972.
11. A. N. Hanna. A Contribution to the Clarification of Rail Shelling. Strasse-Brüke-Tunnel, Vol. 24, No. 1, 1972, pp. 8-13.
12. Y. Yasojima and K. Machii. Residual Stresses in Rails. Bulletin of Permanent Way Society of Japan, Vol. 13, No. 9, 1965.
13. D. M. Burmister. The Theory of Stresses and Displacements in Layer Systems and Applications to Design of Airport Runways. Proc., HRB, Vol. 3, 1943, pp. 126-148.
14. S. Timoshenko and B. F. Langer. Stresses in Railroad Track. Applied Mechanics, Trans., ASME, Vol. 54, No. 23, 1932, pp. 277-293.
15. Stresses in the Rails, the Ballast, and the Formation Resulting From Traffic Loads. Office for Research and Experiments of the International Union of Railways, Utrecht, Netherlands, Question D-71, Rept. 1, April 1965.
16. Concrete Ties (and Fastenings). AREA, Bull. 655, Vol. 77, Nov.-Dec. 1975, pp. 193-236.

Track Structure at Facility for Accelerated Service Testing

Ernest Nussbaum, Metrek Division, Mitre Corporation, McLean, Virginia

An overview of the track structure at the Federal Railroad Administration Facility for Accelerated Service Testing is presented in this paper. The facility consists of a 7.7-km (4.8-mile) loop of relatively conventional railroad track at the U.S. Department of Transportation's Transportation Test Center near Pueblo, Colorado. In September 1976, a loaded freight train began traveling the loop 16 h/d and was scheduled to continue doing so for 1 year, subjecting the track to as much loading as is hauled over an average freight line in 10 years. Many types, makes, sizes, and arrangements of track components (rails, ties, fasteners, and ballast) are used in the 22 track sections of the loop. The rail elements being tested include five types of rails with varying metallurgy or heat treatment, various frogs and guardrails, jointed and continuously welded rail, insulated

and glued joints, and four turnouts. Steel, prestressed concrete, reconstituted, and laminated ties were installed, in addition to several kinds of wooden ties. Differing arrangements of cut, elastic, screw, and lock spikes are used, as are various special rail fasteners and tie plates. Granite, limestone, traprock, and slag ballasts of varying depths and shoulder widths are included. The accelerated service test will provide information on the durability and maintenance requirements of these components. An extensive system of observations and measurements has been scheduled to ensure safety and collect data for immediate and long-range analysis. The results should provide the industry with new tools and knowledge to improve railroad safety, reliability, and operating economy.

Figure 1. Transportation test center (only main tracks are shown).

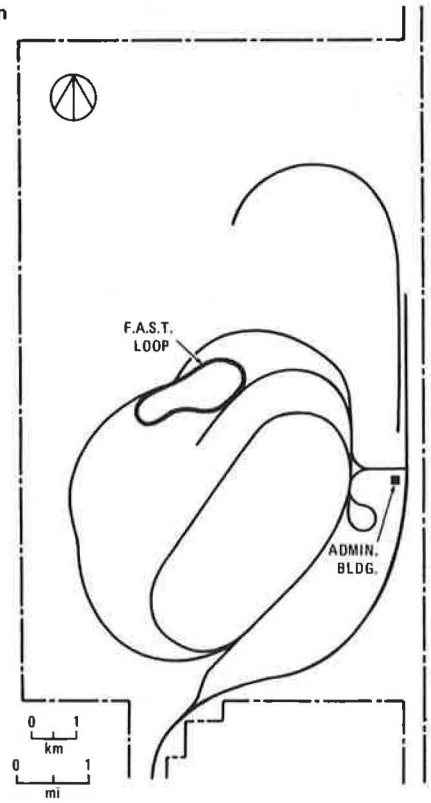

The Transportation Test Center (TTC) occupies an 8.9 by 14.5-km (5.5 by 9-mile) tract of land northeast of Pueblo, Colorado, on the high plateau immediately east of the Rocky Mountains. The Facility for Accelerated Service Testing (FAST) is but the latest addition to a considerable number of research activities there. In terms of length of track, FAST is small among the array of tracks, but in hours of train operation and number of support personnel, it represents one of the largest activities. The layout of TTC is shown in Figure 1.

BACKGROUND AND PURPOSE OF FAST

A railroad track is in some ways a more complicated structure than is a highway and is subject to much higher loads. Freight cars with gross masses of 127 000 kg (140 tons) are common, so that each of the four axle loads is 311 kN (35 tonf)—more than three times the truck axle loads allowed in many states. The initial cost of a track structure is correspondingly high, and much maintenance is required to keep it within required standards of alignment and gauge and to replace the rails and ties that wear out. Track structure has evolved over almost 2 centuries to such arrangements of subgrade, ballast, ties, and rails as are shown in Figure 2.

Although railroads and other agencies have conducted many tests and evaluations of track components, there was felt a need to conduct a comparative test program under controlled conditions. In FAST, these exist to the extent of uniform weather, subgrade, loading, and maintenance.

The purpose of FAST is to compare various types and arrangements of track components under accelerated loading and thus to discover what combinations can yield near-term improvements in railroad safety, reliability, and economy. At the same time, certain aspects of the rolling stock are also being evaluated, e.g., wheel wear. Many of the track components have been used for many years; some have been used more in other countries than in the United States; a very few have been used little or not at all in this country.

Figure 2. Typical track cross section.

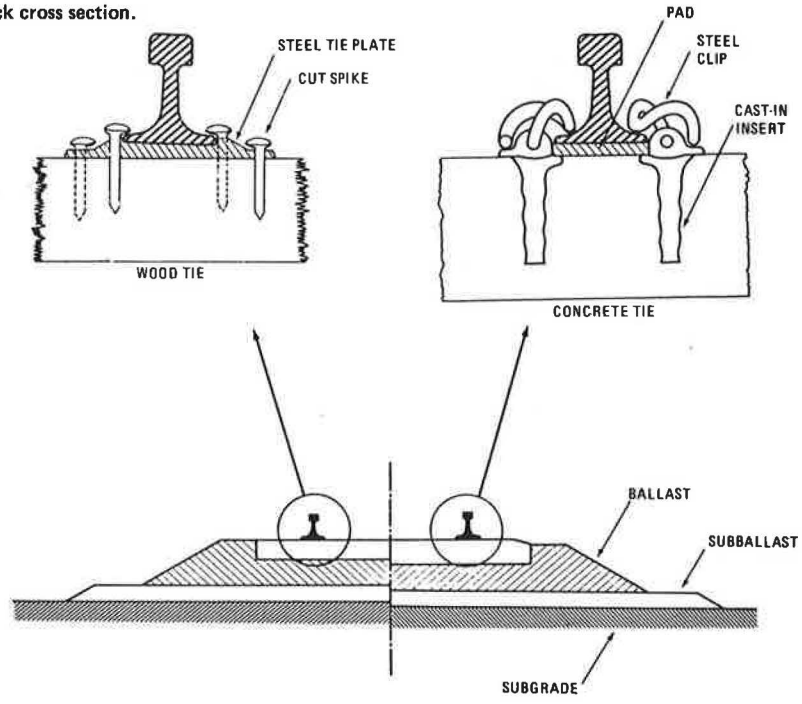

Figure 3. Location of track sections.

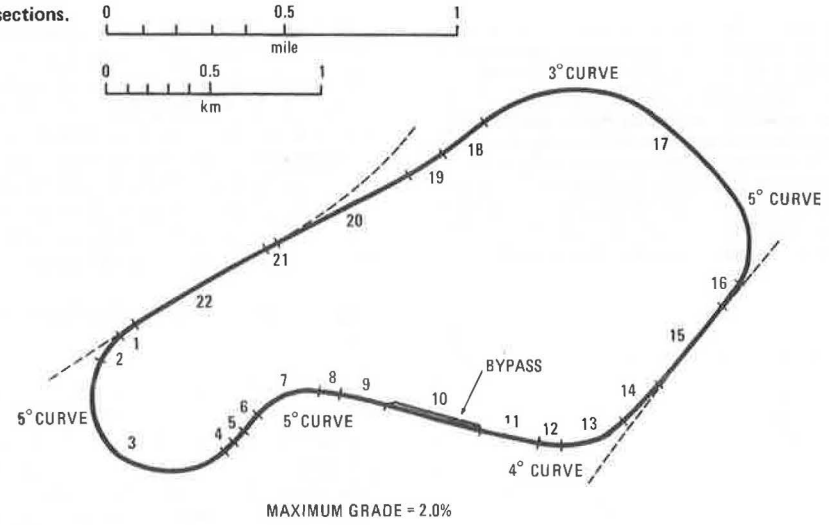

Table 1. Track sections and test items.

Section	Length (m)	Rail[a]	Principal Test Items
1	52	J	No. 20 turnout[b] (existing)
2	100	C	Rubber pads under steel tie plates[c]
3	1140	C	Rail metallurgy; varying tie plates and spiking patterns, ballasts, and shoulder widths
4	64	C	Existing track—no specific test[d]
5	67	J	Bonded rail joints[e]
6	91	C	Steel ties (removed after 4 months)
7	305	C	Special tie plates and fasteners
8	91	C	Existing track—no specific test
9	191	J	Reconstituted and laminated ties
10	472	J(C on bypass)	Elastic rail spikes, frogs, no. 20 turnouts, safety equipment on bypass
11	273	J	Joints, frogs, and guardrails[e]
12	103	J	Existing track—no specific test
13	380	C	Rail metallurgy
14	249	J	No. 20 turnout
15	396	J	Three different ballast shoulder widths
16	52	C	Glued no. 20 turnout[f]
17	1872	C	Various concrete ties and tie pads
18	250	J	Two different ballast depths
19	183	J	Hardwood versus softwood ties
20	694	J	Different types and depths of ballast; rail anchors
21	52	C	Welded no. 20 turnout
22	594	C	Different spiking patterns; rail anchors

Note: 1 m = 3.28 ft.

[a] J = jointed and C = welded.
[b] A turnout is the assembly of rails, ties, switch mechanisms, and such used at point where two tracks meet. Turnout number is related to angle of divergence, with higher numbers indicating smaller angles. (No. 20 is highest normally used.)
[c] Tie plates are usually placed directly on wooden ties. Pads between ties and plates are intended to minimize tie plate cutting, but have been used relatively little.
[d] Existing track sections that were not modified for FAST (nos. 1, 4, 8, and 12) serve as comparison to other sections.
[e] Guardrails are short sections of rail placed inside the regular rail in frog and switch areas to guide the wheels.
[f] Rail joints are most commonly bolted, but the development of modern adhesives has led to the introduction of bonded (adhesive-bonded) joints.

Comparison With AASHO Road Test

Many engineers with highway experience are struck by the apparent similarity of FAST to the AASHO Road Test (1) of 2 decades ago. There are similarities, of course, but there are also differences:

The AASHO Road Test was conceived . . . as a study of the performance of highway pavement structures of known thickness under moving loads of known magnitude and frequency. Both portland cement concrete and asphaltic concrete pavements, as well as certain types of bridges, were included in the test facility.

The test road had six loops of dual-lane roadway with lengths of 1.3 to 4.3 km (0.8 to 2.7 miles). The axle loads ranged up to 214 kN (24 tonf). The test lasted 2 years, during which approximately 20 years of average highway use was simulated. Thus, FAST is similar to the AASHO test in concept and purpose. It is different in that a greater variety of materials are being tested (although no bridges) and that rolling stock and safety-related aspects are also being evaluated.

Limitations of FAST

One limitation of FAST is imposed by the climate at Pueblo. The annual precipitation is only about 30 cm (12 in) of rain plus 81 cm (32 in) or snow, and in recent winters, there has sometimes been less snow. Thus, although the track can be exposed to 10 years' loading in 1 year, 10 years' rainfall or freeze-thaw cycles will not be simulated. (A track can, of course, be watered artificially, but this is not practical at FAST.)

The geometry of the FAST loop causes some limitations, since there can be only a few different grades and degrees of curvature in an 8-km (5-mile) track. The percentage of curved alignment is much higher than on most railroads. Train speed, also, is not as varied as in real-life situations. Nevertheless, FAST will furnish a large amount of comparative, if not always absolute, performance data that should be of immediate use to the railroad industry in achieving more economical construction and maintenance procedures.

TRACK

The FAST track is divided into 22 sections of varying length, as shown in Figure 3. Not quite half the track (sections 16 to 21) was built expressly for FAST; the remainder (sections 22 and 1 to 15) had been built for previous test programs, but was extensively modified for this project. The principal test items are shown in Table 1. The rail elements tested are described below (1 m = 3.28 ft and 1 kg = 2.2 lb).

Item Tested	Section(s)	Description
Rail metallurgy and heat treatment	3	Ten segments, each containing 23.8 m chrome moly rail, 23.8 m high-silicon rail, 23.8 m head-hardened rail, 23.8 m fully heat-treated rail, and 18.9 m standard rail

Item Tested	Section(s)	Description
	13	Four segments, each containing 23.8 m chrome moly rail, 23.8 m high-silicon rail, 23.8 m fully heat-treated rail, and 23.8 m standard rail
Turnouts	1 and 14	Standard no. 20 turnout
	16	Glued (bonded) no. 20 turnout
	21	Welded no. 20 turnout
Frogs and guardrails	10	Two no. 14 60.5-kg spring frogs, long entrance-flare guardrails
	11	Four no. 14 60-kg hammer-hardened manganese frogs, two with standard and two with long guardrails, and four no. 14 60-kg standard cast manganese frogs, two with standard and two with long guardrails
Joints	5	Six different pairs (12 total) glued (bonded) joints, half insulated and half noninsulated
	11	Four different pairs (8 total) insulated (but not bonded) joints

All sections except those specifically otherwise described use mostly standard hardwood ties and switch ties at the turnouts. The types of ties tested are described below (1 cm = 0.39 in).

Type of Tie Tested	Section	Description
Steel	6	Approximately 170 steel ties spaced 53 cm apart, with plastic pads as insulators
Reconstituted and laminated	9	Approximately 84 reconstituted and 100 laminated ties, spaced 50 cm apart (standard spacing)
Concrete	17	Six different concrete ties (approximately 2900 total) distributed among 17 subsections, with varying pad and fastener combinations
Wood	19	Approximately 185 hardwood ties, followed by 185 softwood ties, spaced 50 cm apart (standard spacing)

All sections having wooden ties except those specifically otherwise described use standard tie plates [i.e., 20 by 36 cm (7.75 by 14 in), with eight square spike holes (four on each side), and a cross slope (cant) of 1 to 40 in the rail-seat area] and the usual pattern of two or three spikes on each side. The tie plates and fasteners tested are described below (1 cm = 0.39 in).

Item Tested	Section(s)	Description
Tie plates	2	Standard plates and ties with rubber pads under plates
	3	Three different plates (standard, 22 by 40 cm with 1 to 30 cant, and 20 by 36 cm with 1 to 14 cant) on 5° curve
Spiking pattern	3 and 22	Varied numbers and arrangements
Special spikes	7	Five equal parts of 66 m each that use lock spikes, screw spikes, compression clips, elastic clips, and standard spikes
	10	Subsection with special elastic spikes
Anchors	20 and 22	Varied types and patterns

Sections 1 to 15 and 22, which predated FAST, use blast-furnace slag ballast. Sections 16 and 21 and part of section 20 were also constructed using slag ballast; sections 17, 18, and 19 use granite ballast; and section 20 has four types of ballast—granite, limestone, traprock, and slag. The depth of ballast under the ties is varied in sections 18 and 20 from 15 to 41 cm (6 to 18 in), and the ballast shoulder width varies from 15 to 41 cm in sections 3 and 15.

Track Structure

Track structure on grade consists of five main parts: rails, ties, fasteners, ballast, and subgrade. Space does not permit a detailed description of each, but a short discussion may be appropriate for readers with limited railroad experience.

Rails

Rails are made from rolled steel, with cross sections showing a narrow head, a thin web, and a wide base, which is slightly narrower than the total height. The weight of rail used on mainline track varies between approximately 45 and 74 kg/m (90 and 150 lb/yd). Most of that used in FAST is 67.5 kg/m (136 lb/yd). Various alloys and heat treatments or both are used to produce rail for severe service conditions, especially curves. In the past, almost all rail was laid in 11.9-m (39-ft) sections connected with joint bars (Figure 4). The present trend is toward increasing use of continuously welded rail. FAST incorporates both jointed and welded rail, with heat-treated or alloy steel rails installed in sections 3 and 13. The rail in switches and frogs (points at which two rails cross, as in turnouts and crossings) is particularly subject to severe loading conditions; several such track areas appear in FAST and are test items in sections 1, 10, 11, 14, 16, and 21.

Ties

Crossties are one of the distinguishing marks of a railroad track. (Consider how railroads are denoted on maps.) The ties support the rails and distribute the wheel loads to the ballast. Traditionally, ties are made of wood, preferably hardwood such as oak. The typical size is 17.8 cm (7 in) deep, 22.9 cm (9 in) wide, and 2.6 to 2.7 m (8.5 to 9.0 ft) long; the typical spacing is 49.5 cm (19.5 in) center to center. Most wooden ties are chemically treated to prevent early decay. The life of a treated timber tie may be anywhere from 10 to 50 years, depending on loading, chemical treatment, climatic conditions, type of wood, and track maintenance. In a recent year, about 20 million wooden ties were replaced in the United States (2).

Twenty million is a large number, and suitable timber for ties is becoming increasingly scarce and costly. Hence, substitutes for wooden ties have long been sought. A leading contender is prestressed concrete. (All references hereafter to concrete ties imply prestressed concrete.) In some European countries, concrete ties are rapidly supplanting wooden ones. In North America, wooden ties still predominate, but some railroads are making extensive use of concrete ties. Section 17 of FAST—the longest single section [1872 m (6143 ft)]—consists almost entirely of concrete-tie track, with five manufacturers of them represented. There are about 2900 concrete ties, spaced 61 cm (24 in) center to center; all are new, except one group of 100 that was previously used in the Kansas Test Track, another recent experimental railroad section.

Other substitutes for wood are also being evaluated. One of these is steel; section 6 was built with a recently developed steel tie. (The steel ties were removed after a few months because of fastener problems.) Another is the reconstituted tie, which is made by grinding up used wooden ties and bonding the chips with a suitable resin binder. Laminated ties composed of two pieces are still another approach; these can be made from timber sections that are smaller than those needed for conventional ties. Track section 9 incorporates both reconstituted and laminated ties.

Figure 4. Typical bolted rail joint (new track—ballast not in place).

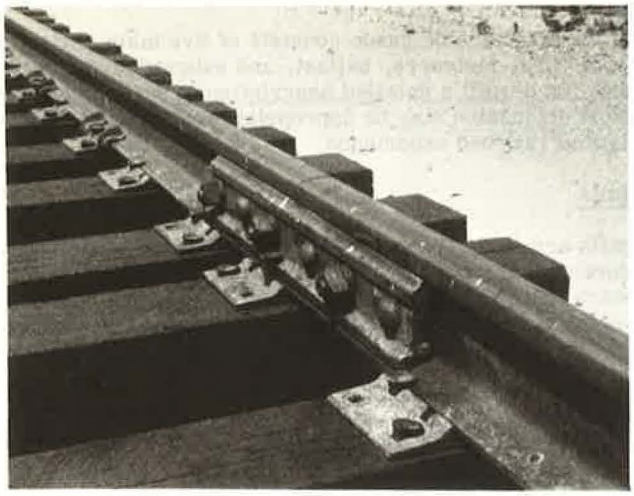

Figure 5. Typical arrangement of tie plates, spikes, and rail anchors (new track—ballast not in place).

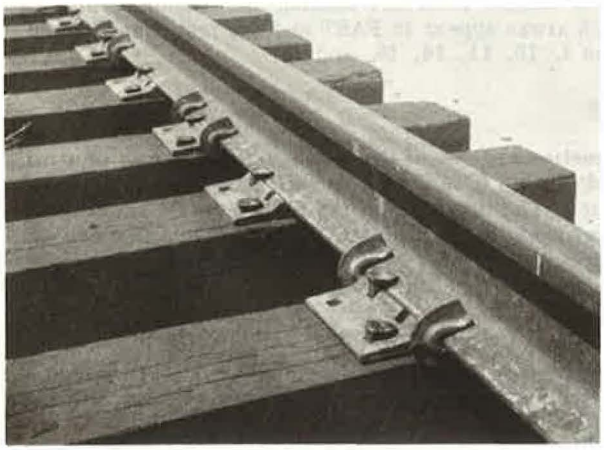

The question is sometimes asked, Why use ties at all? Why not fasten the rails to a (continuous) concrete slab?

Continuous concrete supports for rails have indeed been tested. They are being used extensively on urban rail transit facilities, such as the Washington Metro System. But the loads on passenger lines are relatively light, and what works well on such tracks does not necessarily work well under heavy freight loads. Thus far, the use of continuous concrete supports for rails on freight lines has been minimal in the United States.

Wooden ties will continue to predominate on U.S. railroads for some years (a variety of softwood and hardwood ties are used in FAST), but the quest for timber substitutes will continue. FAST offers the opportunity to evaluate the service life and maintenance characteristics of prestressed concrete, as well as other recently developed, ties.

Fasteners

Rails are supported on ties by fasteners that, as a minimum, maintain the proper gauge—normally 143.5 cm (4 ft 8.5 in)—between the inside faces of the rails.

The typical arrangement on wooden ties consists of a steel tie plate that distributes the rail load to the tie surface and is held in place with square rail spikes driven through holes in the plate (Figures 2 and 5). Not all tie plates are alike, and the square spikes are sometimes replaced by other devices. Some of these variables are tested in sections 2, 3, 7, 10, and 22. In addition, rail anchors are used to prevent longitudinal creep of the rails (Figure 5). A number of types of anchor are being compared on FAST. On concrete ties, the rail and tie are separated by a pad that cushions the interface of the rail and the tie. Several different pad materials are being tested in section 17. Fastening the rail to concrete ties poses special problems. Spikes driven into the tie are obviously not practical. Instead, the ties have inserts cast into the concrete at the time of manufacture; after the rail is in place, a steel fastener connecting to the insert holds the rail to the tie.

Figure 6. Rail fastener on concrete tie.

There are many different fasteners for concrete ties available. In FAST, the type shown in Figure 6 is used on the majority of ties. With several different types of concrete tie and several pad materials being tested on several alignments, it was decided not to introduce still more variables. However, two short segments of track do have fasteners different from the predominant type.

Ballast

Railroad ties are commonly embedded in crushed stone or slag. This ballast resists the horizontal movement of the ties, furnishes drainage, and distributes the tie loads to the underlying subgrade. The ballast bed also helps provide resilience and flexibility to the track structure, thus cushioning the impact loads and prolonging the life of other track components and of the rolling stock.

Ballast possesses all these desirable qualities as long as it is composed of properly sized particles; remains unclogged by oil, soil, windblown sand, or crushed ballast fines; and supports the ties properly (under the rail seats but not in the middle). To keep the ballast in this condition requires periodic maintenance—cleaning, reshaping of the cross section, and tamping. Such maintenance is now carried out mostly with mechanical equipment, but is nevertheless very costly. The particles themselves deteriorate from weathering and crushing by the high axle loads, and eventually the ballast may have to be entirely replaced. Some materials are more durable than others (crushed granite is considered excellent, and limestone, traprock, and blast-furnace slag are also used), but local availability often dictates which will be used.

All of these materials are used in FAST. In addition, the depth of ballast under the ties and the shoulder width (the distance to which the ballast extends beyond the tie ends) are varied. These factors affect the amount of maintenance required for keeping the track geometry within prescribed limits. FAST affords an opportunity to evaluate the cost trade-off between the first cost of ballast and the maintenance cost of the entire track system.

Subgrade

The importance of a good subgrade is the same under a railroad track as under any heavily loaded structure. In FAST, the subgrade is not a test item per se. However, roughly half the subgrade is 3 to 4 years old and thus has had more time to consolidate than the half that was built during the first months of 1976. Hence, the different degrees of consolidation of these two subgrades may affect the performance of the remaining track elements.

TESTS

The test program is aimed at determining the combinations of track components that can yield the greatest near-term improvements in railroad safety and economy. As in all complicated systems, there are interactions among the various elements. For example, the use of wider ballast shoulders at the ends of the ties should reduce the frequency of maintenance needed for keeping the track in proper alignment. But is the extra first cost of the wider ballast justified by the savings due to the lower frequency of track alignment? A more difficult question is posed by the following: Heavier car ladings can increase the productivity of a rail line, but will lead to increased maintenance requirements. What is the cost trade-off between these two factors? The problem is analogous to that in the highway field, where higher pavement maintenance costs are incurred if truck axle loads are permitted to increase.

FAST will provide some answers to such questions. Car loadings will remain essentially constant during the first year of operation, but additional periods of testing with reduced ladings are planned, so as to yield a comparison of maintenance requirements.

The test program, consisting mainly of measurements and observations of material or performance changes in track structure, will in most cases permit comparisons among components or track designs in terms of maintenance or replacement frequency and cost. In some instances, absolute measurements will record the changes that take place with increased loadings or determine the various parameters under loading to provide input for the development of mathematical models that can predict track behavior.

Some measurements are safety or maintenance oriented and are performed over the entire track at frequent intervals, even daily. These include (a) track inspection (a daily visual examination), and (b) track geometry (measurement of gauge, vertical alignment and smoothness, horizontal alignment, and cross-level or superelevation), which is carried on by surveying methods as well as by an instrumented track-geometry car.

Other maintenance-oriented tests and measurements, which are taken at intervals of several days or weeks, include (a) rail-flaw detection (ultrasonic examination of the rail by a specially equipped car), (b) survey of ballast cross section, (c) rail-surface wear, (d) rail hardness, (e) rail and joint insulation (electrical resistivity), (f) rail creep (longitudinal movement), (g) tie-plate cutting (gouging of wooden ties by steel tie plates), and (h) rail stress (longitudinal stress related to temperature changes and rail restraint and anchoring methods).

Measurements made with special instrumentation, generally at selected locations as pertinent to particular track components, include (a) tie-plate load (dynamic live loads on ties), (b) tie stresses (on steel ties), (c) spike-pullout resistance, and (d) horizontal and vertical track stiffness.

A special set of tests and instruments, designed for the concrete-tie section, include (a) ballast and subgrade pressure, (b) subgrade settlement, (c) tie stresses, and (d) rail seat load at pads (analogous to tie-plate load measurement on wooden ties).

There is also a very thorough program for detecting and monitoring cracks or other deterioration in the concrete ties and the various pads being tested.

SUMMARY

An overview of the track at FAST has been presented. The project is expected to improve railroad operating economy, reliability, and safety.

FAST began operating in the fall of 1976. By the end of 1977, a significant number of test results should be available to the railroad industry to provide new knowledge and tools for improving the rail transportation system.

ACKNOWLEDGMENT

The concept and configuration of FAST are the results of coordination and cooperation among many participants in the international government-industry research effort known as the Track Train Dynamics program. Members of that program are the Federal Railroad Administration, the Association of American Railroads, the Railway Progress Institute, and the Transportation Development Agency (of Canada). FAST was constructed by using ballast, track components, rolling stock, and locomotives largely provided by operating railroads and their suppliers. The Federal Railroad Administration funded the construction and maintenance of the track, the operation and maintenance of the train, and the collection and analysis of data. Various consulting firms are also contributing to the effort. The participation by Mitre/Metrek was funded by the Federal Railroad Administration.

REFERENCES

1. AASHO Road Test: History and Description of Project. HRB, Special Rept. 61A, 1961, p. v.
2. Crosstie Crisis. Railway Track and Structures, Dec. 1973, pp. 14-17.

Problems and Needs in Track Structure Design and Analysis

Arnold D. Kerr, Department of Civil Engineering, Princeton University

This paper reviews the design aspects of old and new track systems, the research needs in track structure design, and methods of track analysis.

Railroad tracks have been in use since the eighteenth century. Originally many kinds of track systems were built, but during the nineteenth century, two of these—the longitudinal-tie track and the crosstie track—came to predominate. In the longitudinal-tie track, the rails are continuously supported by wooden or metal beams, and the gauge is maintained by cross bars or crossties. In the crosstie track, the rails are discretely supported by closely spaced wooden or metal crossties. Eventually, the crosstie track became the dominant mode of track construction.

Since World War II, concrete has been increasingly used abroad for the production of ties. The ties currently produced are mainly crossties. However, in view of the historic development of the railroad track and the well-established properties of concrete as a structural material and the ease with which it can be formed into various structural shapes, it is not a priori obvious that the crosstie track is technically and economically the most satisfactory solution when concrete is used as the tie material.

In the first part of this paper, the design aspects of various old and new kinds of track systems are discussed to illustrate this point. This is followed by a discussion of various design aspects of the track system used at present in the United States; i.e., the wooden crosstie track.

The second part of this paper presents a discussion of railroad track analyses. Some of the early papers in this field were published in the middle of the nineteenth century, and there have been many since then. A thorough review and discussion of them is beyond the scope of one paper. Thus, this part of the paper is restricted to a brief review of analyses of static stresses and the stability of track structures, which form a large part of the track analyses published.

PROBLEMS AND NEEDS IN TRACK STRUCTURE DESIGN

The steam locomotive was introduced into regular service during the first half of the nineteenth century. The subsequent rapid improvement of the locomotives resulted in continuously increasing train speeds and higher wheel loads, which in turn continuously increased the demand for stronger and better railroad tracks (1).

During the nineteenth century, both the longitudinal-tie track and the crosstie track were used. In the course of time, the use of the longitudinal-tie track decreased and, at present, the crosstie track is the dominant mode of track construction (2,3). Originally, the crossties were made of wood, as shown in Figure 1a. A number of railways also used metal crossties. For the past two decades, prestressed concrete crossties have been increasingly used on many railways abroad. A typical track with prestressed concrete ties is shown in Figure 1b.

In the U.S., because of the heavy wheel loads, the introduction of concrete crossties caused difficulties. Also, the availability of wooden ties at comparable prices, and the thorough familiarity of our railroad engineers and maintenance crews with their installation and maintenance, did not create the sense of urgency for the rapid development of concrete ties that was the case in many countries abroad. However, work on concrete crossties continues (4). A state-of-the-art survey of the development of concrete crossties in the United States is contained in a recent presentation by Weber (5). The design, production, installation, and maintenance of concrete ties are described by Zolotarskii and others (6) and by Shrinivasan (7). It is expected that a prestressed concrete crosstie suitable for United States conditions will be available for use on main lines in the near future.

When the crosstie track was first introduced, wheel loads were small, and tie spacing was relatively large. As the wheel loads progessively increased, the tie cross section increased, and the tie spacing decreased. But, with current track-maintenance practices, the spaces between the ties cannot be reduced beyond a certain limit. Because of this and other mechanical and economical factors (such as the desire to minimize the increase in track maintenance that is caused by the ever-increasing wheel loads and train speeds), attempts are being made to eliminate the tie spaces altogether by using, instead of discrete ties, a continuous reinforced-concrete slab. The rails, discretely or continuously supported, are secured to the slab by fasteners that are anchored in the slab. Sections of such slab tracks have recently been built by a number of railroads abroad (Figure 2a). In the United States, a track of this type was built and successfully used about 50 years ago (8). Descriptions of design details of recently built slab tracks (also referred to as ballast-free tracks) and their performance have been given by Birmann (9), Lucas and others (10), Miyamoto (11), Bramall (12), Eisenmann (13, 14), and elsewhere (15).

Another noteworthy design is the concrete frame track, which is being developed in the USSR (16, p. 62). For the past several years, this track has been undergoing extensive testing at the Shcherbinka test loop and in a main line in the southern part of the USSR (17). In this system, instead of crossties, 2.50-m long, precast, prestressed concrete frames are placed in the ballast, as shown in Figure 2b. This system has a high lateral rigidity like the slab track, but is lighter and is more accessible, and therefore easier to maintain. In view of the present tamping practice, in which the ballast is compacted only in the vicinity of the rail seats, the frame track is a logical modification of the crosstie track.

The introduction of the slab track, and especially of the frame track, is essentially a return to the longitudinal-tie track, which lost out to the crosstie track some time ago. In this connection, one should note the earlier attempts to introduce the concrete longitudinal-tie track in the U.S. as described elsewhere (18, 19).

According to Winkler (20), one of the main reasons

Figure 1. Crosstie tracks currently in use.

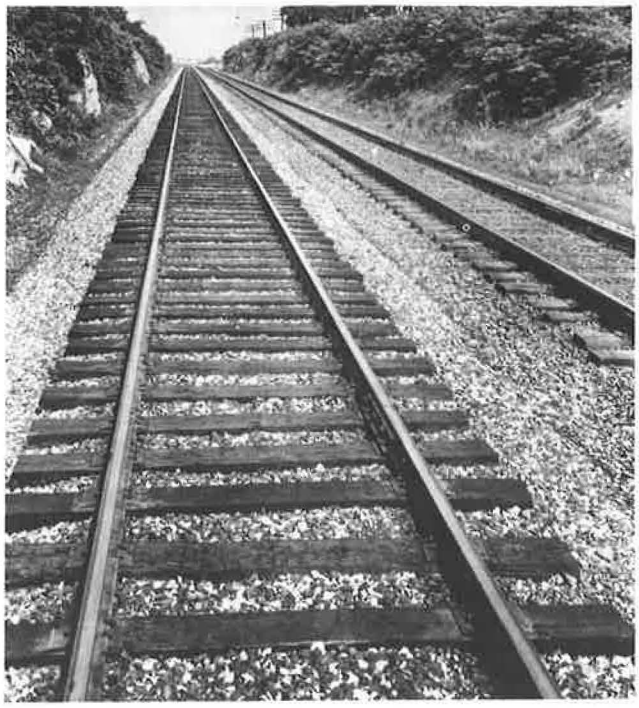

(a)

(b)

for abandoning the longitudinal-tie track in the second half of the nineteenth century was the warping of the long wooden longitudinal ties. Another reason was the difficulty of holding the gauge with the iron rods or wooden crossties that were placed under the longitudinal ties. Also, because the wooden crossties were widely spaced, they contributed to an undesirable periodic disturbance in the ride. This situation is reflected in the railway codes of the period (20, p. 210), which prescribed the use of a crosstie track system when wooden ties were used and the use of a longitudinal-tie track system when metal ties were used.

The slab track and the frame track are free of these limitations, except that the frame track may cause periodic disturbances because of the cross bars in the frames. Whether these disturbances are noticeable will have to be established in tests. Also, when the rails are continuously supported by a slab or frame-track, the height of the rail can be reduced because, as shown by Kerr (21), the slab or frame, when properly designed, will carry part of the load.

These remarks should not be construed as an endorsement of the slab track or the frame track. Their purpose is merely to point out the various new possibilities open to the railroad engineer when concrete is considered as a tie material. In past decades, railroad engineers became used to the crosstie track as the only workable system, and it was natural, when concrete was first considered as tie material, to build concrete crosstie tracks. However, the multitude of other concrete tie systems—e.g., Laval ties and wing ties—that have been proposed recently and the increasing mechanization of track activities mean that the prestressed-concrete crosstie track is not necessarily the most suitable track system for the future.

The development of a proper concrete tie system for U.S. tracks should be a major challenge to railroad engineers. In addition to satisfying the necessary technical criteria, such a track should be easy to install, easy to maintain (this includes replacement of parts), and in general keep costly track maintenance to a minimum.

In the United States at present, the wooden crosstie track is the dominant mode of track construction, and this situation will not change substantially for at least the next several years. Therefore, it is essential to discuss also the design aspects of this track system. This system was developed about 100 years ago. It has performed well for many decades. However, with increasing wheel loads and train speeds some limitations are becoming apparent.

One weak element in the present system is the cut-spike fastener (Figure 3a). As is well known, on main-line tracks that have been subjected to traffic, many cut spikes can be pulled out by hand. One should not wonder why rail turnover occurs sometimes, but rather why it does not occur more often. A recent review of rail turnover has been given by Zarembski (22).

To prevent rail turnovers, a number of European railroads at the turn of the century replaced the cut spikes by screw spikes (Figure 3b) and developed special base plates for use on curves (Figure 3c). Later, the more rigid and elaborate K-type fasteners (Figure 3d) were introduced, and more recently, a variety of spring type fasteners (Figures 3e and 3f), have been developed. A discussion of a large variety of fasteners has been given by Schramm (23).

There were also many attempts in the United States to improve the cut-spike fastener. This is evident from the many fasteners that have been registered with the U.S. Patent Office since about 1860, as shown recently by Posner (24). However, the use of the cut-spike fastener has prevailed until the present.

Because of the increasing wheel loads and train speeds and the problems encountered with cut-spike fasteners, there is a need for the development of an improved fastener for U.S. conditions that will be technically sufficient and economically feasible. Although the K-type fastener may prove to be uneconomical for our railroads, simpler systems (e.g., the types shown in Figures 3b and 3f) may satisfy the necessary criteria.

The technologies of producing and preserving wooden crossties are well established. At present, an average

Figure 2. Nonconventional tracks.

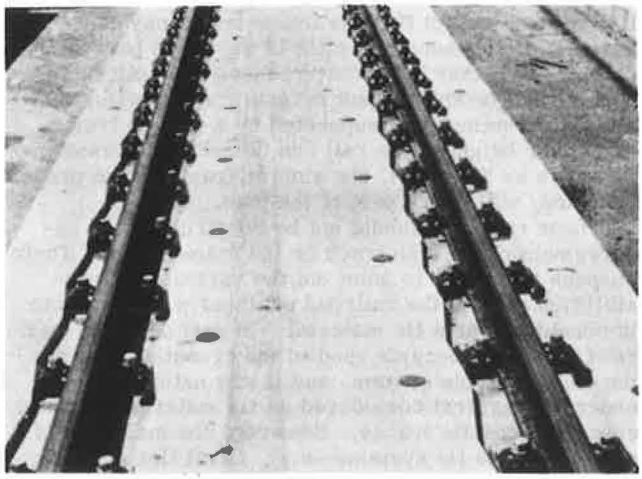

(a)

(b)

Figure 3. Rail-tie fasteners.

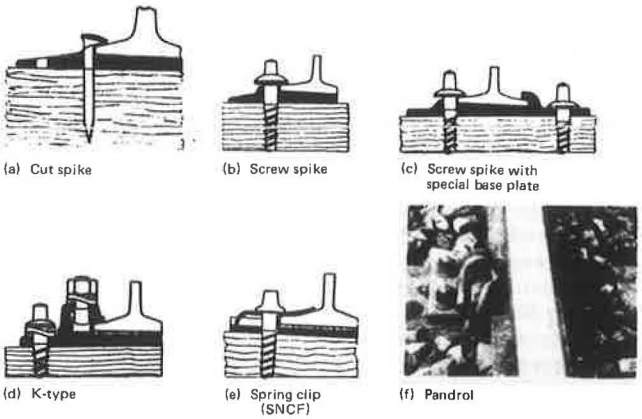

wooden tie stays in main-line service for about 25 years. To extend this period (often on secondary lines), some railroads restore some of the damaged ties. Extensive studies of this subject are given by Lysyuk (25) and Bondarev and Zhuravskii-Skalov (26).

Ballast material has also been the subject of many studies. Recent results have been given by Raymond and others (27), Klugar (28), Shenton (29), and Knutson and others (30). These studies should contribute to a better understanding of the response of ballast to static and dynamic loads, establish useful criteria for choosing ballast material, and lead to economical methods for its maintenance while in line service.

From a design point of view, the ballast section, as used in the United States at present for continuously welded rails, may require modification. According to tests performed abroad and analytical studies conducted recently, wider shoulders than those used by our railroads [15 cm (6 in) on tangents and 31 cm (12 in) on curves] are needed to prevent track buckling. For example, the DB and the railroads of the USSR use ballast shoulders of 35 and 45 cm (14 and 18 in) on tangents and curves respectively.

The observed movement of ballast particles away from the rail-seat region, which is caused by the passage of trains, suggests that ballast shoulders wider than 15 cm may also reduce track degradation and thus track maintenance.

These facts point toward the need for establishing optimal ballast shoulder widths for U.S. conditions, to prevent track buckling and to reduce track maintenance.

There are many other problems in track design—that should be discussed such as clarification of the need for placing expansion joints in continuously welded tracks (especially on bridges), and the proper design of tracks at the approaches to bridges or in the vicinity of track-highway intersection—but these are beyond the scope of this paper.

PROBLEMS IN TRACK STRUCTURE ANALYSIS

Although the development of the railroad track was mainly intuitive, based on a trial and error approach, since the second half of the nineteenth century, railroad engineers have been attempting to analyze the track and its components.

Early workers attempted to determine the bending stresses in the rails and ties. In 1867, Winkler (31) analyzed the stresses in the rails of a longitudinal-tie track by considering the rails as continuously supported beams. The differential equation for the bending of an elastic beam is

$$EI(d^4w/dx^4) + p(x) = q(x) \quad (1)$$

where

$w(x)$ = vertical deflection of point x on track axis,
EI = flexural rigidity of rail and tie,
$p(x)$ = continuous contact pressure between tie and base, and
$q(x)$ = distributed vertical load,

all as shown in Figure 4.

For the response of the base, Winkler proposed the relation

$$p(x) = k_r w(x) \quad (2)$$

where k_r = base parameter for one rail and tie. This is the origin of the well-known Winkler foundation model. The resulting track equation

$$EI(d^4w/dx^4) + k_r w = q \quad (3)$$

is a fourth-order ordinary differential equation and represents the response of a beam that is attached to a spring base (Figure 5).

In 1882, Schwedler (32), in discussing the bending stresses in the rails of a longitudinal-tie track, gave the following solution of Equation 3, for the case when

Figure 4. Equilibrium position of deformed rail.

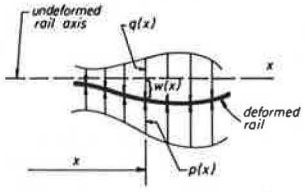

Figure 5. Continuously supported rail subjected to a load q(x).

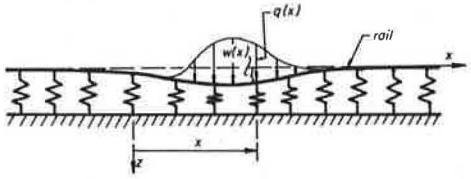

Figure 6. Deflected rail-tie structure.

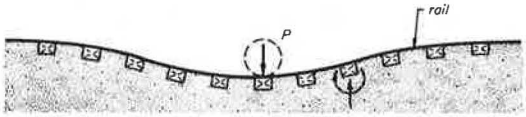

Figure 7. Continuously supported rail with rotational resistance of ties.

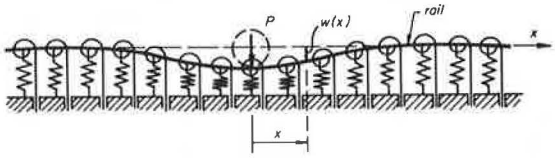

a very long track is subjected to a concentrated force (P)

$$w(x) = (P\kappa/2k_r)\, e^{-\kappa x}\, [\cos(\kappa x) + \sin(\kappa x)] \qquad (4)$$

and the corresponding expression for the bending moments

$$M(x) = (P/4\kappa)\, e^{-\kappa x}\, [\cos(\kappa x) - \sin(\kappa x)] \qquad (5)$$

where $\kappa = (k_r/4EI)^{1/4}$. Schwedler used these expressions as influence functions to determine the effect of several wheel loads.

In 1888, Zimmermann (33) published a book that contained solutions of Equation 3 for many special cases of interest in the analysis of railroad track. Like Schwedler, Zimmermann used the solutions he had obtained to analyze the longitudinal-tie track, but he also analyzed the ties of the crosstie track. He, like Schwedler, compared the analytically obtained and the measured deflection curves of a longitudinal-tie track caused by two loads of 6.3 Mg (7 tons) each. The close agreement found between the measured and the calculated deflections pointed to the conclusion that the bending theory for a beam on a linear Winkler base was sufficient for the analysis of the longitudinal-tie track. More details of the analysis of longitudinal-tie tracks have been given by Kerr (21).

The development of analyses for the rails of a crosstie track was more involved. The rail was first considered as a beam resting on discrete rigid supports, then as one resting on discrete elastic supports, and then as one resting on a continuously supported beam. A critical survey of these rather turbulent developments has been given by Kerr.

The method that ultimately prevailed for the analysis of the bending stresses in the rails is based on the assumption that for a crosstie track also, the rails respond as a continuously supported beam. Thus, Equation 3 is valid for this case also, provided the coefficients EI and k are properly chosen. Early investigators who used this approach were Flamache (34) in 1904, Timoshenko (35) in 1915, and the ASCE-AREA Special Committee on Stresses in the Railroad Track (36) in 1917. The trend toward steadily increasing wheel loads, which has been countered by a steady decrease in the crosstie spacings, increased the justification of the continuity assumption. The analytical solutions based on Equation 3 were compared with corresponding measured results by the ASCE-AREA Special Committee and by Wasiutynski (37). The relatively close agreement found indicated that Equation 3 is also suitable for the analysis of the rails of a crosstie track (21).

Once the continuity of rail support is accepted, the determination of the vertical force the rail exerts on a tie is as follows: It is the contact pressure $p = k_r w$ given in Equation 2 integrated from half span to half span, or approximately the pressure ordinate at the rail seat multiplied by the center-to-center tie spacing. The determined largest force (F_{max}) that each rail can exert on a crosstie caused by the anticipated wheel loads of a moving train is then used for the stress analysis of the crossties.

One deficiency of the track analyses based entirely on Equation 3 is suggested by the observation that, for example, in front of a locomotive, over a certain interval, the track lifts off the ballast. In this liftoff region, Equation 3 is not valid, because $k_r = 0$. Problems of this type have recently been solved by Weitsman (38).

Another deficiency of Equation 3 for the analysis of the bending stresses in the rails has been discussed by Hanker (39, 40), who pointed out that when the rails deflect in the vertical plane, the crossties rotate about their axes and, because the ballast resists these rotations, the ties also exert moments on the rails (Figure 6). By assuming that discrete rotational resistances act at each tie, Hanker proposed an approximate method to remedy this deficiency. In 1974, Kerr (1) suggested that the effect of these reaction moments can easily be taken into consideration by assuming that the reaction moments are also continuously distributed along the beam. By assuming that the distributed reaction moment at point x is proportional to the angle of rotation at x, Kerr obtained the following equation:

$$EI(d^4w/dx^4) - \rho(d^2w/dx^2) + k_r w = q \qquad (6)$$

where ρ = proportionality constant. Equation 6 is a fourth-order ordinary differential equation with constant coefficients. It is identical to the equation of a stretched beam that is attached to a Winkler base. Thus, in the framework of a linear formulation, the effect of the continuous reaction moment is the same as the effect of an axial tension force in the rails of intensity ρ.

To show the effect of the tie-resistance moments on the behavior of the track, let us analyze a long straight track in which each rail is subjected to a wheel load P (Figure 7), by using equation 6. Since the track response is expected to be symmetric, the origin of the coordinate system is placed at the load P, and the analysis is restricted to $x > 0$. From regularity conditions at $x = \infty$ and the matching conditions at P,

$$(dw/dx)|_0 = 0, \qquad (d^3w/dx^3)|_0 = P/2EI \qquad (7)$$

Figure 8. Dependence of deflections and bending moments on ρ.

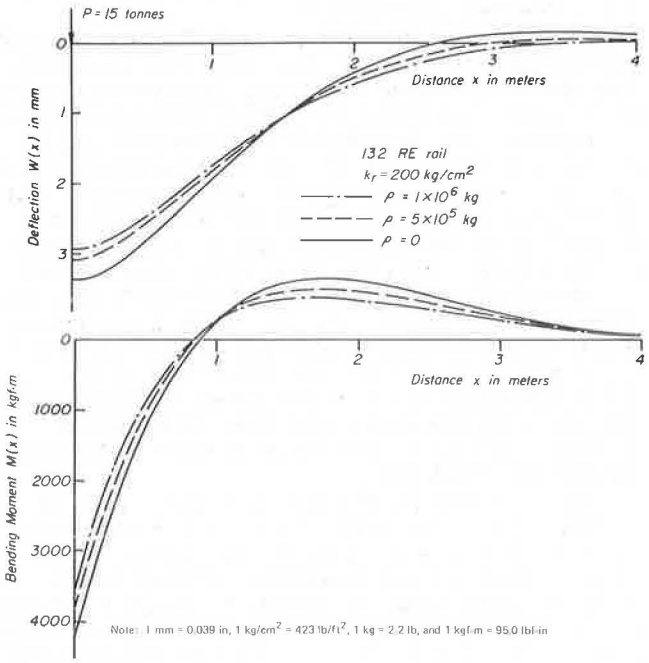

the resulting solution for $x > 0$ is (41, p. 129)

$$w(x) = (P/2k_r)(\kappa^2/\alpha\beta)e^{-\alpha x}(\beta\cos\beta x + \alpha\sin\beta x) \quad (8)$$

and the corresponding moments are

$$M(x) = (P/4)(1/\alpha\beta)e^{-\alpha x}(\beta\cos\beta x - \alpha\sin\beta x) \quad (9)$$

where $\alpha = (\kappa^2 + \rho/4EI)^{1/4}$, $\beta = (\kappa^2 - \rho/4EI)^{1/4}$.

To show the effect of the new parameter (ρ), Equations 8 and 9 were numerically evaluated for a track having a base parameter for one rail of $k_r = 200$ kgf/cm^2 (84 500 lbf/ft^2), various values of ρ, and P = 15 Mg (15.3 tons). The results obtained are shown in Figure 8. For these track parameters, the largest deviation of the deflections and the bending moments is up to 20 percent, a range anticipated by Hanker (40, p. 47).

If, in addition, the base response is improved by replacing the Winkler foundation by a two-dimensional Pasternak foundation (42, 43), then Equation 6 becomes

$$EI(d^4w/dx^4) - (\rho + G)(d^2w/dx^2) + k_r w = q \quad (10)$$

where G = second foundation modulus. Equation 10 is identical to Equation 6 except for the coefficient of the second term. Thus, the solution stated for Equations 8 and 9 is also valid for this case if ρ is replaced by $(\rho + G)$.

When determining the vertical force a rail exerts on a tie, it should be noted that if Equation 6 is used for the analysis of the rails, then the pressure exerted by one rail is as before—i.e., $p(x) = k_r w(x)$. However, if Equation 10 is used, the pressure is $p(x) = k_r w(x) - Gd^2w(x)/dx^2$ (42).

The determination of the base parameter k_r, which enters Equation 3, has been discussed by Kerr (21) who showed that the conducted tests for obtaining k_r, which loaded only one tie, are conceptually incorrect, because k_r depends on the loading area. Because of the simplifying assumptions implicit in Equation 2 and hence also in Equation 3, the determination of k_r should be such that the analytically obtained quantities (such as rail deflections and the stress distribution in the rails) should agree with the corresponding actual quantities as closely as possible.

To achieve this objective, first of all, a test should involve a relatively long section of track. If the actual track is not being tested directly, the size of the ties and their spacing in the test section should be the same as in the actual track. The method of determining k_r from the test data should be such that the analytical and the corresponding test results agree as closely as possible. For example, k_r in Equation 3 can be determined by equating the deflections or stresses at one point only (e.g., at P). Another way is by using a least-squares fit over a specified region. However, this procedure requires measurements at many points along the track, and Kerr (21) has shown that for the determination of k_r, which appears in Equation 3, one measurement at one point is sufficient.

The procedure for determining the two track coefficients (k_r and ρ) that appear in Equation 6 is similar to the one discussed above, except that at least two measurements are necessary. For example, subject each rail of a track to a load P, as shown in Figure 7, measure the resulting (instantaneous) deflections at P and at a point on the track half way between P and the point where the rail deflections approach zero, and equate these two values with the corresponding deflections given by Equation 8. This gives two simultaneous algebraic equations, with k_r and ρ as the only unknowns, whose solution is the two track parameters.

The above analyses assume that the load P is vertical and that it acts centrally through the vertical rail axis. However, in general, a railroad wheel does not act on the rail centrally. Furthermore, the wheels of a moving train also exert lateral forces on the rails. The corresponding stress analyses and test results have been given by Timoshenko (44) and by Timoshenko and Langer (45). More recent discussions of these stresses have been given elsewhere (46, 47).

In the wheel-rail contact region, where very large loads are transmitted from the wheel to the rail over a very small area, the actual stresses deviate considerably from those calculated by the beam theories. The occurence of shelling rail failures has prompted many analytical and experimental studies of this problem. An extensive survey of these analyses and tests has been given by Paul (48) and related papers that discuss rail reliability and rail failures by Steele (49) and Stone (50).

The determination of the stress distribution in the ballast has been discussed by Clarke (51) and more recently by Lundgren, Martin, and Hay (52) and So and others (53).

Another research effort has been an investigation of thermal track buckling. This problem increased in importance and urgency with the introduction of continuously welded rails on main lines shortly after World War II. A thermally buckled track is shown in Figure 9. Since the early 1930s many analyses of track stability and results of track-buckling tests have been published, but in spite of this, there is no generally accepted method available for analyzing this problem.

A critical survey of the analyses of thermal track buckling and related tests has been given by Kerr (54). This survey showed that the majority of the published results are not suitable for analyzing thermal track-buckling problems, because they are based on formulations that do not describe correctly the physical problems under consideration. One of the deficiencies is the omission of consideration of the decrease in the axial force in the rails due to buckling. Those few analyses that are conceptually correct have analytical faults with unknown effects on the final results.

Figure 9. Thermally buckled track.

To eliminate some of these problems, Kerr has given an improved analysis of track buckling in the lateral plane (55, 56). This analysis was subsequently used to determine the validity of a conjecture made by Kerr (57) that many track-test facilities, especially those used by British Railways and the German Federal Railroad were too short. The results obtained (58) show that the data recorded on short test tracks may deviate strongly from those obtained on long tracks in main-line service. These results also provide a guide for choosing the proper track length for thermal-buckling tests and for interpreting the test results obtained on short test tracks.

The mathematical level of Kerr's analyses is relatively high. Therefore, to simplify their use, the results obtained were evaluated numerically for a wide range of the track parameters encountered in the United States and the results presented graphically. Examples that show their use are given in a recent paper that also contains a general discussion of track buckling and measures for preventing it (59).

When a track is very rigid in the lateral plane (such as a slab track) or when a conventional crosstie track is prevented from moving sideways by adjacent structures, then the track can buckle in the vertical plane by lifting off the ballast. This problem has been analyzed recently by Kerr and El-Aini (60), and by El-Aini (61).

In all of the track-buckling analyses published, it is assumed that the track buckles either in the lateral or in the vertical plane. The effects of these restrictions on the results obtained have been studied by Kish (62).

The track-buckling studies are not yet complete. A complete clarification of this problem will require additional analyses, as well as laboratory and field tests, in which heated tracks will be subjected to moving trains, to validate the criteria used and the analytical results obtained.

CONCLUSION

A review of past and present track designs and their performances has shown the need for improvements in the present crosstie track system and for establishing the proper track system for the future, if concrete is used as tie material. Searching for these innovations should take into consideration that they must be economically feasible as well as technically sufficient.

Experimental and analytical investigations of the response of the track and its components to static and dynamic load are being made in many countries. Some areas are by now well understood, but others require more research. Although some areas of investigation are amenable to analytical studies, many less explored areas will at first require extensive experimental research programs.

It is reasonable to expect that in the United States, the recently intensified research activities will contribute in a relatively short time period to the solution of many problems of interest to our railroads. In view of the almost complete absence of railroad-related courses in the curricula of our engineering schools, special attention should be given to the transfer of these new results to the practicing railroad engineer, so that they may be used for improving our railways.

ACKNOWLEDGMENTS

This research was supported in part by the National Science Foundation and in part by the Association of American Railroads.

REFERENCES

1. A. D. Kerr. The Stress and Stability Analyses of Railroad Tracks. Journal of Applied Mechanics, Vol. 41, No. 4, 1974; Federal Railroad Administration, Rept., 1974.
2. A. Haarmann. Das Eisenbahn Geleise. W. Engelmann, Leipzig, Vol. 1, 1891, and Vol. 2, 1902.
3. J. E. Watkins. The Development of American Rail and Track. Trans., ASCE, 1890.
4. Manual Recommendations: Special Committee on Concrete Ties. Proc., AREA, Vol. 78, Nov.-Dec., 1976.
5. J. W. Weber. Development of the Prestressed Concrete Tie in the USA. In Railroad Track Mechanics and Technology (A. D. Kerr, ed.), Pergamon, New York, 1978.
6. A. F. Zolotarskii, A. A. Balashov, N. M. Isaev, V. V. Serebrennikov, and V. F. Fedulov. Zhelezodorozhnyi Put' na Zhelezobetonnykh Shpalakh. Izdatelstvo Transport, Moscow, 1967.
7. M. Shrinivasan. Modern Permanent Way. Somaiya Publications, Bombay, 1969, Chaps. 11-14.
8. P. Chipman. Permanent Track Construction on the Pere Marquette. Railway Engineering and Maintenance, Vol. 24, No. 10, 1929.
9. F. Birmann. German Federal Railway Experiments With Concrete Track Beds. Railway Gazette, April 1969.
10. J. C. Lucas, D. Lindsay, and W. K. Aitken. Experimental Concrete Track-Bed at Radcliffe. Railway Gazette, June 1969.
11. T. Miyamoto. Maintenance-Saving Track. Japanese Railway Engineering, Vol. 16, No. 2, 1976.
12. B. Bramall. The Mechanics of Rail Fasteners for Concrete Slab Tracks. In Railroad Track Mechanics and Technology (A. D. Kerr, ed.), Pergamon, New York, 1978.
13. J. Eisenmann. Eisenbahnoberbau für Hohe Geschwindigkeiten. Eisenbahntechnische Rundschau, No. 6, 1972.
14. J. Eisenmann. Railroad Track Structure for High-Speed Lines. In Railroad Track Mechanics and Technology (A. D. Kerr, ed.), Pergamon, New York, 1978.
15. Railways Research Slab Track. International Railway Journal, March 1977.
16. V. G. Albrekht, E. M. Bromberg, K. E. Ivanov, V. N. Lyashchenko, S. P. Pershin, and V. Ja. Shulga. Besstykovoi Put' i Dlinnye Relsy. Izdatelstvo Transport, Moscow, 1967.

17. S. G. Guins. Railroad Track Technology in the USSR: The State of the Art. Office of Research and Development, Federal Railroad Administration, Rept. FRA-ORD-76-12, Oct. 1974.
18. Permanent Way for Railways. Engineering News and Railway Journal, Vol. 41, No. 1, 1899; Proc., AREA, Vol. 28, 1927, pp. 852-882.
19. Concrete-Supported Railway Track. Portland Cement Association, Publ. T-26-8M-12-37, 1937, and Publ. T-26-3M-12-45, 1945.
20. E. Winkler. Der Eisenbahn-Oberbau. Verlag von H. Dominicus, 3rd Ed., Prague, 1875.
21. A. D. Kerr. On the Stress Analysis of Rails and Ties. Proc., AREA, Vol. 78, 1976; Federal Railroad Administration, Rept. FRA-ORD-76-285.
22. A. M. Zarembski. Rail Rollover: The State of the Art. Research and Test Department, AREA, Bulletin 664, Sept.-Oct. 1977, pp. 1-26.
23. G. Schramm. Oberbautechnik und Oberbauwirtschaft. Otto Elsner Verlagsgesellschaft, Darmstadt, West Germany, 3rd ed., 1973.
24. H. Posner III. Potential Improvements to Railroad Track Fastenings: A Review of Expired Patents. Department of Civil Engineering, Princeton Univ., NJ, senior thesis, 1977.
25. V. S. Lysyuk. Iznos Derevyannykh Shpal i Borba s Nim. Trudy CNII MPS, Vypusk 445, Izdatelstvo Transport, Moscow, 1971.
26. A. L. Bondarev and D. L. Zhuravskii-Skalov. Remont Derevyannykh Shpal. Izdatelstvo Transport, Moscow, 1972.
27. G. P. Raymond, P. N. Gaskin, and O. Svec. Selection and Performance of Railroad Ballast. In Railroad Track Mechanics and Technology (A. D. Kerr, ed.), Pergamon, New York, 1978.
28. K. Klugar. Contribution to the Mechanics of Ballast. In Railroad Track Mechanics and Technology (A. D. Kerr, ed.), Pergamon, New York, 1978.
29. M. J. Shenton. Deformation of Railway Ballast Under Repeated-Loading Conditions. In Railroad Track Mechanics and Technology (A. D. Kerr, ed.), Pergamon, New York, 1978.
30. R. M. Knutson, M. R. Thompson, T. Mullin, and S. D. Tayabji. Materials Evaluation Study: Ballast and Foundation Materials Research Program. Univ. of Illinois, Federal Railroad Administration, Rept. FRA-ORD-77-02, Jan. 1977.
31. E. Winkler. Die Lehre von der Elasticität und Festigkeit. Verlag von H. Dominicus, Prague, 1867, section 195.
32. J. W. Schwedler. On Iron Permanent Way. Proc., Institute of Civil Engineers, London, 1882, pp. 95-118.
33. H. Zimmermann. Die Berechnung des Eisenbahnoberbaues. Verlag W. Ernst und Sohn, Berlin, 1888.
34. A. Flamache. Researches on the Bending of Rails. Bull. International Railway Congress (English Ed.), Vol. 18, 1904.
35. S. Timoshenko. K Voprosu o Prochnosti Rels. Trans., Institute of Ways of Communication, St. Petersburg, Russia, 1915.
36. First Progress Report. ASCE-AREA Special Committee on Stresses in Railroad Track, Trans., ASCE, Paper 1420, Nov. 1917.
37. A. Wasiutynski. Recherches Experimentales sur les Déformations Elastiques et le Travail de la Superstructure des Chemins de Fer. Annales de l'Academie des Sciences Techniques à Varsavie, Dunod, Paris, Vol. 4, 1937; Experimental Research on the Elastic Deformations and Stresses in a Railroad Track. Federal Railroad Administration, Rept. FRA-ORD-76-10, 1976.
38. Y. Weitsman. On Foundations That React in Compression Only. Journal of Applied Mechanics, Dec. 1970.
39. R. Hanker. Die Entwicklung der Oberbauberechnung. Organ für die Fortschritte des Eisenbahnwesens, Vol. 93, No. 3, 1938.
40. R. Hanker. Eisenbahnoberbau. Springer, Vienna, 1952.
41. M. Hetényi. Beams on Elastic Foundation. Univ. of Michigan Press, Ann Arbor, 1946.
42. A. D. Kerr. Elastic and Viscoelastic Foundation Models. Journal of Applied Mechanics, Vol. 31, 1964.
43. A. D. Kerr. On the Derivation of Well-Posed Boundary-Value Problems in Structural Mechanics. International Journal of Solids and Structures, Vol. 12, No. 1, 1976.
44. S. Timoshenko. Method of Analysis of Statical and Dynamical Stresses in Rail. Proc., 2nd International Congress for Applied Mechanics, Zürich, 1927.
45. S. Timoshenko and B. F. Langer. Stresses in Railroad Track. Applied Mechanics, Trans., ASME, Vol. 54, 1932.
46. J. Eisenmann. Stress Distribution in the Permanent Way Due to Heavy Axle Loads and High Speeds. Proc., AREA, 1969.
47. Stress Distribution in the Rails. ORE, Question D71, Interim Rept. 2, Utrecht, Netherlands, 1966.
48. B. Paul. A Review of Rail-Wheel Contact Stress Problems. In Railroad Track Mechanics and Technology (A. D. Kerr, ed.), Pergamon, New York, 1978.
49. R. K. Steele. Requirements for the Reliability Assessment of Railroad Rail in Service. In Railroad Track Mechanics and Technology (A. D. Kerr, ed.), Pergamon, New York, 1978.
50. D. H. Stone. An Introduction to Fracture Mechanics of Railroad Rails. In Railroad Track Mechanics and Technology (A. D. Kerr, ed.), Pergamon, New York, 1978.
51. C. W. Clarke. Track Loading Fundamentals. Railway Gazette, Pt. 3, 1957.
52. J. R. Lundgren, G. C. Martin, and W. W. Hay. A Simulation Model of Ballast Support and the Modulus of Track Elasticity. Civil Engineering Studies, Univ. of Illinois, Champaign-Urbana, Transportation Engineering Series 4, 1970.
53. W. So, G. C. Martin, B. Singh, I. C. Chang, and E. H. Chang. Mathematical Models for Track Structures. Research and Test Department, Association of American Railroads, Rept. R-262, April 1977.
54. A. D. Kerr. Lateral Buckling of Railroad Tracks due to Constrained Thermal Expansions: A Critical Survey. In Railroad Track Mechanics and Technology (A. D. Kerr, ed.), Pergamon, New York, 1978.
55. A. D. Kerr. The Effect of Lateral Resistance on Track Buckling Analyses. Rail International, No. 1, 1976.
56. A. D. Kerr. An Analysis of Thermal Track Buckling in the Lateral Plane. Princeton Univ., Federal Railroad Administration, Rept. FRA-ORD-76-285, 1976; Acta Mechanica, in preparation.
57. A. D. Kerr. Principles and Criteria for the Design of a Railroad Track Test Facility. Proc., AREA, Vol. 77, 1975.
58. A. D. Kerr. On Thermal Buckling of Straight Railroad Tracks and the Effect of Track Length on

the Track Response. Department of Civil Engineering, Princeton Univ., NJ, Res. Rept. 76-TR-19, 1976.
59. A. D. Kerr. Thermal Buckling of Straight Tracks: Fundamentals, Analyses, and Preventive Measures. Princeton Univ., NJ; Federal Railroad Administration, Rept., 1977.
60. A. D. Kerr and Y. M. El-Aini. Determination of Admissible Temperature Increases to Prevent Vertical Track Buckling. Department of Civil Engineering, Princeton Univ., NJ, Res. Rept. 75-SM-3, 1975; Journal of Applied Mechanics, in preparation.
61. Y. M. El-Aini. Effect of Foundation Stiffness on Track Buckling. Engineering Mechanics, Proc., ASCE, Vol. EM 3, 1976, pp. 531-545.
62. A. Kish. On the Nonlinear Bending-Torsional Equations for Railroad Track Analyses. New York Univ., PhD thesis, Sept. 1974.

Use of Floating-Slab Track Bed for Noise and Vibration Abatement

George Paul Wilson, Wilson, Ihrig, and Associates, Oakland, California

Underground rail rapid transit systems can produce ground-borne vibration and noise from trains that creates intrusion in buildings located close to the underground facilities. This intrusion is usually a low-frequency (31.5- to 125-Hz range) noise or rumble transmitted via the intervening ground to the building structure. The use of floating-slab track bed, concrete slabs supported on resilient elements, to isolate the vibration of the rail support from the subway structure has been effective in reducing the transmission of vibration and noise to the surrounding ground and nearby buildings. This paper presents details on two types of lightweight floating-slab track bed; i.e., the continuous and the discontinuous designs. Some sections of continuous floating-slab track bed are in service at the Washington Metropolitan Area Transit Authority Metro System, and measurements of the reduction of the noise and vibration levels are presented.

Rail transit vehicles produce ground-borne vibration and noise that can and do create intrusion in nearby buildings, and this is particularly so for underground transit facilities that may be very near to buildings. This noise and vibration, which originates at the interface of the wheel and the rail, has been a significant problem along some subway corridors. With modern, lightweight vehicles and continuously welded rail, the vibration is seldom of sufficient amplitude to be felt as mechanical vibration or motion, and the only sensation is that of a low-frequency noise or rumble. But with older vehicles and jointed rail, the noise is sometimes accompanied by noticeable vibration.

Ground-borne noise can be reduced by vibration isolation of the track bed to interrupt the transmission path. The use of a floating-slab track bed, which consists of a concrete slab supported on resilient pads, can provide a vibration-isolated inertial base for support of the running rails. This design has been found effective in reducing the transmission of vibration and noise to the surrounding ground and nearby buildings in a manner similar to that of the inertial bases on springs that are used to support stationary machines. The use of floating-slab track bed provides for both reduced intrusion in nearby buildings and the placement of new rail transit subways in closer proximity to buildings.

A number of designs for vibration-isolated track bed have been developed ranging from heavy bridgelike structures with thick rubber support pads and damping applied to the bridge deck to relatively light concrete slabs without damping supported on thin resilient pads. Two basic forms of the relatively light slabs have evolved: (a) continuous slabs that are cast in situ and (b) discontinuous precast slabs. The original lightweight floating-slab design now in use in North America was developed in 1970 for the Washington Metropolitan Area Transit Authority and is of the continuous configuration. Trains have been operating on these slabs since 1975 with excellent performance. No operational information is yet available about the second-generation discontinuous-slab design, which was developed in 1974; the installations using it are not yet operational.

In the design of subway transit facilities, floating slabs are used only in critical areas where it is necessary to reduce ground-borne noise because of the critical proximity of buildings. These track beds add significantly to the cost of the subway structure, and their use is not appropriate except to avoid unacceptable noise intrusion.

DESIGN

The lightweight floating-slab design is based on the concept of the inertial mass-on-spring vibration isolator and uses a simple single-degree-of-freedom analysis for the vertical motion of the floating slab. A maximum deflection of 3 mm (0.125 in) under the static load of the train is generally imposed to limit the rail deflections to acceptable values. To avoid modal interactions and provide adequate control of the motion of the slab along with achieving a significant reduction of the ground-borne noise, the slab mass is made at least equivalent to the train mass and three times the bogie unsprung mass, considering the masses to be distributed over the vehicle length. The vertical fundamental resonance frequency for uniform motion of the slab, loaded with the bogie mass as a dynamic load, must be less than 16 to 18 Hz to provide reduction of the low-frequency audible sound. The design goal is generally 13 to 15 Hz; lower frequencies can be used only if greater rail deflection is allowed or if more space is used, to allow for the greater mass of the slab.

With a loaded resonance of 15 Hz for uniform vertical harmonic motion and a maximum live-load static deflection of 3 mm, the mass of modern rail transit vehicles leads to a design consisting of concrete slabs 275 to 375 mm (11 to 15 in) thick and 3.0 to 3.5 m (10 to 11.5 ft) wide and supported on 75-mm (3-in) thick elastomeric pads. The slabs must be completely isolated from the subway structure and, therefore, the lateral and longi-

tudinal supports are also elastomeric pads. The lateral natural frequency is designed to be less than, but not less than half, the vertical resonance frequency for uniform motion of the slab. The dynamic vertical stiffness of the vertical and lateral support pads and any entrained air must all be included in the calculations of the resonance frequencies and the determination of the elastomeric-pad characteristics required to achieve the design goals.

Figure 1 illustrates the cross section of the design for the continuous floating slabs developed in 1970 for the Washington, D.C., Metro box-section structures. This design uses 305-mm (12-in) thick slabs 3.4 m (11 ft 2 in) wide, supported on resilient pads spaced 600 mm (2 ft) on center. The support pads are 150-mm (6-in) square, load-bearing fiberglass, 150-mm diameter, round natural rubber, or 140-mm (5.5 in) diameter, round polyurethane, all 75 mm (3 in) thick. The side or perimeter isolation is a continuous pad of expanded neoprene or continuous strips of neoprene cemented in place. A detailed performance specification was prepared for use in purchase of the resilient pads to ensure long life and the appropriate stiffness range. The concrete is poured in situ by using a waterproofed sheet-metal form placed on top of the resilient pads and turned up at the sides.

Figure 1. Cross section of continuous floating-slab design.

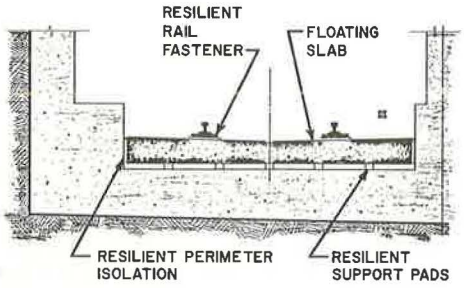

Figure 2. Plan view of discontinuous floating-slab design.

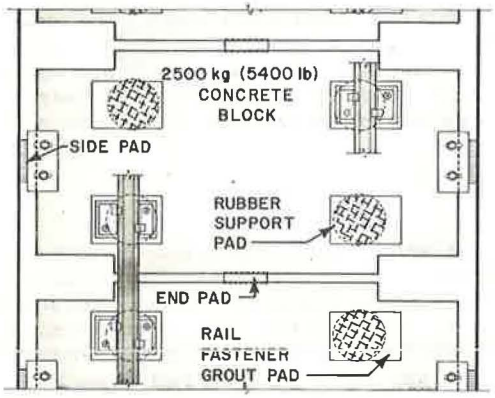

Figure 3. Configuration for floating-slab track bed tests.

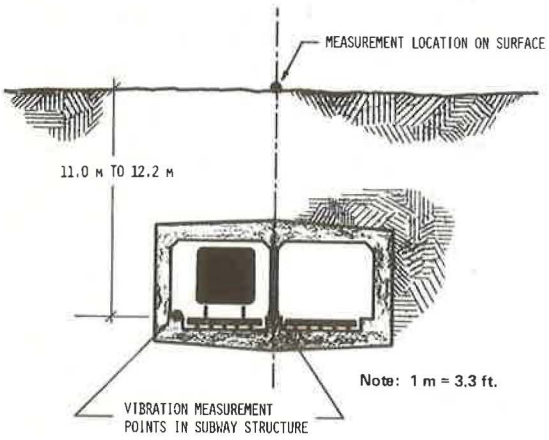

Figure 2 illustrates the plan view of the design for the discontinuous floating-slab design developed in 1974 for use in an extension of the Toronto rail transit system. The cross section is similar to that shown in Figure 1. For box-section structures, this design uses individual precast concrete blocks about 300 mm (11.8 in) thick and 3.2 m (10 ft 6 in) wide, weighing 2500 kg (5400 lb) and supported on four resilient pads each. Side and end pads are provided for lateral and longitudinal restraint. For this design, the support pads are larger because only two rows at larger spacing are used. In the Toronto system, the support pads are of natural rubber, 330 mm (13 in) in diameter and 75 mm thick and spaced 760 mm (30 in) on center longitudinally. The side pads are 300 by 150 by 50 mm (12 by 6 by 2 in) and the end pads are 300 by 150 by 75 mm (12 by 6 by 3 in), both of natural rubber. The side pads are preloaded by about 15 kN (4000 lbs) via the slotted mounting angles and anchor bolts. Similar designs have been adopted for use in the Atlanta; Melbourne, Australia; and Hong Kong transit facilities. Support pads of 330 mm to 375 mm (13 in to 14.75 in) diameter have been used.

The use of either design in single-track round tunnels requires a narrower slab and, because of available space, the mass is usually less than that used for the box section, but still can be made adequate to give the desired results. An advantage of the discontinuous slab design is that it has no entrapped air, which results in a lower natural frequency than that of the continuous design for an equivalent static deflection under load.

The rails are fixed to both types of floating slab by using the same procedures and resilient direct-fixation fasteners as for standard rigid-invert installations. With the precast blocks, recesses for the rail-fastener anchor bolts can be cast in the block, which simplifies the rail installation.

RESULTS

Figure 3 illustrates the configuration that was used for tests of the effectiveness of the continuous floating slabs installed in the Washington, D.C., Metro subway structures. The rail was 11 to 12 m (36 to 40 ft) below the surface on a section of subway where there were uniform conditions and both a standard rigid track bed and a long floating-slab track bed. The tests were performed in October 1975; the results are shown by Figures 4, 5, and 6. A two-car train was operated at constant speeds of 32, 48, and 64 km/h (20, 30, and 40 mph) through the test area. The vibration was measured on the subway structure at the side curbs and center bench and on the ground surface by using a sidewalk or a parking-lot slab for mounting the accelerometer. Several accelerometer locations were used and the results averaged, although the differences between the results at the different locations were actually small.

Figures 4 and 5 illustrate typical results, showing the vibration levels by one-third-octave band and the reduction with the floating slab for frequencies above 20 Hz. These results showed only a small amplification of the vibration levels near the fundamental resonance fre-

quency and a substantial reduction at frequencies above 31.5 Hz. At the surface, the background noise and vibration from surface traffic prevented obtaining accurate data for frequencies above 100 Hz with the floating slab.

Because the lightweight continuous floating slab is an undamped concrete plate, it can radiate the noise in the subway due to its bending-mode vibrations. The level of this noise could affect patrons riding in the cars and has been of some concern. During the tests, noise outside the train was also measured; Figure 6 illustrates the comparison of reverberant noise levels around the train with the continuous floating slab and the standard rigid invert for single-track slabs. The floating slab causes an increase in noise level, primarily low-frequency noise, outside the car, but the change in the noise level in the car interior is not noticeable and barely measurable.

Figure 4. Subway-structure vibration levels with two-car Metro train passing at 64 km/h (40 mph).

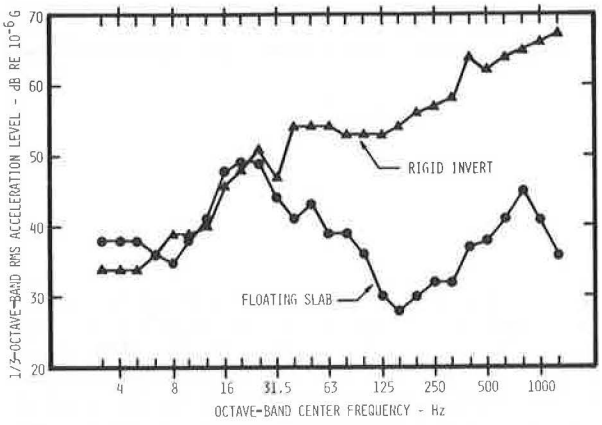

Figure 5. Ground-surface vibration levels with two-car Metro train passing at 64 km/h (40 mph).

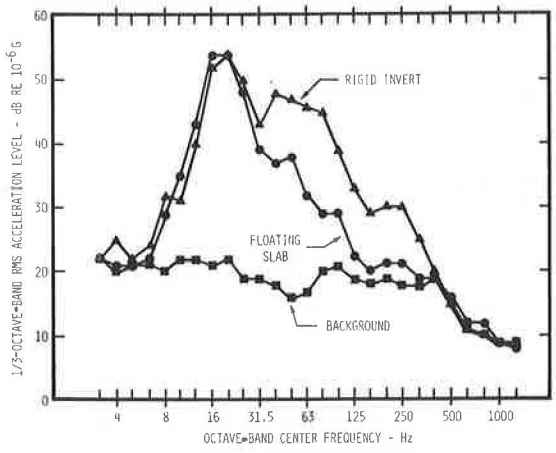

Figure 6. Average wayside noise level in subway with two-car Metro trains passing.

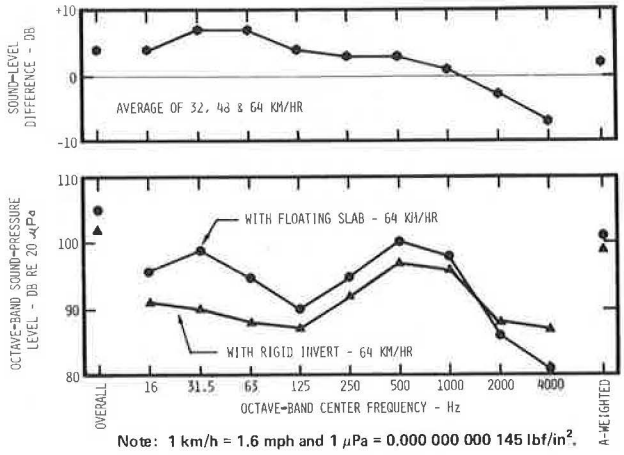

Note: 1 km/h = 1.6 mph and 1 μPa = 0.000 000 000 145 lbf/in^2.

Although several kilometers of discontinuous floating slabs have been installed, because the installations are not yet complete, no tests have been made with operating trains. Preliminary low-speed tests with towed cars indicate favorable performance. A reduction in the ground-borne vibration similar to that of the continuous floating slab is expected, and a reduced level of noise radiation in the subway is also expected because of the elimination of the large-area slabs.

One of the significant factors in the lightweight floating-slab design is that no special damping is used, only the natural damping of the resilient-pad material, the entrapped air, and energy radiation. The damping factor at the fundamental resonance of the continuous floating slab was expected to be 5 to 10 percent of critical and was measured to be 17 to 18 percent. For a single-degree-of-freedom system with a steady-state excitation, the amplification at the resonance of such a system would be expected to be 8 to 14 dB, as shown by Figure 7. However, for impact excitation, the amplification would be less than 1 dB with this degree of damping. At the time of the original analysis in 1970, it was estimated that the combination of train excitation, random impact, and periodic forces moving along the slab would lead to results between those of the steady-state response and the impact response—i.e., an estimated amplification at resonance of 2 to 3 dB, as shown by Figure 7.

Figure 8 shows the average results for the continuous floating slab plotted as a response function and indicates that the amplification at resonance is only 3 dB with a moving train as the vibration source and that the results above resonance are closer to those for a simple system than had been expected.

A second factor of importance for the costs and construction complexity of the lightweight floating-slab designs is that no special precision is required for the concrete invert surface in the subway. The standard tolerance and finish for concrete surfaces is adequate and appropriate for supporting the resilient pads. With the continuous slab, the sheet metal form bends when the concrete is poured, so that each pad is loaded uniformly even though the concrete invert may be uneven. With the precast blocks for the discontinuous design, the use of rubber-sheet shims, 3 or 6 mm thick as required, under one of the four pads for each block is sufficient to adjust the supports to a plane and give essentially equal loads on each pad. The need for the shims is determined by using a four-point jig placed at the location of each block during assembly.

During the construction of the continuous slabs, the support pads are cemented to the concrete invert to maintain their position during the placement of the metal form and concrete. In the precast discontinuous slab design, pockets are provided in the bottom of the block for mechanical retention of the support pads. The rubber pads are cemented to the blocks to hold them in place during installation of the block. The shim pads are not cemented or otherwise retained. Dynamic load tests have shown that no fastening is necessary to hold the rubber pads or shims in place after the load of concrete is applied.

Figure 7. Force transmissibility response for single-degree-of-freedom vibration-isolation system.

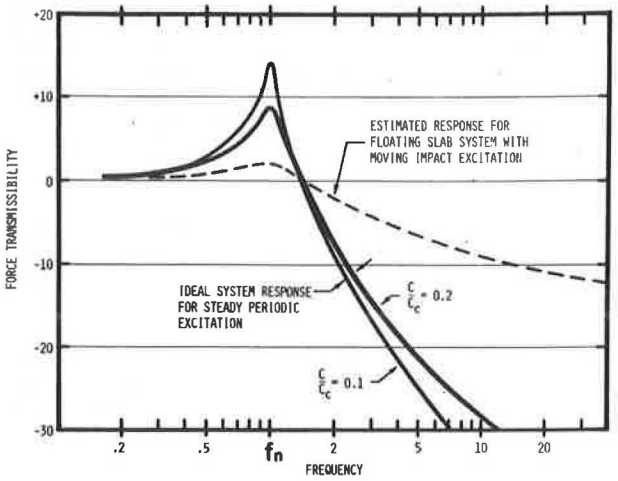

Figure 8. Insertion-loss performance of continuous floating-slab track bed as measured on surface and subway structure with two-car trains.

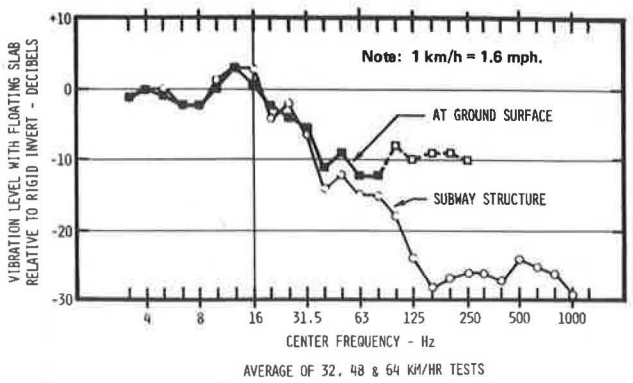

SUMMARY

A lightweight floating-slab design, requiring small space, has been developed that is effective in reducing ground-borne noise from subway transit trains. The design has two forms, one of which produces an approximately 15-dB reduction of the ground-borne noise in the low-frequency range that is most noticeable in nearby buildings and a more than 20-dB reduction of higher frequency noise. The installation, while requiring special techniques for placing the floating slab itself, requires no special tolerance or finish for the subway structure.

Assistance of New York State Department of Transportation to Railroad in Solving Soils and Foundation Problems

Harry E. Schultz and Taylor J. McDermott, Delaware and Hudson Railway Company
Stephen E. Lamb, New York State Department of Transportation

This paper describes the informal assistance that soils engineers from the New York State Department of Transportation have provided to the Delaware and Hudson Railway Company for the solution of several embankment failures that interrupted traffic operations. Under the present New York State Railroad Service Preservation Bond Act, engineering assistance is available to the railroads, and soils engineers are investigating areas of recurring track maintenance problems caused by soils and water conditions. The goal is to develop solutions for permanent stabilization that will be more economical than continual maintenance. Geotechnical engineering can have a significant input into reducing some of the costs of track operation and maintenance caused by soils, water, and foundation problems. In this case, the service was provided by a highway geotechnical organization. Highway and railroad soils and foundations problems are shown to be similar.

This paper discusses the type of engineering assistance that a state Department of Transportation soils and foundation organization can provide to a railroad for the timely repair of foundation problems that disrupt operations and for other soils-related problems that require continuing maintenance.

Soils and foundation engineering has developed rapidly in the last 30 years. Many state transportation agencies have established units in their organizations to implement geotechnical engineering into the extensive highway design and construction programs over the last 2 decades. In this same time span, most railroads have not had major construction programs, and there has been little stimulus for them to develop soils and foundation expertise in their engineering staffs. Railroads and highways are similar facilities except for the travel way. Their problems with embankments, embankment foundations, and rock or earth cut slopes have similar solutions. Tracks and pavements are both located on the ground surface, and the travel ways are both subjected to the same climatic freeze-thaw and wet-dry cycles that affect the performance of the subgrade soils and the pavement or ballast.

For the last 15 years, members of the soils staff in the New York State Department of Transportation (NYSDOT) have provided informal assistance to the Delaware and Hudson Railway Company (D and H RR) in solving major soils and roadbed problems. The bases for this relationship are that the headquarters of both organizations are in Albany and that several NYSDOT engineers formerly worked for the railroad.

The D and H RR system in New York State extends from Pennsylvania to the Canadian border, as shown in Figure 1. New York is a glaciated state, and the major valleys contain soils deposited by large quantities of glacial-melt water as the ice sheet receded northward. The northern portion of the D and H RR is located in the Lake Champlain Valley, which contains plastic clays of limited strength and other water-laid deposits of coarser sand and gravel.

Both the embankment problems described in this paper were major failures that disrupted service and required immediate repair without taking the time for subsurface exploration and laboratory testing. Therefore, there was a need for a soils engineer having experience with similar foundation problems to advise on the most expedient and correct action to take.

The first embankment-failure problem occurred at Spar Mill Bay in 1963 and involved a 6.1-m (20-ft) high embankment located near the shore of Lake Champlain. Several days before the major failure, maintenance

Figure 1. Delaware and Hudson Railway Company system in New York State.

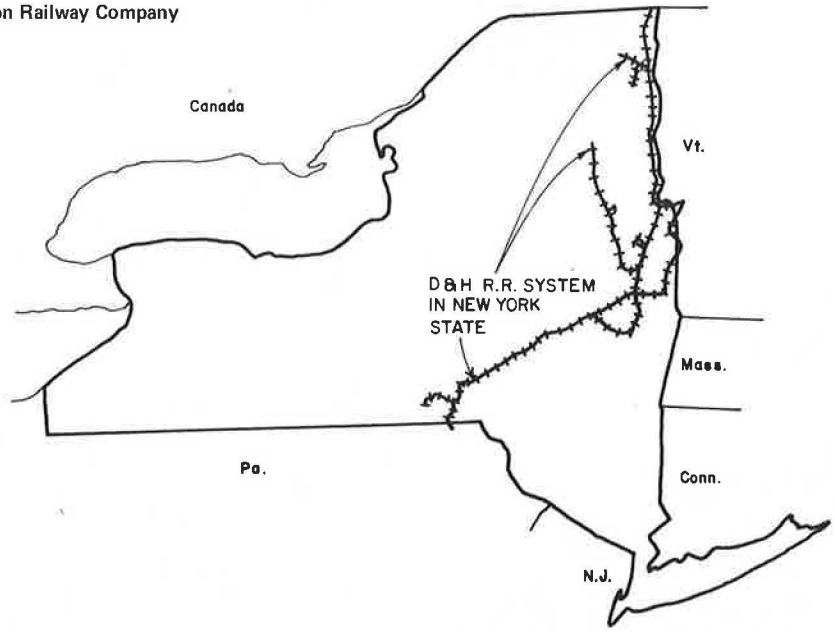

Figure 2. Section of slide: Spar Mill Bay.

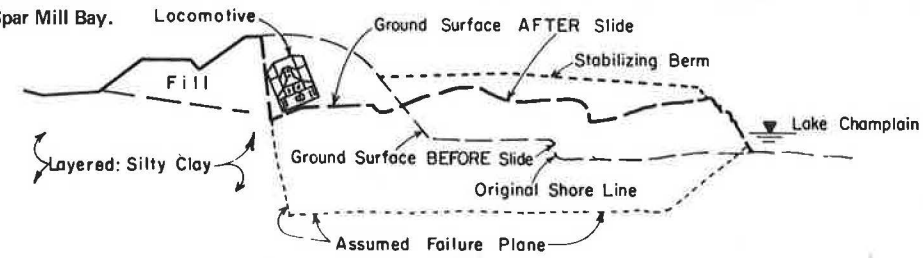

Figure 3. Location plan of slide: Spar Mill Bay.

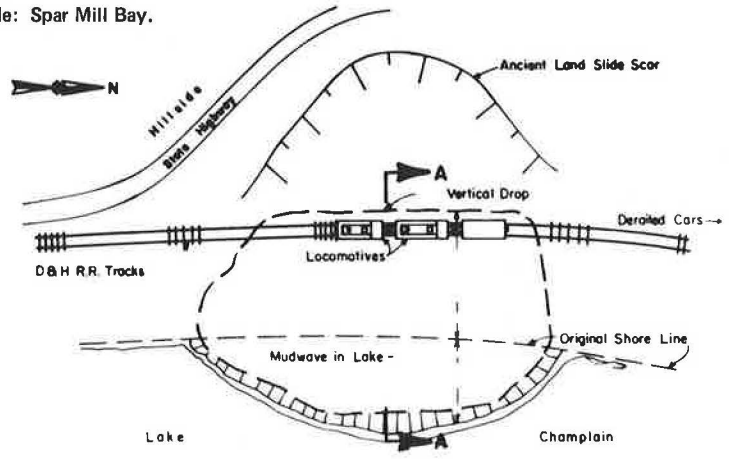

Figure 4. Embankment failure: Spar Mill Bay.

Figure 5. Mud wave: Spar Mill Bay.

crews had repaired some minor track settlement at the site. Additional settlement occurred, and the next day a northbound freight was derailed, scattering numerous cars along the track north of the future failure area. A work train was sent to the site, cleared the tracks, and unfortunately backed onto the unstable embankment-settlement area while waiting for orders. Suddenly, the embankment and locomotives dropped 6.1 m (20 ft) and simultaneously the bottom of Lake Champlain 45.6 m (150 ft) distant rose 3.5 m (12 ft) above the water. The details of this failure are shown in Figures 2 and 3. Figures 4 and 5 show the locomotives and the mud wave that exposed the lake bottom.

Soils engineers in NYSDOT were asked for an appraisal of the failure and recommendations for restoration of the embankment to reestablish main-line service. On inspection, it was found that the area was underlain by a layered silt and clay deposit and that the topography of the adjacent hillsides showed evidence that this was an area of ancient landslides. It was concluded that the initial settlements observed had been caused by minor movements in the underlying clay. Although the embankment had been stable for 30 years, high groundwater conditions may have cause minor plastic movements in the foundation soil and contributed to the settlement that caused the derailment. However, the major movement was caused by the mass of the locomotives and the vibrations of the idling engines. These vibrations apparently caused the liquefaction and complete loss of strength in an underlying silt layer that resulted in the spectacular failure. The recommendations were to construct a stabilizing counterweight berm over the mud wave to the elevation shown in Figure 2. After the berm was completed, the embankment was brought back to grade. This was done in 2 d, and the area has presented no problem during the last 14 years.

At a location further north at Port Kent, a failure occurred in the spring of 1971. At this location, the roadbed is on a side hill fill 12 m (40 ft) above Lake Champlain, as shown in Figure 6. The embankment was constructed 50 years ago against the face of a delta deposit of sand laid down by postglacial rivers flowing from the Adirondack Mountains. Suddenly, during the spring thaw, a portion of the fill liquified and slumped

Figure 6. Conditions before failure: Port Kent.

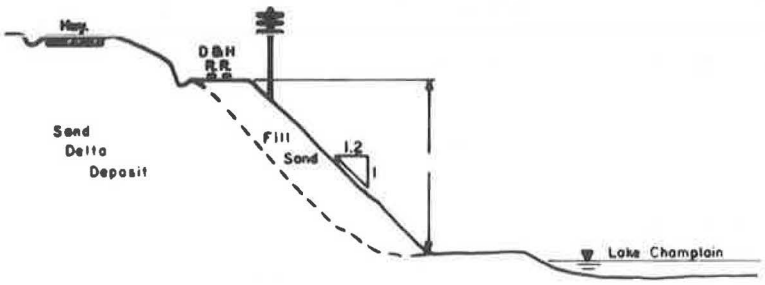

Figure 7. Failure and repair sequence: Port Kent.

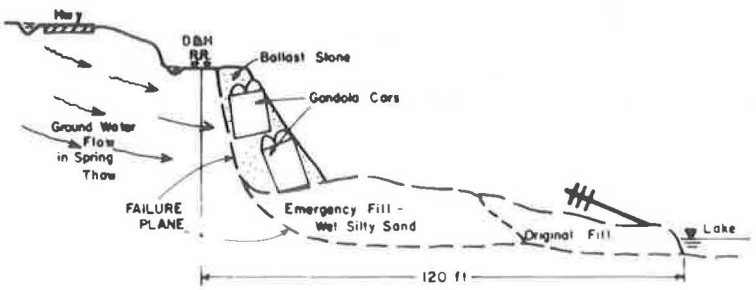

into the lake. Railroad maintenance forces placed an emergency fill, but this also became unstable and flowed into the lake.

NYSDOT soils engineers were requested to make recommendations for stabilizing this failure of the main-line embankment. An examination of the site showed that groundwater was emerging from the slide face. This groundwater flow must have increased significantly immediately before the failure; the winter frost had just become completely thawed, and the accumulated surface groundwater could flow downward to the delta deposit where the natural direction of subsurface drainage was toward the lake. The embankment had less permeability than the natural deposit, and the groundwater head and seepage forces caused the fill to become unstable at its steep angle of repose, which resulted in the failure. The solution recommended was the reconstruction of the embankment with a pervious material that would allow drainage and a lightweight material that would reduce the load on the unstable fill. Readily available materials were ballast stone to provide permeability and a number of old gondola-car bodies to decrease the embankment weight. The embankment was constructed to grade with the cars upside down as shown in Figure 7. The main line was reopened to traffic in 2 d, and the embankment has been stable since then.

These two case histories demonstrate the potential for technical assistance that an experienced soils organization can provide to a railroad for the solutions of major foundation problems. This assistance was conducted on an informal basis.

In the past 5 years, there has been an increase in federal and state funding for improvements to existing railroad systems. In 1970, New York State voters approved the Railroad Service Preservation Bond Act, which authorized $250 million for the maintenance and improvement of rail transportation facilities and services. NYSDOT was designated to administer this program, and its engineering assistance is available for the identification and development of projects eligible for funding.

The D and H RR has recognized the value of the previous soils engineering services for their emergency problems. Under the new engineering-assistance arrangement, they requested a soils investigation of an unstable embankment area adjacent to Lake Champlain. Subsurface explorations and laboratory testing and analyses were conducted to determine the most economical method to provide a stable embankment, and a design report was prepared for the railroad.

Under the same engineering-assistance arrangement, NYSDOT soils engineers and D and H RR engineers and maintenance personnel have recently made a field survey of 160 km (100 miles) of main line track to locate areas of perennial maintenance problems caused by soil and water conditions. Some of the conditions causing maintenance problems are subgrade pumping of fine-grained soils, erosion of finer soils through riprap protection, unstable embankment foundations and cut slopes, and stream-bank erosion. A report is being prepared indicating the locations of the soils-related maintenance problems and suggesting methods of permanent stabilization. It is probable that the cost of some recommendations will be greater than that of continuing maintenance. However, for other problems, permanent stabilization may be economically practical, making long-term savings possible through reduction of maintenance costs.

This engineering-assistance arrangement does not obligate the railroad to comply with the NYSDOT recommendations to be eligible for state funds. The railroad is responsible for the final decisions and policies involving engineering operations. The geotechnical engineering services of NYSDOT are available to provide the most economical and adequate solution of maintenance and operation problems for the mutual benefit of the railroad and the state.

Part 2
Related Railroad Topics

Mechanical Testing at Facility for Accelerated Service Testing

Walter L. Piotrowski, OAO Corporation, Beltsville, Maryland

Test operations are being conducted on the 7.7-km (4.8-mile) Facility for Accelerated Service Testing loop at the Transportation Test Center. The 9000-Mg (10 000-ton) test train operates 16 h/d at an average speed of 67 km/h (42 mph). The goal is an accelerated service test of track and rolling stock to determine comparative performances, wear rates, and maintenance and life-cycle costs. The consist is composed of 90 rail freight cars prepared in accordance with test specifications. Of the 90 test cars, 76 are available each day for testing. At least 1 year of test operations is planned. Four cars are removed daily from the consist for a 24-h period of test measurements and data collection. Inspection and gauging of components common to all cars occur every 22 d. Measurements of specific test components are made in accordance with the objects of each experiment. All measurements will be repeated at least five times during the test period so that a wear rate can be established for each component. The components involved in these experiments include wheels, journal roller bearings, adapters, trucks, springs, center plates, side bearings, brake shoes, wear plates, and couplers. The experiments and test measurements on each component are described.

TEST OPERATIONS

The operation of a compressed life-cycle test installation of track and rolling stock has begun at the Transportation Test Center near Pueblo, Colorado. The emphasis at the 7.7-km (4.8-mile) closed-loop track—the Facility for Accelerated Service Testing (FAST)—is on accelerated wear and fatigue tests of track and mechanical components. This will be accomplished by the continuous operation of a 76-car, 9000-Mg (10 000-ton) train over the FAST loop configuration, 16 h/d, at an average speed of 67 km/h (42 mph).

The nature of freight car and component test facilities and testing in revenue service and the need for rapid accumulation of car distance traveled place severe limitations on the usefulness of different mechanical tests. FAST will provide an opportunity for the comparative testing with respect to wear and fatigue life of freight cars and their components under near-actual conditions. In addition, FAST testing can be achieved in a relatively short time under controlled conditions.

Rolling stock will be tested in an accelerated-service manner to determine relative performances, wear rates, and maintenance and life-cycle costs. The tests will simulate, in a limited environment, the service life of a typical open-hopper car and will evaluate the in-service deterioration of its components.

The FAST consist is composed of 90 railroad freight cars prepared in accordance with test specifications. Of the 90 cars, 76 are available each day for testing. The test train is approximately 1.6 km (1 mile) long and weighs about 9000 Mg. Power is supplied by four GP-38 locomotives of 1 500 000 W (2000 hp) each. The consist includes three 63-Mg (70-ton) piggyback cars, 90-Mg (100-ton) tank cars, three hopper cars with specially fabricated trucks, three bathtub gondolas, and sixty-three 90-Mg open-hopper cars. Except for the 63-Mg piggyback cars, which contain loaded trailers, and six of the tank cars, which are run empty, all cars are loaded to the 119.3-Mg (131.5-ton) maximum gross mass allowed for 90-Mg freight cars in interchange service.

The testing environment includes a limited amount of available trackage that is oval shaped. The consist is operated so that the resulting component wear is equalized at all locations on the test cars. Every other day, the train is turned to compensate for wheel wear and asymmetric forces, and on alternate days, the locomotives are moved from one end of the consist to the other to vary the leading axle. Thus, the train travels clockwise around the loop one day and counterclockwise the next. Operating speeds are controlled, and the cars will remain unchanged during the test.

Each car is on a 22-d shop-inspection and data-collection cycle. Every day, a block of four cars is removed from the front of the consist for test measurements and data collection, after which the cars are reinserted at the rear of the train. During the 22 d between measurement cycles, the cars migrate from the rear to the front of the train. Some measurements are required at shorter intervals and are taken in the field. Others are taken into the shop every second, third, or even fourth cycle.

The car components being tested include trucks, center plates, side bearings, wheels, journal bearings, bearing adapters, springs, couplers, wear plates, and brake shoes. The object of each experiment is to compare the performances of various designs of a particular car component and determine the most cost-effective.

MATERIALS

The most commonly used material in the construction of freight cars and their components is steel. Steels are generally classified by their significant alloy components and by the method of processing; i.e., worked (wrought) or unworked (cast). The strength of steel is increased by the presence of particular other elements, the most important of which is carbon. Carbon increases steel strength without significantly decreasing ductility. Manganese, phosphorus, sulfur, copper, silicon, chromium, and molybdenum are also commonly used.

Ferritic steels of a given hardness or hardenability have the same tensile strength, whether cast or wrought, regardless of the alloy content. For design purposes involving tensile and yield properties, wrought and cast steels can be reliably interchanged. Cast steels do not show directional properties. The longitudinal properties of wrought steels are slightly higher than those of cast steel, but the transverse properties are lower by an amount that depends on the degree of working. If the directional properties are averaged for wrought steels, the values obtained are comparable to those for cast steels of similar composition. Resistance to wear and corrosion, machinability, and hardenability of cast and wrought steels are also similar.

COMPONENTS

Trucks

The railroad freight car is supported by a truck at each end, which also provides for the attachment of wheels and axles. A body center plate at each end of the car rests on a truck center plate.

The conventional freight-car truck weighs about 4500 kg (10 000 lb) and is a three-piece arrangement with cast-steel frames and bolsters. The truck components include center plates, side bearings, springs, snubbers,

wheels, axles, journal bearings, and bearing adapters. On some trucks, the brake rigging is integral with the truck.

Three different types of commonly used standard trucks and four different types of limited-use trucks are being compared. One of the standard trucks is 63 Mg; the others are 90 Mg. Three of the types of premium trucks are conventional three-piece arrangements with cast-steel side frames and bolsters. The fourth type, a 90-Mg truck, was fabricated of two side frames and a bolster with a secondary spring group in a somewhat conventional arrangement, but it also has a tie between the side frames and is equipped with hydraulic snubbers. Pads directly over the side frames carry the vertical load, and the truck pivots on a conventional center plate that does not transmit vertical loads.

A minimum of three cars are involved in each truck-test program to fulfill statistical requirements. At 44-d intervals, wear is measured within 0.025 mm (0.001 in) on those truck components exposed to it, including friction castings, bolsters, side frames, gibs, and stops. At 88-d intervals, hardness is measured at maximum localized-wear points on the same components.

Center Plates

The center plate about which trucks swivel not only functions as a pivot, but also normally transmits the mass of the entire car body into the truck structure. (Center bearing is a general term used to designate the whole arrangement and the functions it performs.) The body (male) center plate is attached to the underside of the car body and rests on the truck center plate. The truck (female) center plate is either attached to the top side or cast integral with the truck bolster. The center pin (king bolt) passes through both truck and body center plates, but does not really serve as a pivot. The truck turns about the bolt, but the stress is absorbed by the center plates.

The body center-plate surfaces can be cast or forged from a variety of steels and the bowl bearing surfaces can be modified by local hardening. Center plates of cast-steel truck bolsters have a manganese or carbon-steel wear liner applied before the bolsters are assembled into the trucks.

The center plate on 90-Mg freight cars is normally 35.6 cm (14 in) in diameter, but 40.6-cm (16-in) diameter center plates are also used. The nominal static load on these center plates is 56.2 Mg (62 tons) at a unit pressure of more than 6.9 MPa (1000 lbf/in^2). Rocking occurs at critical speeds, and it is not uncommon to have a center-plate reaction on 90-Mg cars of three times the static mass.

The experiments being done on center plates consist of comparing 35.6 versus 40.6-cm diameter center plates, unlined versus lined truck center plates, and standard versus manganese car-body center plates. Center-plate performance is being measured on 27 cars at 44-d intervals. Wear is measured on both truck and body center plates at eight locations on the plate. Surface hardness is determined at the locations showing maximum wear and on a nearby unworn portion of the plate surface.

Side Bearings

The center plate normally carries the mass of the car body into the truck structure, but when the car is tilted, as on a curve or during rocking, part of the mass is carried on the side bearings. Side bearings are attached to the bolsters of both the car body and the truck, on each side of the center plate, to prevent excessive rocking. The upper (body) side bearing and the lower (truck) side bearing are sometimes merely large flat surfaces. Other types of side bearings use rollers, springs, and friction elements to maintain constant contact and control the relative movement between body and truck.

The side bearings of the body are the upper pair of two side-bearing assemblies and are attached to the car-body bolster. The body side bearing is generally a flat plate, sometimes covered with a renewable, wear-resistant, hardened-steel wear plate through which loads from the car body are transmitted to the side bearing of the truck. Body side bearings are usually manufactured from medium-high-carbon rolled steel and heat treated for proper hardness.

Truck side bearings can be large flat plates, blocks, rollers, or elastic units. They are attached to the top of the truck bolster, under a corresponding bearing that is attached to the car-body bolster. Side-bearing housings are generally manufactured from high-carbon, high-manganese rolled steel.

Under normal operating conditions, vertical side-bearing loads will approach three-fifths of the loaded car mass, and, on poor track, this reaction may exceed two-thirds of it.

Many cars are equipped with roller side bearings to overcome the resistance in curves caused by friction at the side bearings. Roller side bearings for 90-Mg freight cars are of the double roller type. Their housings are manufactured from high-carbon, high-manganese rolled steel. Urethane constant-contact side bearings are available for use as replacements for existing double solid-steel rollers.

Some constant-contact side bearings are designed to control truck swivel and are not intended to control car rocking. Others use energy absorption to control the rocking of cars.

The experiments being made on side bearings compare double roller, friction block, and four types of constant-contact side bearings. The measurements are being made on 34 cars at 44-d intervals and include cage and roller wear for double-roller side bearings, permanent set and precompression for constant-contact side bearings, and hardness for all.

Wheels

Freight cars of 90-Mg capacity use 91.4-cm (36-in) wheels. Except for the three piggyback cars, which have 83.8-cm (33-in) wheels, all cars in the consist are of 90-Mg capacity and have 91.4-cm wheels. One-wear, two-wear, and multiple-wear wheels are available in both wrought and cast carbon steel for use on 90-Mg freight cars. One-wear wheels are not intended to be reprofiled; two-wear wheels can be turned at least once; and multiple-wear wheels have sufficient rim thickness to permit turning full flange and tread contours at least twice. One-wear wrought (H-36) and cast (CH-36) steel wheels differ significantly from two-wear wrought (J-36) and cast (CJ-36) steel wheels only in rim thickness.

The type of heat treatment and the carbon content are indicated by a suffix on the wheel nomenclature. Class U untreated high-carbon wheels are intended for general-service use where an untreated wheel is satisfactory. Class C heat-treated high-carbon wheels are intended for light braking conditions and high wheel loads or for heavier braking conditions where off-tread brakes are used, and there are other standards for classes L, A, and B wheels.

The heat treatment for class C cast-steel wheels consists of treating the rim only. The heat treatment for wrought-steel wheels consists of treatment of only the rim or of the entire wheel. After heat treatment and

quenching, the wheels are tempered to meet hardness requirements. The contour of the tread and flange is machined and smooth finished for wrought-steel wheels. The tread and flange contours of cast-steel wheels can be machined, ground, or cast.

The experiments being made on wheels compare wrought versus cast, one-wear versus two-wear, treated versus untreated, and standard versus Canadian National (CN) profile on 91.4-cm steel wheels. Thirty-two cars in the consist will be assembled with new wheels, bearings, and the two types of freight-car trucks most commonly used. The test is a symmetrical design; half the test elements are of one design and will be compared to the other half, which are of another design. Half the cars have 35.6-cm diameter center plates; the other half have 40.6-cm center plates. Half the trucks are of one type, and the other half are of another type. The wheels are wrought or cast, one-wear or two-wear, treated or untreated, and have standard or CN profiles. The journal roller bearings are regular or premium. The cars have the same type of truck at both ends, and both trucks have wheels of the same profile, heat treatment, and wear type, but one has wrought wheels and the other has cast wheels. One truck on each car has regular journal roller bearings, and the other has premium bearings. The center plates, brake shoes, roller-bearing adapters, and side bearings are the same for both trucks.

Wheel measurements are being taken on 71 cars at 22-d intervals. Wheel profiles will provide a complete record of flange and rim wear to within 0.25 mm (0.01 in). Wheel hardnesses (Brinell) are being determined at 44-d intervals.

Journal Bearings

At one time, almost the entire American freight-car fleet rolled on plain bearings, the failures of which required setting off cars at about 240 000-car-km (150 000-car-mile) intervals. Cylindrical roller bearings also were used at one time, but are no longer in use on heavy freight cars in the United States.

The tapered, journal roller bearing is now the most commonly used. These bearings have multiple-row designs and are installed on all new freight cars used in interchange service. They are well suited to the support of combination radial and thrust loads, but are limited to freight train speeds. The package type of roller bearing, a grease-lubricated assembly developed for freight-cars, is characterized by its rotating end cap secured to the axle by three cap screws. Roller bearings are designed for a minimum life expectancy of 804 500 km (500 000 miles) of service with a load factor of 80 percent, which is a full rail load in the radial direction for half the distance. The life expectancy represents a statistical reliability of 90 percent.

Bearings and enclosures are designed either for no field lubrication or for efficient periodic lubrication at a minimum specified interval. Roller bearings with housing end covers that rotate are lubricated at 48-month intervals. Extended-life bearings are designed to go without reconditioning or relubrication for 965 000 km (600 000 miles) or 10 years, whichever comes first.

The experiments being made on journal roller bearings compare three types of regular and three types of premium (extended life, no field lubrication) roller bearings. Measurements are being made on 30 cars of the wheel-test group. Grease loss will be determined within 2.8 g (0.1 oz) by cleaning the bearing exterior and weighing the bearing when the test is completed. The properties of the grease will be determined by conducting a penetration test and by inspecting the grease for foreign matter. Wear on the outer ring is being measured at 88-d intervals and when the bearings are replaced.

Bearing Adapters

The roller-bearing adapter ensures proper seating of a roller bearing in the pedestal type of side frame. The side-frame lugs on either side of the adapter transmit the lateral-thrust loads through the adapter side slots to the bearing cup. The top of the adapter is crowned to evenly distribute the load between the bearing seats. The crown also minimizes the shift in the center of the bearing load as the side frame rocks. Relief grooves in the center and on each end of the bore form the bearing seats that place the load directly over the rollers in the bearing.

Excessive adapter wear can cause improper loading of the bearing raceways, which will result in reduced bearing service life. Thrust-shoulder face wear, which is caused by contact with the end of the bearing outer ring, can result in damage to one or both of the bearing seals.

The experiments being done on bearing adapters compare nonhardened, crown-hardened, and crown-and-thrust-shoulder-hardened adapters. Wear and hardness measurements are being taken on 31 cars at 22-d intervals at all adapter wear points; i.e., adapter crown, thrust shoulder, and relief grooves.

Springs

The bolster spring is the main spring of a car and supports the truck bolster on which the mass of the car body rests. Some cars are equipped with stabilizing springs as part of the friction snubber on the truck. This spring also carries part of the load.

Freight-car truck springs are heat-treated helical compression springs and made of carbon-steel or alloy-steel round bars, by coiling on a preheated mandrel. These springs have inner and outer coils. The D-5 outer coil (carbon spring) has a left-hand winding of 14 cm (5.5 in) outside diameter, and the inner coil (alloy spring) has a right-hand winding of 8.6 cm (3.375 in) outside diameter. An alloy outer spring of the same winding, size, and spring parameters as the carbon outer coil has received conditional approval, but is not in widespread use. The recommended arrangement of D-5 springs for 90-Mg freight cars is 8 each inner and outer coils/spring nest. The solid (fully compressed) capacity per spring nest is 43 000 kg (95 000 lb).

Some newer freight-car trucks use the D-7 long-travel helical compression spring. The outer coil of this spring has the same winding and diameter as the D-5, but its solid capacity is slightly greater. Its total travel is 10.8 cm (4.28 in).

The experiments being made on springs compare D-5 carbon versus D-5 alloy outer springs and D-5 versus D-7 springs. The permanent set of all springs is being measured within 0.25 mm (0.01 in), the spring deflection is being measured within 0.25 mm (0.01 in) for load carrying springs, and the spring rates are being determined for all springs on 34 cars at 44-d intervals.

Snubbers

Standard bolster springs recoil with approximately the same force as that of the shock causing them to be compressed, which results in a periodic vibration of compression and recoil. This action is usually controlled by snubbing springs, friction dampeners, or hydraulic shock absorbers. Some type of mechanical system for preventing the development of harmonic car-body motion is

incorporated in all current truck designs. However, spring group or side-frame snubbing devices are not being tested or considered as a test variable. If installed on any test car received, they were removed or deactivated.

Couplers

Freight-car couplers automatically connect one rail vehicle to another, or conversely, disconnect them. The longitudinal (drawbar) forces at the couplers between cars or between cars and locomotives can be either tensile (draft) or compressive (butt), depending on the operation of the train at the time. Coupler-centering devices maintain the coupler in the center line of draft, but allow it to move to either side when a car is rounding a curve while coupled to another car.

The type E coupler, the basic coupler used in freight-car service, was adopted by the railroads as standard in 1932. It has undergone numerous design modifications, including continued metallurgical refinements to improve the physical properties of the steels used in its manufacture. Couplers made of grades C and E steels have the same chemical composition, but differ in heat treatment, hardness, and strength.

The rigid-shank, type E coupler has a flat butt surface that is seated on the draft-gear follower. This arrangement requires a lateral coupler movements to compress the draft gear. This reaction maintains the alignment of cars in pusher service or under dynamic braking conditions and tends to retain the coupler to a centered position on the car.

The type F interlocking coupler does not allow vertical disengagement when mated with a similar coupler and has a support shelf that retains an E coupler in the event of a failure or a pullout. An alignment control on the shank counteracts lateral car forces and coupler jackknifing under butt loading. The type F coupler is available in various shank lengths that allow curve negotiations for longer cars.

The most recently adopted standard freight-car coupler is the E/F coupler. By design, the coupler head is the standard E type, and the shank is the standard F type. It is widely used on longer freight cars.

Some freight cars have a rotary-shank coupler that allows coupled open-top, full-size railroad or mine cars to be unloaded in car dumpers without uncoupling and is widely used in unit train operations transporting bulk material such as coal.

The performance of type E couplers in grades C and E steel is being measured on 9 cars at 44-d intervals. Wear and hardness at all wear points, the permanent sets of the shank length, and butt thicknesses are being measured.

Coupler Shank and Carrier Wear Plates

The coupler shank rests on a carrier whose opening allows the coupler to swing laterally to permit passage of the car around curves. Some coupler-shank designs have a 0.64-cm (0.25-in) thick wear plate on the bottom wall to provide for wear due to contact with the carrier. The material for shank wear plates is spring steel or a suitable substitute, hardened and tempered to prolong its life.

The wearing surface of the flexible carrier on which the coupler shank bears must be long enough and wide enough to cover the full width of the coupler shank in the maximum angled position. Type E coupler carriers are integral with the striking plate. The type F coupler has a spring-supported carrier. Renewable, wear-resistant, hardened-steel carrier wear plates are used on carrier surfaces where wear is greatest.

The experiments being made on shank and carrier wear plates compare J-alloy AR-360, C-1045, and manganese-steel wear plates on 15 cars at 44-d intervals and when the plates are replaced.

The wear depths of both plates are measured near the plate center at the maximum localized wear. The hardness of both plates is measured at the maximum localized wear and where there is no wear.

Draft Gears

Draft gears are shock-absorbing devices designed to receive and dissipate coupler forces without damage to the car structure and lading. The draft gear forms the connection between the coupler rigging and the center sill. It receives the shocks incidental to train movements and car coupling and cushions the force of impact so that the maximum unit stress is within the capacity of the car structure.

Draft gears are not being tested or considered as a test variable. All test cars are equipped with draft gears conforming to the same specifications that require a minimum capacity at a specified level of reaction force.

Brake Shoes

Dynamic braking can be used to control train speed and to brake a train to a low speed, after which air brakes can bring it to a full stop. On most freight cars now in service, braking forces are developed in a single body-mounted cylinder and transmitted to the wheel treads by cast-iron brake shoes through a system of rods and levers. However, some cars are equipped with truck-mounted or composition brake shoes.

Brake shoes are made of a material that will provide friction and shaped to fit the tread of the wheel and held together by a steel backing plate. Composition brake shoes have characteristics considerably different from those of the standard metal brake shoe. The coefficient of friction of composition shoes is relatively constant throughout the entire speed range, but the standard metal shoe has a coefficient that increases as the speed decreases, which results in a tendency of the wheels to slide at slow speeds when a constant braking force is exerted throughout deceleration. The retardation performance of vehicles with composition brake shoes is more closely parallel to rail adhesion than is that of vehicles with cast-iron shoes, because the friction value is more uniform. The composition high-friction shoe develops a higher coefficient of friction than does the cast-iron shoe and allows a smaller force against the shoe to develop the same retarding effect.

The experiments being made on brake shoes compare high-phosphorus cast-iron and three types of composition high-friction shoes. Performance is being measured on 16 cars at 7-d intervals and on 47 cars at 22-d intervals by weighing the brake shoes before, during, and after testing to obtain the rate of wear and the total wear.

BATHTUB COAL GONDOLAS AND TRAILERS ON FLATCARS

The three bathtub gondola cars are being compared with the sixty-six 90-Mg hopper cars in the consist. Trailer-on-flatcar performance is being measured on the three 63-Mg flatcars and compared to that of the 90-Mg open-top hopper cars. Components unique to the gondolas and flatcars, such as king pins, trailer-hitch jaws, and side plates, will be measured at 66-d intervals.

ACKNOWLEDGMENT

This research was sponsored by the Office of Research and Development, Federal Railroad Administration.

Solar-Powered Refrigeration System for Railway Refrigerator Cars

David R. Conover,* Fruit Growers Express Company, Alexandria, Virginia

The potential of an available method to reduce the fuel consumption of the mechanically refrigerated railcars used for transporting perishable commodities has been investigated. An energy-oriented engineering analysis showed that a compact refrigeration system deriving its power from photovoltaic cells could be used in the design of railcar equipment for transporting perishable produce. Maximum load-respiration data and a heat-loss analysis for mechanically refrigerated railcars in service today were used to develop the energy design requirements of an alternative system. A solar-energy system was used to eliminate the need for fossil fuels, which also eliminates the emission of air pollutants and reduces acoustical emissions. The results reflect the present state of the art for designing and supplying power to railcar refrigeration systems and the way in which these systems could be used to alleviate projected energy problems in refrigerated transport.

Perishable produce has been shipped in refrigerated railcars since 1851 when ice was first used to cool a load of butter in shipment from upstate New York to Boston. Six years later, 30 insulated cars with ice-boxes in the doorways were constructed for use on the Pennsylvania Railroad. In 1868, patents for the ice tank car, which had iron tanks filled with ice and salt, were issued, and this design led to the Hutchins wool-insulated cars, which established the usefulness and practicability of railway refrigerator cars.

In the early twentieth century, research and development efforts in the area of refrigerated transport by rail were intensified. Numerous arrangements were designed and tested, some of which proved to be of great importance. The most important advance in the pre-World War II era was the interior fans, driven by the movement of the railcar wheels, which circulated ice-cooled air throughout the load. As the shipment of perishable produce by highway increased, so too did the activities by the railroads to develop new equipment and methods for the transport of perishable produce.

Mechanical refrigeration equipment, commercially introduced to railcar design in 1949, uses a separate diesel-engine power plant in each car to power a mechanical refrigeration system. In the past 25 years, both the equipment and the general design of the railcar have been improved, and together they now provide a reliable way of cooling perishable and frozen produce during transit; however, further development is needed. With the cost of diesel fuel and machinery escalating, and the share in the transport of perishable shipments carried by the railroads decreasing, there is a great need for a new energy-conserving railcar design for shipping items requiring refrigeration.

Solar energy, which is considered our ultimate energy resource at present, is a perpetual source that can be converted directly into electrical power by photovoltaic cells. At present, research in the area of photovoltaic cells is being increased; the proposed spending for fiscal year 1977 is more than $60 million. With increased research, the cost and availability of these cells is expected to become comparable to that of other energy sources, while the technology of the product itself will increase. It is therefore pertinent to investigate the possibility of using solar cells for the bulk generation of electricity in railcars.

This paper presents an analysis of the use of these cells mounted on a railcar roof to produce electricity to power a refrigeration system. Although many limitations exist today, the theoretical analysis shows that the concept is sound and possesses the capability of reducing the dependence of the rail industry on fossil fuels.

CAR DESIGN AND USE

The railcar designed for use with the solar-panel refrigeration design would be similar in construction to the refrigerated railcars presently manufactured (Figure 1). The specific car would be a 91-Mg (100-ton) capacity refrigerator car with a 50.8-cm (20-in) travel hydraulic cushioning device incorporated in the underframe. The interior dimensions are given below (1 m = 3.3 ft):

Dimension	Value
Inside length, m	16.0
Inside width, m	2.7
Inside height, m	2.9
Interior volume, m^3	128.2

The exterior sides, ends, roof, and doors would be constructed of steel design standard to present railcar technology and in compliance with all Association of American Railroads and Federal Railroad Administration specifications. The door and side-wall lining would be reinforced fiberglass, the ceiling aluminum sheets, and the ends and floors plywood. Alternative materials, such as high-density foam, could be considered for interior construction. Wood would be used for structural members between the interior lining and the exterior steel shell. The entire railcar would be insulated with 38.4 kg/m^3 (2.4-lb/ft^3) density polyurethane foam. Railcars of this design have been built with tested heat losses of 47.5 J/s·°C (90 Btu/h·°F). The design car would be heavily insulated, using alternative materials wherever possible, and built to eliminate hot spots in the interior. The calculation of the theoretical heat loss of the railcar designed is described below.

$$Q_c/dT = kA/dx \quad (1)$$

where

- Q_c = rate of heat flow by conduction in material,
- dT = temperature difference,
- k = thermal conductivity of material [(for polyurethane foam, k = 0.025 J/s·m·°C (0.015 BTU/h°·ft°·F)],
- A = area of section through which heat flows by conduction perpendicular to the heat flow, and
- dx = distance or thickness of insulation in direction of heat flow.

The following assumptions are made:

1. Heat flow is one dimensional through the car body,
2. Conduction is in the steady state,
3. Thermal and mechanical properties of the car-

body construction are constant,

4. No heat is generated in the car-body structure,
5. The metal exterior car structure and interior lining are neglected,
6. The car structure is all foam insulated; there is an additional heat loss of 15 percent for areas around the door and interior hot spots, and
7. The corner and edge sections of the car structure are neglected.

The data used in the calculations are given below (1 m = 3.3 ft).

Term	Definition	Value
A_1, m^2	Ceiling area	43.9
A_2, m^2	Interior floor area	43.9
A_3, m^2	Area of B-end interior	8.36
A_4, m^2	Area of A-end interior	8.36
A_5, m^2	Area of interior sides and doors	97.6
dx_1, m	Thickness of roof insulation	0.203
dx_2, m	Thickness of floor insulation	0.178
dx_3, m	Thickness of B-end wall insulation	0.178
dx_4, m	Thickness of A-end wall insulation	0.305
dx_5, m	Thickness of side and door wall insulation	0.178

By modifying Equation 1, the total heat loss for the entire design car can be calculated. Thus,

$$Q_c/dT = \text{heat loss in (roof + floor + A-end + B-end + side and door walls)}$$
$$= kA/dx(\text{total})$$
$$= k[(A_1/dx_1) + (A_2/dx_2) + (A_3/dx_3) + (A_4/dx_4) + (A_5/dx_5)] \quad (1a)$$

$= 0.025\,[(43.9 \div 0.203) + (43.9 \div 0.178) + (8.36 \div 0.178) + (8.36 \div 0.305) + (97.6 \div 0.178)] = 28.9$ J/S·°C (53.4 Btu/h·° F). To add the 15 percent heat loss allowed in assumption 6, this becomes $Q_c/dT = 32.4$ J/s·°C (61.5 Btu/h·° F). Thus, for the railcar design analysis, the total heat loss by conduction through the railcar structure can be considered as 32.7 J/s·°C (62.0 Btu/h·° F).

To design the system for the test car, it was necessary to determine a theoretical maximum for the heat generation by the load. Even after harvest, all fresh commodities respire or breathe, i.e., take in oxygen and give off carbon dioxide. This phenomonon produces heat that must be removed by the refrigeration system to maintain the product at the proper temperature until it reaches its destination. All types of produce have different respiration rates and, therefore, the maximum amount of heat produced will be determined by the commodity shipped. The maximum possible respiration heat is that of sweet corn. This value, which was used in the refrigeration-system design calculations, is calculated below. A frozen load would generate a negligible amount of heat.

$$Q_{gen} = \text{Resp} \times 1/24 \times 1/3600 \times \text{Den} \times \text{Cap} \quad (2)$$

where

Q_{gen} = rate of heat produced by load due to respiration,
Resp = maximum respiration rate for all U.S. Department of Agriculture commodities (1),
$1/24$ = conversion factor days to hours,
$1/3600$ = conversion factor hours to seconds,
Den = maximum density of commodity, and
Cap = volume capacity of railcar.

The following assumptions are made:

1. The entire load is precooled before shipment,
2. Heat within the load is generated in the steady state and uniformly, and
3. Heat generated by boxes, pallets, or shipping containers is neglected.

The data used in this calculation are given below [1 (J/d)/kg = 0.86 (Btu/d) ton, 1 kg/m^3 = 0.062 lb/ft^3, and 1 m^3 = 35.3 ft^3].

Term	Value
Resp, (J/d)/kg	8140
Den, kg/m^3	537
Cap, m^3	128

By substituting the above data into Equation 2, the maximum heat generated by the load can be calculated: $Q_{gen} = 8140 \times 1/2000 \times 1/24 \times 1/3600 \times 537 \times 128 = 6482$ J/s (22 121 Btu/h). Thus, for the calculation of maximum refrigeration load in the design railcar, the maximum heat generated by the load is 6475 J/s (22 100 Btu/h) at 0°C (32° F).

The photovoltaic-cell panels would be secured on a roof area of 55.7 m^2 (600 ft^2), arranged transversly in 1.52 by 0.61-m (5 by 2-ft) sections. The refrigeration system would be located on the A-end of the railcar.

Initially a prototype should probably be limited to a

Figure 1. Railcar design.

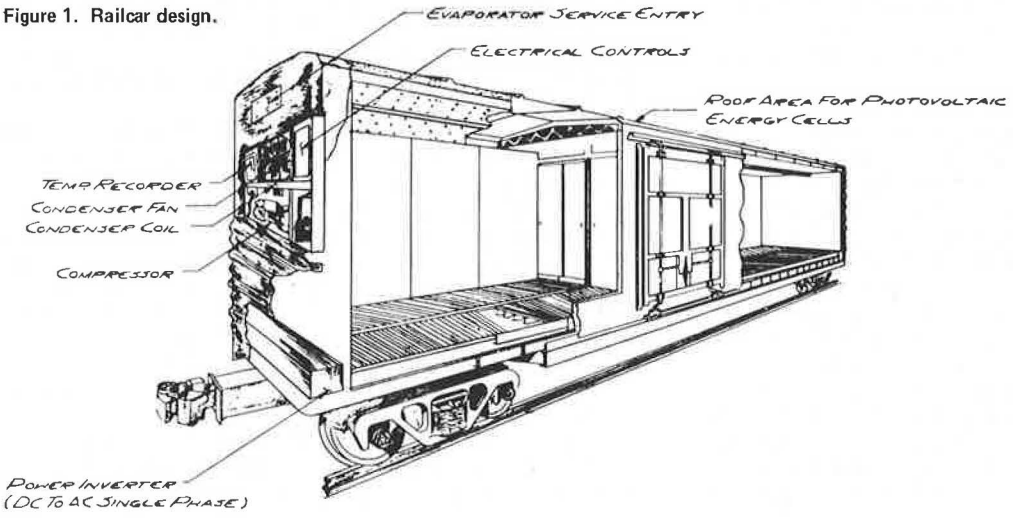

private operation, which would permit closer evaluation under controlled movement conditions. The train operation should be planned to achieve the maximum travel distance during the day, when the solar system could be in operation, and eliminate the need for large numbers of batteries. With a 12-h daylight period during the summer and a projected speed of 113 km/h (70 mph) average, the operating distance would be 1352 km (840 miles). The shorter winter daylight or some night operation would not be a problem because of the lower ambient temperatures, lower car heat losses, and lower refrigeration loads under those conditions. (Specific details of train operation were not developed here and would require further study.)

REFRIGERATION SYSTEM

Heat is defined as a quantity of energy transferred across boundaries because of a temperature difference between those boundaries. Because heat moves from an area of high temperature to one of low temperature, a low-temperature substance must be introduced into the railcar interior sufficient to remove the heat inside. The specific purpose of the refrigeration or heat-pump system in a railcar is to create a low-temperature heat sink capable of removing the railcar heat.

The refrigeration system most commonly used today (Figure 2) uses a system of an evaporator, a compressor, a condenser, and an expansion valve to circulate the refrigerant fluid. The refrigeration cycle begins when gaseous refrigerant at a low temperature and a low pressure is introduced into the compressor. The temperature and pressure of the refrigerant are increased by the operation of the compressor. The refrigerant then flows through the condenser coils where it is liquefied, giving up heat to the environment. Still at a high pressure, but now at a lower temperature, the liquid refrigerant flows to an expansion valve where its pressure and temperature are reduced. The low-temperature refrigerant next flows into the evaporator, where air from inside the car is blown over the cooling coils. The refrigerant absorbs the heat from this interior air and carries it to the compressor where the cycle begins again.

The particular design selected for this study was an 8790-J/s (2.5-ton) refrigeration system similar to that used in refrigerated containers, adapted to fit on the top end section of the railcar (Figure 3). A flue would be constructed at this end of the car to allow air to circulate from the ceiling, through the evaporator, and down along the floor area. A plan of the system, shown in Figure 4, would have cooling capacities of 8790 J/s (30 000 Btu/h) for a perishable load at 35°C (95°F) ambient temperature and 2930 J/s (10 000 Btu/h) for a frozen load at 37.8°C (100°F) ambient temperature respectively.

This system using R-22 refrigerant is capable of refrigerating the maximum possible heat load under the most extreme environmental design conditions. The arrangement has an 8790-J/s (30 000-Btu/h) cooling capacity for a perishable load at 35°C ambient temperature and a 2930 J/s (10 000 Btu/h) capacity for a frozen load at 37.8°C ambient temperature. For the frozen load, where minimal heat is generated within the load, the system will have more than ample refrigerating capacity. At ambient temperatures lower than those used in the design calculations, the efficiency of the system would be higher, and the refrigeration load would be lower. When all environmental and perishable-loading factors are considered, the system as designed is capable of refrigerating most loads under normal ambient temperatures. The calculations below present an analysis of this system and its thermodynamic states for the most extreme conditions of temperature and pressure. (The numbered points refer to Figure 4.) (SI units are not given for these calculations because they were developed for U.S. customary units.)

$$Q_{tot} - W_{tot} = \Delta H + \Delta u^2/2g_c + \Delta z(g/g_c) \quad (3)$$

where

Q_{tot} = all heat transfered into or out of system,
W_{tot} = amount of work or energy put into the system,
ΔH = enthalpy change of system,
$\Delta u^2/2g_c$ = kinetic energy of system, and
$\Delta z(g/g_c)$ = potential energy of the system.

The following assumptions are made:

1. The system is steady state and steady flow;
2. Compression and expansion of the refrigerant fluid is adiabatic, but not reversible;
3. Kinetic energy = 0; and
4. Potential energy = 0.

(Other equations and assumptions will be introduced as required.) The data used are given below:

Term	Definition	Value (Btu/h)
Q_{gen}	Respiration heat generated by commodity	22 100
Q_c	Rate of heat flow into interior loading space of car	3 906
Q_e	Heat generated by 0.75-bhp evaporator blower model	1 909
Q_{tot}	$Q_{gen} + Q_c + Q_e$	27 915

At point 1, the evaporator temperature = 28.00°F, the amount of superheat in refrigerant = 10°F, and therefore the saturated vapor temperature = 18.00°F. The corresponding pressure from the pressure-enthalpy (P-H) diagram (Figure 5) for 18.00°F saturated vapor = 55.551 lbf/in^2 (absolute). Interpolation of tables of properties of refrigerant 22 in the superheated region at 28.00°F and 55.551 lbf/in^2 (absolute) gives the following results: H_1 = enthalpy at point 1 = 108.4400 Btu/lb (mass) and S_1 = entropy at point 1 = 0.229 64 Btu/lb (mass)·°R.

At point 4, the condenser temperature = 95.00° F (from the maximum ambient temperature), and the state is saturated liquid. The corresponding pressure from the P-H diagram for saturated liquid at 95.00°F = 196.51 lbf/in^2 (absolute). Interpolation of the R-22 tables for the saturated liquid at 95.00°F and 196.51 lbf/in^2 (absolute) gives the following results: H_4 = enthalpy at point 4 = 37.7050 Btu/lb (mass) and S_4 = entropy at point 4 = 0.076 68 Btu/lb (mass)·°R.

At point 2′, there is isentropic compression from point 1 to a pressure of 196.51 lbf/in^2 (absolute), which is equal to P_4, the pressure at point 4—because the compression is isentropic, the entropy at point 1 must be equal to the entropy at point 2′, or $S_2' = S_1 = 0.229\ 64$ Btu/lb (mass)·°R. From S_2', interpolation of the R-22 tables in the superheated region gives the following results: H_2' = enthalpy at point 2′ = 122.6970 Btu/lb (mass), and T_2' = temperature at point 2′ = 148.23°F.

At point 2, there is compression from point 1 to a pressure of 196.51 lbf/in^2 (absolute) in the superheated region. This calculation requires the following assumptions: (a) compressor efficiency = 70 percent = 0.70, and (b) the compressor is adiabatic or Q_c from the compressor is 0. From Equation 3,

Figure 2. Operation of refrigeration system.

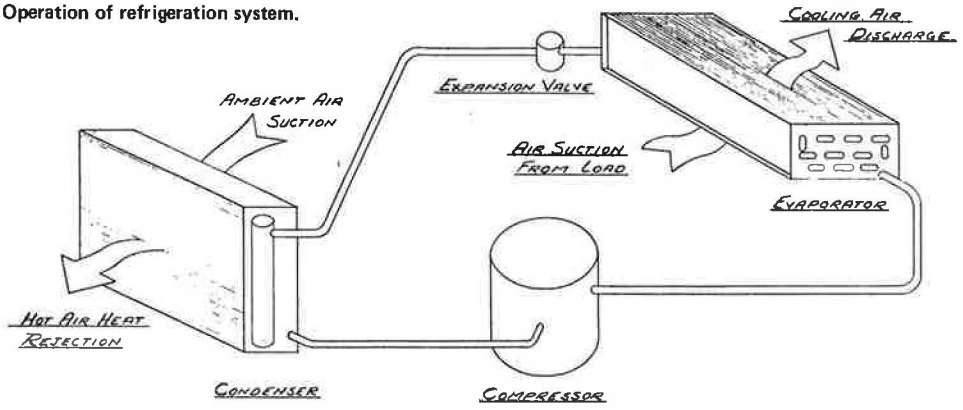

Figure 3. Arrangement of refrigeration system.

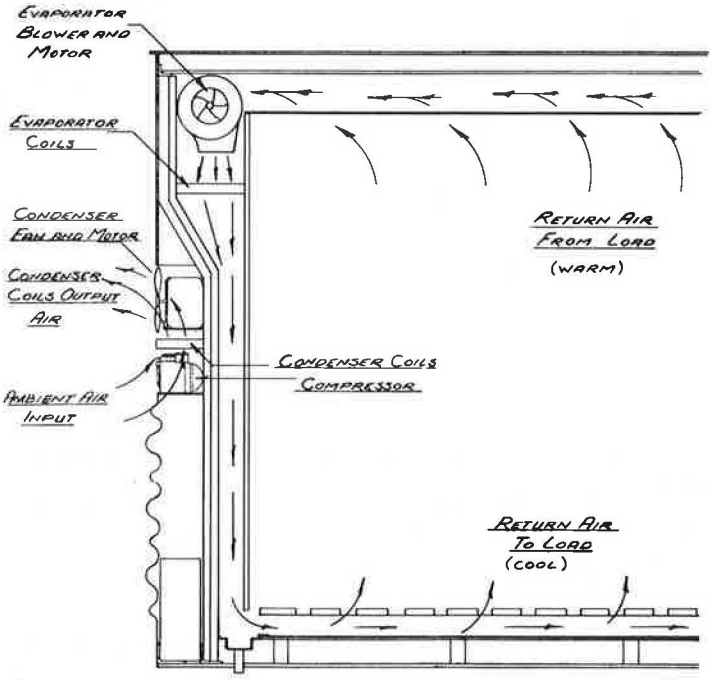

Figure 4. Plan of refrigeration system.

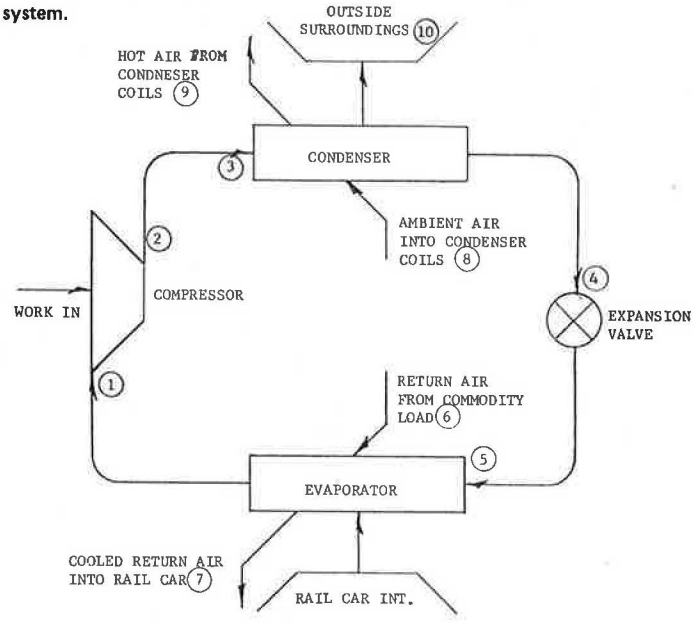

Figure 5. Pressure versus enthalpy: refrigerant 22.

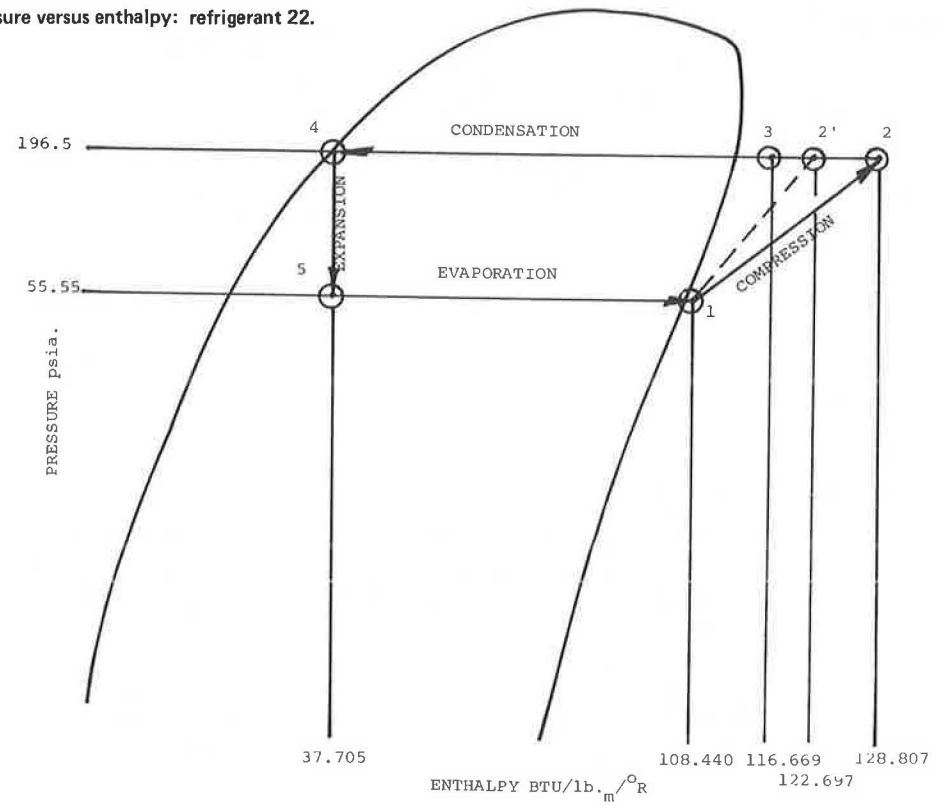

$$W_{c_{rev.}} = H_{2'} - H_1 = (H_2 - H_1)n_c \quad (3a)$$

The reversible work of the compressor = actual work × efficiency. From Equation 3a, H_2 = enthalpy at point 2 = $[(H_{2'} - H_1)/n_c] + H_1 = [(122.6970 - 108.4400)\ 0.70] + 108.4400 = 128.8070$ Btu/lb (mass). Interpolation of the R-22 tables for superheated vapor at 196.51 lbf/in^2 (absolute) and $H_2 = 128.8070$ Btu/lb (mass) gives the following results: T_2 = temperature at point 2 = 181.95°F, and S_2 = entropy at point 2 = 0.239 49 Btu/lb (mass)·°R.

At point 3, because of cooling of the refrigerant between the compressor and the condenser, the temperature decreases. T_3 = temperature at point 3 = T_4 + 20°F = 115.0°F, and P_3 = pressure at point 3 = pressure at point 2 = 196.51 lbf/in^2 (absolute). Interpolation of the R-22 tables for superheated liquid at 115.00°F and 196.51 lbf/in^2 (absolute) gives the following results: H_3 = enthalpy at point 3 = 116.6690 Btu/lb (mass), and S_3 = entropy at point 3 = 0.219 42 Btu/lb (mass)·°R.

At point 5, the refrigerant has been expanded isentropically from point 4; i.e., there is no work or heat exchange in the process. H_4 = enthalpy at point 4 = H_5 = enthalpy at point 5 = 37.705 Btu/lb (mass), P_5 = pressure at point 5 = 55.551 lbf/in^2 (absolute), and T_5 = temperature at point 5 = 18.00°F. For a second-law analysis of the dynamics of wet refrigerant,

$$H_5 = 37.705 \text{ Btu/lb (mass)} = H_{f5} + x_5(H_{fg5}) \quad (4)$$

H_{f5} = tabulated value of enthalpy for dry refrigerant = 15.44 Btu/lb (mass), H_{fg5} = enthalpy for dry refrigerant - enthalpy for saturated refrigerant = 91.48 Btu/lb (mass), and x_5 = degree of saturation = $(H_5 - H_{f5})/H_{fg5} = (37.705 - 15.440)/91.480 = 0.2434$,

$$S_5 = \text{entropy at point 5} = S_{f5} + x_5(S_{fg5}) \quad (5)$$

S_{f5} = tabulated value of entropy for dry refrigerant = 0.0341 Btu/lb (mass)·°R, and S_{fg5} = entropy for dry refrigerant - entropy for saturated refrigerant = 0.1916 Btu/lb (mass)·°R. Thus, $S_5 = 0.0341 + 0.2434\ (0.1916) = 0.080\ 74$ Btu/lb (mass)·°R.

The following calculations of sensible and latent heat are required to find the properties of air at points 6 to 9.

$$q_s = \text{sensible heat change} = 1.08 \times \text{air flow} \times TD_{db} \quad (6)$$

$q_s = 0.25Q_{gen} + Q_c + Q_{em} = (0.25 \times 22\ 100) + 3906.0 + 1908.75 = 11\ 339.75$ Btu/hr, air flow = 2500 ft^3/min, and TD_{db} = temperature difference (dry bulb) between air entering and leaving the evaporator coils = $q_s/(1.08 \times 2500) = 11\ 339.75/(1.08 \times 2500) = 4.20$°F(dry bulb). T_7 = temperature of air entering interior of car from evaporator = 29.0°F, T_6 = temperature of air entering evaporator from car interior = 29.0 + 4.2 = 33.2°F, and $P_6 = P_7$ = pressure of air at evaporator = 41.697 lbf/in^2 (absolute).

$$q_l = \text{latent heat change} = 4.5 \times \text{air flow} \times \Delta H_L \quad (7)$$

$q_l = 0.75 \times Q_{gen} = 0.75 \times 22\ 100 = 16\ 575$ Btu/h, and ΔH_L = change in enthalpy of air (latent heat) = $q_l/(4.5 \times 2500) = 16\ 575/(4.5 \times 2500) = 1.4733$ Btu/h.

$q_t = q_s + q_l$ = total heat change = 11 339.75 + 16 575.0 = 27 914.75 Btu/h = 4.5 × air flow × ΔH_t. Thus, ΔH_t = total enthalpy change of supply air to the evaporator = $q_t/(4.5 \times 2500) = 27\ 914.75/(4.5 \times 2500) = 2.4813$ Btu/lb (mass). SHR = sensible heat ratio = $q_s/q_t = 11\ 339.75/27\ 914.75 = 0.4062$.

At point 6, air at 80 percent degree of saturation and 33.2°F is going from the car interior to the evaporator coils. H_t = total enthalpy change in air = 2.4813 Btu/lb (mass) = $H_6 - H_7$, and H_6 = enthalpy at point 6 = $H_{a6} + x_6(H_{as6})$ (from Equation 4). From the American Society of Heating, Refrigerating, and Air-Conditioning Engineers air tables, H_{a6} = tabulated value of enthalpy of dry

Table 1. Thermodynamic properties of refrigeration system.

Point	State	Temperature (°F)	Pressure [lb/in² (absolute)]	Enthalpy [Btu/lb (mass)]	Entropy [Btu/lb (mass)°R]
1	Superheated vapor	28.00	55.551	108.4400	0.229 64
2	Superheated vapor	181.95	196.510	128.8070	0.239 49
2	Superheated vapor	148.23	196.510	122.6970	0.229 64
3	Superheated vapor	115.00	196.510	116.6690	0.219 42
4	Saturated liquid	95.00	196.510	37.7050	0.076 68
5	Saturated liquid	18.00	55.551	37.7050	0.080 74
6	Moist air	33.20	14.697	11.3968	0.024 15
7	Moist air	29.00	14.697	8.9155	0.018 99
8	Dry air	95.00	14.697	22.8270	0.045 13
9	Dry air	108.32	14.697	26.0301	0.050 84
10	Dry air	95.00	14.697	22.8270	0.045 13

air = 7.975 Btu/lb (mass), and H_{as6} = enthalpy of dry air - enthalpy of saturated air = 4.2772 Btu/lb (mass). x_6 = degree of saturation = 80 percent = 0.80, and thus $H_6 = 7.975 + 0.80(4.2772) = 11.3968$ Btu/lb (mass). S_6 = entropy of air at point 6 = $S_{a6} + x_6(S_{as6}) + S_{cl}$ (from Equation 5), S_{a6} = tabulated value of entropy for dry air = 0.016 764 Btu/lb (mass)·°R, S_{as6} = entropy for dry air - entropy for saturated air = 0.009 112 Btu/lb (mass)·°R, and S_{as6} = entropy correction factor = 0.000 10 Btu/lb (mass)·°R. Thus, $S_6 = 0.016\ 764 + 0.80\ (0.009\ 112) + 0.000\ 10 = 0.024\ 153\ 6$ Btu/lb (mass)·°R.

At point 7, air at 29.0°F is being circulated from the evaporator to the railcar interior. H_7 = enthalpy at point 7 = $H_6 - 2.4813 = 11.3968 - 2.4813 = 8.9155$ Btu/lb (mass). $H_{a7} = H_{a7} + x_7(H_{as7})$ (from Equation 4). H_{a7} = tabulated value of enthalpy of dry air = 6.966 Btu/lb (mass), and H_{as7} = enthalpy of dry air - enthalpy of saturated air = 3.540 Btu/lb (mass). x_7 = degree of saturation = $(H_7 - H_{a7})/H_{as7} = (8.9155 - 6.9660)/3.540 = 0.5507$. S_7 = entropy of air at point 7 = $S_{a7} + x_7(S_{as7}) + S_{cl}$. S_{a7} = tabulated value of entropy of dry air = 0.014 70 Btu/lb (mass)·°R. S_{as7} = entropy of dry air - entropy of saturated air = 0.007 61 Btu/lb (mass)·°R, and S_{cl} = entropy correction factor = 0.000 10 Btu/lb (mass)·°R. Thus, $S_7 = 0.014\ 70 + 0.5507\ (0.007\ 61) + 0.000\ 10 = 0.018\ 99$ Btu/lb (mass)·°R.

The air-flow and refrigerant-flow requirements are $q_t = \dot{m}_{air}(H_6 - H_7)$ (from Equation 3) = total heat change = 27 914.75 Btu/h. $H_6 - H_7$ = enthalpy change of air over evaporator = 2.4813 Btu/lb (mass), and $\dot{m}_{air}$ = air mass required to remove heat $q_t = 27\ 914.75/2.4813 = 11\ 250.05$ lb (mass)/h. Air flow required at evaporator = $m_{air}/(p_{air} \times 60)$, where p_{air} = air density at 32°F, = $11\ 250.05/(0.081 \times 60) = 2314.80$ ft³/min. For an energy balance at the evaporator, the heat leaving the air must be equal to the heat transfered to the refrigerant. Therefore, $q_t = \dot{m}_r(H_1 - H_5)$ (from Equation 3) = total heat change = 27 914.75 Btu/hr. H_1 = enthalpy at point 1 = 108.440 Btu/lb (mass), H_5 = enthalpy at point 5 = 37.705 Btu/lb (mass), $\dot{m}_r$ = mass-flow rate of refrigerant = $q_t/(H_1 - H_5) = 27\ 914.75/(108.440 - 37.705) = 394.64$ lb (mass)/h.

For an energy balance, the condenser coils must remove to the environment the heat transferred by the evaporator and the energy put into the compressor. $q_t + W_c = TD_{db} \times 1.08 \times$ air flow (from Equations 6 and 7). q_t = total heat change = 27 914.75 Btu/lb (mass), W_c = work put into compressor = $\dot{m}_r(H_2 - H_1) = 394.64\ (128.807 - 108.440) = 8037.63$ Btu/h. TD_{db} = temperature difference dry bulb through the condenser = $(q_t + W_c)/(1.08 \times 2500) = (27\ 914.75 + 8037.63)/(1.08 \times 2500) = 13.32°$ F.

At point 8, ambient air enters the condenser coils at a temperature of 95.0° F and atmospheric pressure. H_8 = enthalpy of dry air at point 8 = 22.827 Btu/lb (mass) (from the air tables), and S_8 = entropy of dry air at point 8 = 0.045 13 Btu/lb (mass)·° R.

At point 9, air leaves the condenser coils with added heat from the refrigerant. T_9 = dry air temperature at point 9 = $T_8 + 13.32°F = 108.32°F$, H_9 = enthalpy of dry air at point 9 = 26.0301 Btu/lb (mass), and S_9 = entropy of dry air at point 9 = 0.050 84 Btu/lb (mass)·°R. These results are summarized in Table 1.

The power requirements of the system are calculated below. $Comp_{bhp}$ = power requirement of compressor = $W_s \times \dot{m}_r = (H_2 - H_1) \times \dot{m}_r$, where heat loss from the compressor = 0 (from Equation 3), = $(128.807 - 108.440) \times 394.64 = 8037.6328$ Btu/h = 3.1582 brake horsepower (bhp). The closest commercially available compressor is a 3⅓-bhp model having 2 cylinders, which would be the type used to run the refrigeration system.

$Evap_{bhp}$ = power requirement of evaporator fan motor = (air flow × P_t)/(6356 × n_{er}). Air flow = 2314.80 ft³/min, n_{er} = assumed motor efficiency = 80 percent, and P_t = maximum static pressure through evaporator coils = 1.5 in of mercury. Thus $evap_{bhp} = (2314.80 \times 1.5)/(6356 \times 0.80) = 0.6829$ bhp. The closest commercially available motor is a ¾ bhp model, which would be used to run the blower for the evaporator air.

$Cond_{bhp}$ = power requirement of condenser fan motor = (air flow × P_t)/(6356 × n_{con}). Air flow = $\dot{m}_r(H_9 - H_4)/[(H_9 - H_8)/(p_{air} \times 60)]$, where p_{air} = air density at 95°F, = $394.64(116.6690 - 37.7050)/[(26.0301 - 22.8270)/(0.0684 \times 60)] = 2370.57$ ft³/min, P_t = maximum static pressure through condenser coils = 1.0 in of mercury, n_{con} = assumed motor efficiency = 80 percent. Thus, $cond_{bhp} = (2370.57 \times 1.0)/(6356 \times 0.80) = 0.4662$ bhp. The closest commercially available motor is a ½-bhp model, which would be used to run the blower for the condenser air.

ANALYSIS OF ENERGY AVAILABILITY

By using an energy-availability analysis of a system, it is possible to establish a program of energy management for it. This type of analysis, which is currently needed in all areas of energy use, will be used to show how fuel oil is consumed in the present railcar environment and the advantages in energy consumption of the smaller refrigeration system powered by solar cells.

Available energy is defined as that portion of energy added to a system that is converted directly to work by a reversible process (i.e., a process in which the total amount of energy put in can be recovered at any time). Unavailable energy is defined as that portion of energy added to a system that cannot be converted directly into work, but is lost to the environment because of friction, heat loss, or inefficiency of the components of the system.

These two definitions are the basis for the thermodynamic energy analysis of any system using energy or transferring heat. According to the first law of thermodynamics, mechanical systems convert fuel into useful work, and this useful work is recoverable at any time. According to the second law of thermodynamics, of the work produced by a fuel, some is transformed into un-

recoverable energy or work, and the remainder is used for the final goal of the system. The calculations below show how much of the total energy input will be used for the refrigeration itself in the new design as compared with that used at present in railcars.

e = effectiveness
= ideal power input to system/actual power input to system (8)

b = availability function = $(H - T_o S)$ (9)

$\dot{I}$ = irreversibility = maximum work - actual work
= amount of heat or work lost because of effects such as friction
= $\dot{m}_r \Delta b$ (10)

The operating data are shown below.

Item	Value
Refrigerant	R-22
$\dot{m}$, lb(mass)/h	394.64
Electric input to compressor, Btu/h	8 483.32
n_c	0.80
Compressor heat loss, Btu/h	0
Condenser air-flow rate, ft^3/min	2 370.57
Electric input to fan motor, Btu/h	1 272.50
n_{con}	0.80
Evaporator air-flow rate, ft^3/min	2 314.80
Electric input to evaporator fan motor, Btu/h	1 908.75
n_{ev}	0.80
Maximum energy absorbed from railcar interior, Btu/h	27 914.75
Interior temperature	491.67°R
Ambient temperature	554.67°R

b_1 = availability function at point 1 = $H_1 - T_0S_1$ = 108.440 - (554.67 × 0.229 64) = -18.934 41 Btu/h, b_2 = availability function at point 2 = $H_2 - T_0S_2$ = 128.8070 - (554.67 × 0.239 49) = -4.030 91 Btu/h, b_3 = availability function at point 3 = $H_3 - T_0S_3$ = 116.6690 - (554.67 × 0.219 42) = -5.036 69 Btu/h, b_4 = availability function at point 4 = $H_4 - T_0S_4$ = 37.7050 - (554.67 × 0.076 68) = -4.827 095 Btu/h, and b_5 = availability function at point 5 = $H_5 - T_0S_5$ = 37.7050 - (554.67 × 0.080 74) = -7.079 055 Btu/h.

The actual power input into the system = compressor power input + condenser-fan motor input + evaporator-fan motor input = 8483.32 + 1272.5 + 1908.75 = 11 664.57 Btu/h. The ideal power input into the system = $\dot{m}_{air} T_0 (S_7 - S_6)] - (H_7 - H_6)$ = IP_{in} = 11 250.05 × 554.67 (0.018 99 - 0.024 15) - (8.9155 - 11.3968) = -4283.9875 Btu/h.

e = effectiveness of system = IP_{in}/actual power = 4283.9875/11 664.57 = 0.3673. $\dot{I}_{comp}$ = irreversibility of compressor = $\dot{m}_r(H_2 - H_1) - \dot{m}_r(b_2 - b_1)$ = 8037.6328 - 5881.9603 = 2155.6725 Btu/h, $\dot{I}_{e\,fan}$ = irreversibility of evaporator fan motor = T_L/T_H × electric input to evaporator motor = (491.67/554.67) × 1908.75 = 1691.952 Btu/h, $\dot{I}_{cond}$ = irreversibility of condenser = $\dot{m}_r(b_5 - b_1)$ = 394.64[-5.036 69 - (-7.8271)] = 1101.2911 Btu/h, $\dot{I}_{con\,fan}$ = irreversibility of condenser fan motor = 0 Btu/h (because no energy from the fan motor is available to the system), $\dot{I}_{ev}$ = irreversibility of expansion valve = $\dot{m}_r(b_5 - b_4)$ = 394.64[-7.07906 - (-7.82710)] = 295.2065 Btu/h, $\dot{I}_{evap}$ = irreversibility of evaporator = $\dot{m}_r(b_5 - b_1) - (1 - T_L/T_H)\dot{m}_r(H_5 - H_1)$ = 394.64[-7.079 06 - (-18.934 41)] - [1 - (491.67/554.67)] × 394.64(37.7050 - 108.440) = 1478.6313 Btu/h, $\dot{I}_{dl}$ = irreversibility of discharge line from compressor = $\dot{m}_r(b_2 - b_3)$ = 394.64 [-4.030 91 - (-5.036 69)] = 396.9210 Btu/h. The ideal power input into the system + the total of all $\dot{I}$ = actual power into system = 4283.9875 + 7119.6744 = 11 403.662.

The present railcar refrigeration system hourly converts an average of 3.2 L (0.85 gal) of diesel fuel into the energy necessary to power a 35.2-kJ/s (10-ton) refrigeration system. The effectiveness of this system is about 15 percent of the actual power available from the fuel. The remaining 85 percent of the fuel is eventually converted into wasted heat and cannot be recovered. This can and should be improved on. One solution would be the use of smaller refrigeration systems, incorporated in better designed railcar structures, and deriving power from solar energy.

The refrigeration system proposed here would require no diesel fuel. Its effectiveness would be 37 percent, which is an increase of over 200 percent in the use of the energy delivered to the system.

SOLAR CELL SYSTEM

A railcar refrigeration system can operate on electricity produced by a diesel engine, drawn from storage batteries, taken from the electric wires above the train, or produced by photovoltaic energy cells. The first three alternatives all rely on petroleum resources that at the present rate of growth in use of 7.3 percent will be exhausted in 31 years (3). Solar energy as an alternative energy source could also be used to provide electricity to refrigerate the railcar. The amount of solar energy falling on the ground is 10 000 times the present world consumption, which establishes the sun as a major energy source.

The photovoltaic effect is the direct production of electricity through absorption of sunlight by semiconductors that can convert light energy into electrical energy.

The annual average incidence of solar energy on the ground in the United States is 720 W/m^2 (67 W/ft^2) (3). Photovoltaic cells are currently available made from silicon or cadmium sulfide having efficiencies of 14 percent. A system of photovoltaic cells operating at this efficiency and receiving the average solar power would produce 101 W/m^2 (9.38 W/ft^2). By using cells having a 12.5 percent efficiency and a roof area of 55.74 m^2 (600 ft^2), the average power output available from a railcar solar system would be 5 kW, which would be sufficient to power its refrigeration system.

Although these theoretical figures indicate that the solar array is capable of supplying the needed power, the present cost of $4000/kW would put the cost of the array at $20 000. Cost reduction in this area can be expected: The Energy Research and Development Administration has set goals of $2000/kW for 1980, $500/kW for 1985, and $100/kW for 2000. If the refrigeration system and the railcar design described above prove to be adequate, the 1980 cost of a 5-kW array would be $10 000. By eliminating the present costs of $6100 and $900 for the diesel engine and the fuel tank respectively and $900/year for the fuel, the cell cost would be offset in 3 years. The following (2) summarizes the position that has been taken on the possibilities of solar cells to produce large quantities of electrical power.

> In order to justify these (photovoltaic) expenditures, however, it is necessary to demonstrate that, when these array-cost goals are reached, photovoltaic solar-energy systems will have a good chance of competing successfully for a significant place in the nation's energy market.

Preparing for the future needs of refrigerated transport is vital to the railroad industry. The power capabilities of photovoltaic cells will provide an alternative power source as sources of diesel fuel diminish and costs of operation increase.

ENVIRONMENTAL CONSIDERATIONS

Air and noise pollution have recently become major concerns in present and projected transportation operations.

New federal and state air pollution standards have been set and are being enforced. The diesel engines powering the present railcar refrigeration systems are contributors to air pollution, control of which will be very costly. The elimination of the diesel engine by using solar panels would not only eliminate chemical air pollutants, but could also save the costs of pollution-control equipment, which would offset a portion of the first cost of the solar panels.

Noise levels, recently regulated by the Environmental Protection Agency, are another major concern. Certain projected state noise-emission controls now under consideration could force the industry into costly and time-consuming programs of redesigning or retrofitting existing equipment. The elimination of the diesel engine as a power source would therefore provide additional environmental-control benefits.

DISCUSSION AND CONCLUSIONS

The refrigeration of a perishable load can be theoretically accomplished with an 8.8 kJ/s (2.5- ton) refrigeration system powered by the direct current generated by photovoltaic cells. This affords the operator of this type of equipment almost total independence from energy-oriented problems.

However, there are limitations that must be considered because they dictate the circumstances under which such a system could be used and the extent of engineering technology that must be perfected.

1. At present, only daytime operation is feasible. Further advances in fuel-cell or storage-battery technology are required before continuous day-night operation could be used.
2. Some loads would still require precooling to a predetermined temperature level, mainly because of their respiration rates. The system as designed could precool an item with a low respiration rate such as oranges or cantaloupes. Corn or peas, which have higher respiration rates, would require precooling before release for shipment and probably top icing to provide the proper humidity.
3. Along with precooling before shipment, the railcar would require a storage battery to power the system until the solar energy was sufficient to operate it.
4. Maximum efficiency would be obtained only if the railcars were operated as a unit train, thereby benefiting from maximum travel distance during daylight operation.
5. If for some reason the railcars were stopped in a classification yard for any length of time, standby power sources would be necessary for continuous operation.
6. The solar panels would require careful and scrupulous maintenance.

RECOMMENDATIONS

Railroad refrigerator cars operating independently of fossil fuels may be an immense asset in the near future. An existing mechanically refrigerated railcar could be modified in construction to lower the structural heat loss. A smaller, more efficient refrigeration system could then be incorporated into the railcar for analysis and testing, using standby electrical power, to achieve maximum efficiency and system effectiveness. When the costs of photovoltaic-cell arrangements become lower and their technology is improved, a solar-assisted system could be attached to the roof of the prototype.

A model of this type of system could be operational by 1980. The tempo of technological advancement and our dwindling energy supplies make it mandatory for the transportation industry to play a leading role in the development of new methods for storing and transporting perishable commodities.

ACKNOWLEDGMENT

I wish to express my appreciation to the following individuals who gave freely of their time and energies toward the preparation of this paper: Albert L. Creel, Jr., Lydia V. McClary, and Charles C. Necessary of the Fruit Growers Express Company and James B. Kelly, Ivor S. Pelsue, and Edward F. Russ of the Carrier Transicold Company.

REFERENCES

1. W. H. Redit. Protection of Rail Shipments of Fruits and Vegetables. Agriculture Handbook Number 195, July 1969.
2. S. S. Leonard. Mission Analysis of Photovoltaic Conversion of Solar Energy. 11th IEEE Photovoltaic Specialists Conference, 1975.
3. J. H. Krenz. Energy Conservation and Utilization. Allyn and Bacon, Boston, 1976.
4. J. A. Merrigan. Prospects for Solar Energy Conversion by Photovoltaics. MIT Press, Cambridge, 1975.

Mr. Conover is now with the American Gas Association, Arlington, Virginia.